Zebrafish posterior lateral line organogenesis regulation by Notch signaling

Thesis

Zebrafish posterior lateral line organogenesis regulation by Notch signaling

Agnė Kozlovskaja-Gumbrienė B.Sc., M.Sc.

A thesis submitted in fulfillment of the requirements of the Open University

for the Degree of Doctor of Philosophy

The Stowers Institute for Medical Research

Kansas City, USA

an Affiliated Research Center of the

Open University, UK

Kansas City, MO, January 2017

Abstract

Organ morphogenesis depends on the precise orchestration of cell migration, cell fate specification and cell shape chages. Results in this thesis demonstrate that Notch signaling is an integral part of the feedback loop between Wnt and Fgf signaling that underlies the self-organization of rosette-shaped sensory organs in the zebrafish lateral line system. Notch cell autonomously induces apical constriction and cell adhesion downstream of Fgf signaling and organizes lateral line organs into rosettes independent of patterning cues normally provided by a Wnt/Fgf signaling system. We also show that the ectopic Notch signaling induces larger organs independently of proliferation and the Hippo pathway. Transplantation and RNASeq analyses revealed that Notch signaling induces cell adhesion and tight junction proteins that interact with cytoskeleton causing cells to self-organize into fewer larger organs rather than several smaller ones. Thus, Notch plays an essential role in coordinating actomyosin induced cell shape changes and their transmission throughout the tissue via adhesion molecules.

Dedication

To my parents…

Acknowledgements

My deep gratitude goes first to my mentor Tatjana Piotrowski, who expertly guided me through my graduate education and was critically important for my scientific development and success. She also helped me to become a more confident and thoughtful person and I am very thankful for her hard work and dedication.

This dissertation would not have been completed without the support, advice and critique from my committee members Tatjana Piotrowski, Matt Gibson, Paul Trainor, Rong Li and Robb Krumlauf. The financial and the core facility support form the Stowers Institute was critical for my work and I am very grateful for it. I also want to thank Leanne, Shelly and Lisa for organizing everything related to Open University and Marina, Mark and Kristin for helping me to polish this thesis.

My appreciation also extends to my laboratory collegues. Marina, my first and dearest teacher in the lab, who was always attentive, devoted and fun. I thank Nina for her continuous support and companionship, and Helena for her kindness and friendship. Thanks also goes to Mark for his steady hand in guiding me through the multiple experiments and Joaquín for his inspiring enthusiasm, love for science and sincere friendship. All current and previous Piotrowski lab members were instrumental in my graduate journey and I am very appretiative for their help.

My gratitude goes to my wonderful sisters, parents, grandparents and all my friends back at home who always believed in my success and were incredibly supportive despite many miles and scarce meetings that separated us. I am also very grateful to my mother-in-law Nijolė and Aleishia for their tremendious help when my family most needed it.

Foremost, I want to thank my other half Aurimas for his unconditional love and constant encouragement to be true to myself, and Joris- my miracle child, for inspiring me to be a better human being.

Table of Contents

Table of Figures

Chapter 1

Introduction

Organogenesis and organ size regulation

The control of body and organ size is a key developmental process that impacts the anatomy and physiology of an animal. Misregulation of size control may not only affect fundamental phenotypic traits of an organism, but also result in multiple pathologies, such as dwarfism and gigantism, hypo- and hyperplasia, cancer and organ degeneration (Gokhale and Shingleton, 2015). The regulation of individual cells to form multicellular three-dimensional structure of specific shape and size is enforced by coordinated gene action. Molecular signaling regulates cell proliferation, migration, growth and differentiation patterns to shape the tissue in precise manner. Intrinsic as well as nonautonomous, short-range and long-range signals guide cells to achieve unique developmental goals. Nevertheless, how these myriad components work together to generate an organ of correct size and shape is still largely unknown. The main processes that regulate organ size are: 1) growth rate, 2) growth duration, 3) target size, 4) apoptosis and systemic growth coordination (Gokhale and Shingleton, 2015). These functions are most famously implemented by, but not limited to Insulin/IGF, RAS/RAF/MAPK, TOR, JNK and Hippo signaling pathways and their combinations (Keshet and Seger, 2010; Laplante and Sabatini, 2012; Teleman, 2010; Weston and Davis, 2007; Yu and Guan, 2013). These pathways deploy different strategies to regulate organ size. For example, the Insulin/IGF pathway deactivates negative regulators of growth, such as FOXO family proteins (van der Vos and Coffer, 2011). The role of RAS/RAF/MAPK signaling on size regulation is complex and context dependent. Many of the nuclear and cytoplasmic targets of this pathway are positive regulators of cell-cycle progression, however, the overexpression of Raf proteins can lead to cell cycle arrest

and apoptosis (McCubrey et al., 2007). Besides its function with respect to nutrition, cellular energy and oxygen regulation, the TOR pathway is known to regulate cell size through actin cytoskeleton organization (Jacinto et al., 2004). The JNK-signaling pathway mainly functions in response to cellular stress and is crucial in regulating cell death, tissue regeneration and wound healing (Igaki, 2009; Johnson and Nakamura, 2007). Lastly, Hippo is the novel signaling pathway in the organogenesis field. Hippo signaling regulates growth by inhibiting the activity of growth-promoting YAP/TAZ genes (described in more detail below; (Huang and Ingber, 2005; Song et al., 2010)). Despite the classical mechanisms, such as cell proliferation and cell death regulation, in this thesis, we provide an insight into a previously underappreciated mechanism for organ size regulation whereby zebrafish lateral line organs are formed through cell allocation regulated by the Fgf/Notch signaling.

1.1 Multicellular rosettes in organogenesis

The morphogenetic movement of cells and tissues predisposes the formation of adult organs. Hence, it is critically important to understand how tissue shaping is regulated at the cellular and molecular level. Over the past 20 years, it has become apparent that in multiple species cells transition through a stage when five or more cells connect at a central point and form stable or transient epithelial rosettes that drive tissue modeling during their organ development (Harding et al., 2014). Such epithelial rosettes are observed in *Drosophila* axis elongation and retina development, mouse pre-implantation embryo morphogenesis, pancreas development, zebrafish lateral line sensory organ formation, brain tumors or the neural stem cell niche (Bedzhov and Zernicka-Goetz, 2014; Blankenship et al., 2006; Harding et al., 2014; Martin and Goldstein, 2014; Wippold and Perry, 2006). Whereas the intracellular mechanisms that regulate epithelial rosette formation remain conserved, the extracellular cues are highly dependent on the developmental context.

There are two main mechanisms for rosette formation: 1) planar polarized constriction and 2) apical constriction. Usually, rosettes formed through the planar polarized mechanism dissolve relatively quickly and typically are involved in tissue elongation processes, such as *Drosophila* epithelial elongation (Bertet et al., 2004; Blankenship et al., 2006; Irvine and Wieschaus, 1994). By contrast, rosettes that are formed through the apical constriction mechanism are more stable and may or may not resolve, but instead they remodel to form a functional structure or organ. One of the better-studied examples of apical constriction driven rosette formation is the development of the zebrafish lateral line sensory organs (Figure 1-1B, B'; (Harding et al., 2014)). Due to the scope of this thesis on zebrafish lateral line development, I will focus on the apical constriction formation principles.

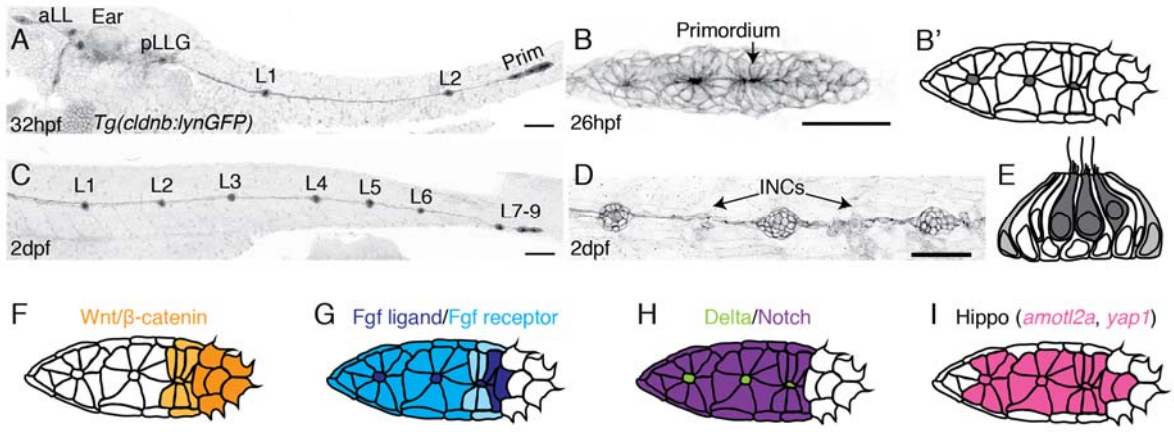

Figure 1-1. Zebrafish posterior lateral line development and cell signaling in the primordium

(A-D) Zebrafish posterior lateral line in the *Tg(cldnB:lynGFP)* background, which allows visualizing cell mebranes in the lateral line and the skin. (A) Anterior and posterior lateral lines at 32 hpf. Anterior lateral line (aLL) migrates anterior from the ear and splits into two paths surrounding the eye. Posterior lateral line develops along the embryonic tail and by 32hpf primordium deposits 2-3 proneuromasts. (B and B') The schematics of posterior lateral line primordium, which is composed of mesenchymal unpatterned cells in the leading domain and apico-basally polarized cells, which form 3-4 rosettes in the trailing domain. The most nascent rosette (arrow in B) forms just behind the leading domain. (C) Posterior lateral line primordium deposits ~6 neuromasts along the trunk and 3 terminal neuromasts in the tail at 2 dpf. (D) Along with proneuromasts, primordium also deposits a chain of interneuromast cells (INCs), marked with arrows. (E) Schematic representation of mature neuromast architecture at 2dpf with hair cells (dark gray) in the middle surrounded by support cells (white) and mantle cells (light gray) in the periphery. (F-I) Schematic

representation of the different signaling pathways activities in the primordium. (A and C) scale bar is 100μm, (B and D) scale bar is 50μm.

Every apico-basaly polarized cell has distinct apical, basal and lateral plasma membrane domains, which are established by polarity proteins and each have discrete functions in tissue maintenance and function (Rodriguez-Boulan and Macara, 2014). Apical constriction occurs upon the narrowing of the cell at its apical side (Figure 1-2A, A'; (Martin and Goldstein, 2014; Sawyer et al., 2010)). Coordinated apical constriction of multiple neighboring cells can result in bending of sheets of cells or/and the formation of a multicellular rosette that is comprised of cells pointing their apical domains into one location (Figure 1-1B', Figure 1-2A'). The apical constriction that underlies multicellular rosette formation is usually regulated through the contraction of an acto-myosin network (Figure 1-2B; (Ernst et al., 2012; Harding and Nechiporuk, 2012; Nishimura and Takeichi, 2008)), which is a dynamic meshwork of the Non-muscle myosin II (NMII) and filamentous actin (F-actin) molecules established by cell polarity and cell-cell junction regulators (see below). The apical meshwork contraction is goverened by NMII motor activation through a Myosin II subunit, Myosin regulatory light chain (MRLC) phosphorylation (Sawyer et al., 2010). An apically constricted cell acquires a teardrop form, and when multiple such cells are combined, they form a garlic bulb-shaped multicellular rosette (Figure 1-1E).

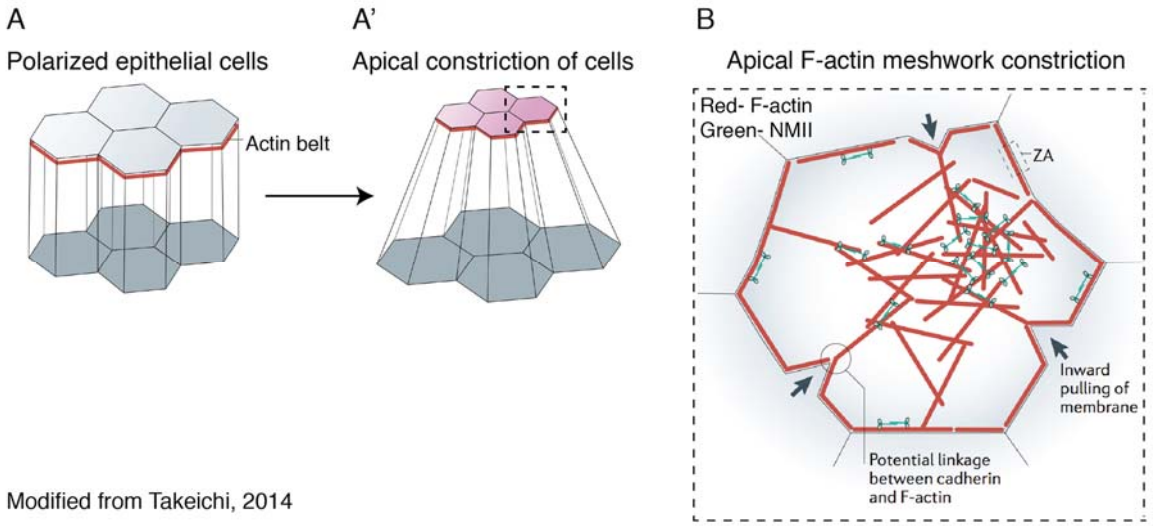

Figure 1-2. Apical actin cortex shrinkage drives cell apical constriction
(A-A') Apical adherens junctions (AJs) accumulate around the actin belt and link cells, allowing apical actomyosin constriction to drive shape changes in the tissue. (B) Key components regulating apical constriction include F-actin (red) and NMII (green), which form contractile networks that underlie the apical cortex. Shrinkage of apical cortex (black arrows) is driven by actomyosin constriction (Takeichi, 2014).

The extracellular cues that trigger apical constriction-dependent rosette formation vary highly depending on the organism and tissue (reviewed in Harding et al. (2014)). However, since this mode of cell organization is common among multiple species, understanding the molecular signals driving rosette formation is essential to get a better insight into tissue formation and maintenance.

1.2 Zebrafish posterior lateral line development

1.2.1 Introduction: Posterior lateral line system

To successfully navigate in their habitat amphibians and fish have developed a "touch at a distance" sensory system called the lateral line (Dijkgraaf, 1963). This system allows to perceive information in response to changes in water motion around the animal body and use it to perfom functions such as schooling, sexual courtship, rheotaxis (swimming against current), predator avoidance and pray detection (Ghysen and Dambly-Chaudiere, 2004). The lateral line system has disappeared in the terrestrial tetrapods,

however its sensory organ cell ultrastructure and molecular signaling program required for development is surprisingly similar to an auditory system found in the ear (Fritzsch, 1987; Nicolson, 2005; Whitfield, 2002).

The lateral line system organs were disovered in the seventeenth century by Steno and Lorenzini in elasmobranchs (sharks, skates and rays) (Figure 1-1E; reviewed in Piotrowski and Baker (2014)). For a long time, lateral line organs were thought to be mucus-secreting glands and later assigned an auditory function. However, in the beginning of the twentieth century elegant cell transplantation, cell labeling and cell ablation studies performed in anuran and urodele amphibians by Harrison and Stone, revealed the lateral line function in mechanosensation (reviewed in Wright (1951); (Piotrowski and Baker, 2014)). Since then, the lateral line system has become an excellent model to study important developmental paradigms such as cell migration, cell fate specification, morphogenesis and organogenesis. From all the aquatic animals, the zebrafish (*Danio rerio*) lateral line is the most well studied due to the wealth of genetic tools and transperancy of the embryos, which allows lateral line studies performed at cellular and molecular levels (Kimmel et al., 1995; Nüsslein-Volhard, 2012).

Both electrosensory and mechanosensory organs are present in multiple species of fish, but zebrafish maintained only the mechanosensory system (Piotrowski and Baker, 2014). The zebrafish lateral line mechanoreceptive organs are called neuromasts, that induce neuron signals through their sensory cell deflections caused by the moving water (Figure 1-1E). Neuromasts are distributed in stereotypical paths along the body of the animal together with neurons that innervate them and convey information to the adjacent hindbrain (Ghysen and Dambly-Chaudiere, 2004). There are two major branches, the anterior lateral line, which extends on the head around the eyes and jaw, and a posterior part that develops along the trunk and tail (Figure 1-1A, C). The posterior lateral line system

is better studied so far, likely because it is easier to be identified at an early stage of its development and it is more ameanable for imaging.

1.2.2 Zebrafish posterior lateral line development

The lateral line originates from the ectodermal thickening called the placode (Ghysen and Dambly-Chaudiere, 2004). The anterior and posterior lateral lines develop, respectively, from the migrating anterior and posterior lateral line placodes called primordia (Figure 1-1A,B,B'; reviewed in Piotrowski and Baker (2014)). Posterior lateral line primordium initially separates from the posterior lateral line ganglion, situated posterior to the developing ear, and deposits sensory organs along the wake of migration to the tail tip (Figure 1-1A,C). Since experimental evidence for this thesis was acquired entirely from studies in the posterior lateral line, I will focus on its development from now on.

After segregation from the ganglion at ~18 hours post fertilization (hpf), the posterior lateral line primordium forms first proneuromast in its most trailing part. Proneuromast formation occurs when around 20 apico-basally polarized cells constrict their apices into one point and form a garlic bulb-shaped cellular rosette within the primordium (Hava et al., 2009; Lecaudey et al., 2008). Soon after, the primordium starts migrating under the epidermis along the trunk towards the tail, which takes ~ 24 hours to complete. The process by which primordium migration is initiated is still poorly understood. Upon the beginning of migration, additional posteriorly located cell clusters fuse to the primary primordium and thereby primordium formation is completed (Breau et al., 2012). The primordium comprised of ~100 cells starts to segment into additional proneuromasts (Figure 1-1B,B'). The most nascent rosette is formed next to the leading, seemingly unpatterned mesenchymal cells (Figure 1-1B arrow). Once the primordium subdivides into 4 rosettes, the most mature proneuromast slows down and is ready to be deposited from

the trailing part of the primordium (Gompel et al., 2001; Haas and Gilmour, 2006). The fascinating feature of the lateral line development is that proneuromast formation and deposition process is iterative and sustained by continious cell proliferation in the primordium to provide enough cells for 5-6 deposition cycles along the trunk of the fish (Aman et al., 2011). Once the primordium reaches the tail tip it breaks down into the last 3 neuromasts (Figure 1-1C). Importantly, analyzing molecular strategies deployed in primordium development and proneuromast formation contributes to our broader understanding about organ morphogenesis and how cells form into rosettes in certain brain tumors.

Along with the proneuromasts, the primordium also deposits a chain of cells called interneuromast cells (INCs), which span the distance between neuromasts and postembryonically develop into sensory organs (Figure 1-1D arrows; (Grant et al., 2005; López-Schier and Hudspeth, 2005; Lush and Piotrowski, 2014)). Moreover, primordium migration is accompanied by the axons extending from the posterior lateral line ganglion that later innervate the fully formed neuromasts (Gilmour et al., 2002; Metcalfe et al., 1985).

The proneuromast cells start to express differentiation markers already inside the primordium, however the neuromasts will only become functional sensory organs at ~ 2 days post fertilization (dpf) and fully mature by 5 dpf (Figure 1-1B', E dark gray). Mature neuromasts are composed of sensory hair cells surrounded by two types of accessory cells: support cells and mantle cells in the periphery (Figure 1-1E white and light gray, (Hernández et al., 2007)). Hair cells stick their cilia out into the water and depending on their orientation the information about their deflection pattern is registered and transmitted to the brain. Contrary to mammals, lateral line hair cells are capable to regenerate throughout the liftetime of the fish, thus investigating the molecular mechanisms behind their regeneration

might be very insightful for mammalian deathness treatment (Nicolson, 2005; Whitfield, 2002). Interestingly, the “distant-touch” lateral line system has also been explored by the biomimetics field to improve underwater vehicles and marine robots so that they can similarly to fish sense hydrodynamic events in three-dimensions (Fan et al., 2002; Yang et al., 2010).

1.3 Molecular signaling coordinating zebrafish lateral line development

1.3.1 Wnt/β-catenin and Fgf signaling interplay regulates primordium patterning

Primordium cells acquire stereotypical morphologies along the anterior-posterior axis in the primordium, which ultimately contribute to sensory organ formation. Specifically, the leading 10-15% of primordium cells are flat, unpatterned and with multiple protrusions reaching out into the direction of migration, whereas, the larger trailing domain of the primordium is composed of apicaly constricted epithelial cells organized into rosettes (Figure 1-1B, B’; (Lecaudey et al., 2008)). These two completely distinct cell morphologies are maintained by mutually antagonistic interractions between the Wnt/β-catenin signaling in the front and Fgf signaling in the trailing domain of the primordium (Figure 1-2F, G; (Aman and Piotrowski, 2008)). Wnt/β-catenin signaling induces Wnt target genes, such as *wnt10a*, *lef1*, *axin2* and Fgf ligands *fgf3* and *fgf10a* in the leading cells, also Fgf receptor *fgfr1* and *fgf10a* expression in the back of the primordium (Aman and Piotrowski, 2008; Lush and Piotrowski, 2014; Nechiporuk and Raible, 2008). A recent study showed that Fgf ligands deploy heparin sulfate proteoglycans (HSPGs) for diffusion to the trailing domain of the primordium where they activate the expression of the Fgf receptor and Fgf target genes *pea3*, Di-pERK1/2 and *dkk1b* expression (Galanternik et al., 2015). Together with Fgf signaling components, Wnt also induces the cytoplasmic membrane-associated Fgf inhibitor *sef*, which protects leading mesenchymal cells from acquiring epithelial

morphology by blocking the Fgf receptor function (Aman and Piotrowski, 2008). Conversly, Fgf signaling ensures epithelial integrity in the trailing compartment by stimulating expression of *dkk1b*, a diffusible inhibitor of Wnt/β-catenin signaling pathway. These interactions establish a balance between Wnt and Fgf signaling domains that is critical for primordium migration and sensory organ formation (Aman and Piotrowski, 2008).

1.3.2 Wnt/β-catenin and Fgf regulate primordium segmentation through cell proliferation and chemokine signaling

As the primordium does not contain enough cells at the beginning of migration to deposit all 8-9 neuromasts, the primordium needs to compensate for the cell loss, thus cell renewal is necessary for the complete lateral line formation and it is achieved by a coordinated cell proliferation process (Aman and Piotrowski, 2008). The pattern of proliferating cells is not homogeneous across the primordium with more proliferation at the overlapping region between Wnt/β-catenin and Fgf signaling domains and in the trailing domain (Figure 1-1F, G lighter color; (Dalle Nogare et al., 2016)). It has been demonstrated that a combined activity of Wnt/β-catenin and Fgf is required for normal cell proliferation in the primordium (Aman and Piotrowski, 2008). Depleted proliferation leads to a significant reduction in the number of deposited neuromasts due to primordium shortening and subsequent obstruction of proneuromast placement into the deposition zone (Aman and Piotrowski, 2008).

Chemokines are chemotactic, secreted proteins that signal through G-protein coupled receptors and control the migratory patterns of immune and cancer cells, also they are critically important for progenitor germ cell, neuron and neural crest cell guidance in the embryo (Dumstrei et al., 2004; Killian et al., 2009; Svetic et al., 2007). Likewise, it has been demonstrated that directional migration of the primordium is not regulated by

extrinsic guidance molecules, but rather by the asymmetric expression of the chemokine receptors, *cxcr4b* and *cxcr7b*, in the primordium and the expression of a chemokine ligand *cxcl12a* in a narrow stripe along the myoseptum (Dambly-Chaudière et al., 2007; David et al., 2002; Haas and Gilmour, 2006; Valentin et al., 2007). The Cxcr7b receptor utilizes and removes Cxcl12a ligand from the trailing part of the primordium, thereby generating a gradient of Cxcl12 and guiding the primordium forward by Cxcr4b chemoattraction towards Cxcl12a in the myoseptum (Dambly-Chaudière et al., 2007; Donà et al., 2013; Valentin et al., 2007; Venkiteswaran et al., 2013). The *cxcr4b* receptor is expressed in the leading cells, overlapping with the Wnt domain in the primordium. However, Wnt/β-catenin signaling is rather a permissive than a direct regulator of *cxcr4b* expression in the primordium (Aman and Piotrowski, 2008). Similarly, the *cxcl12a* ligand expression is also not affected by Wnt/β-catenin or Fgf signaling perturbations in the primordium (Aman and Piotrowski, 2008). However, *cxcr7b* expression, which marks the neuromast deposition zone in the trailing domain is repressed in the leading primordium cells by Wnt/β-catenin signaling. The *cxcr7b* expression is dependent on where cells are positioned within the primordium; it shrinks just after proneuromast deposition and expands upon next rosette maturation (Aman and Piotrowski, 2008). Therefore, one might expect to increase proneuromast deposition periodicity upon *cxcr7b* domain expansion in the primordium. To conclude, apart from regulating Fgf signaling in the primordium (see above), Wnt/β-catenin is also crucial for cell proliferation and chemokine signaling transduction in the lateral line, that are essential processes for primordium migration and sensory organ deposition (Aman et al., 2011; Aman and Piotrowski, 2008).

1.3.3 Fgf signaling is required for posterior lateral line organ formation

Blocking Fgf signaling pharmacologically or genetically disrupts the primordium cell

organization into epithelial rosettes (Lecaudey et al., 2008; Nechiporuk and Raible, 2008). Fgfs are secreted molecules that regulate multiple developmental processes, such as cell survival and cell fate specification (Ornitz and Itoh, 2015). Upon binding to transmembrane receptors (Fgfrs) the Fgfs activate numerous signaling pathways, including the Ras-MAPK (Erk) pathway, which was shown to mediate proneuromast formation through an apical constriction process (see below) in the lateral line (Harding and Nechiporuk, 2012; Tsang et al., 2004). Expression of the Fgf ligand (*fgf10a*) is uniform in the leading region, but then becomes restricted to the central cells in the forming proneuromasts (Figure 1-1G dark blue; (Nechiporuk and Raible, 2008)). Fgf ligand activates Fgf signaling in the peripheral cells through the *fgfr1*-Ras-MAPK pathway that regulates cell apical constriction and thereby ensures proneuromast formation and maintenance (Durdu et al., 2014; Harding and Nechiporuk, 2012; Lecaudey et al., 2008; Nechiporuk and Raible, 2008). Specifically, Fgf signaling cell-autonomously induces the transcription of the scaffolding and actin-binding protein *shroom3*, which is a known regulator of apical constriction in multiple processes, such as chicken neural tube closure and *Xenopus* gastrulation and gut formation (Ernst et al., 2012; Hildebrand and Soriano, 1999; Lee et al., 2007; Nishimura and Takeichi, 2008; Plageman et al., 2011). Fgf also induces the expression of Rho-associated kinase 2a (Rock2a) that phosphorylates the Non-muscle myosin II (pNMII) in proneuromast cells, driving acto-myosin constriction (Harding and Nechiporuk, 2012). The loss of *shroom3*, Rock2a or pNMII function individually is comparable to Fgf signaling inhibition whereby, proneuromast formation is disrupted (Ernst et al., 2012; Harding and Nechiporuk, 2012). Together, these data suggest a model in which *shroom3* expression is activated downstream of Fgfr1-Ras-MAPK pathway to recruit Rock2a to the apical side of the cell where it activates actin constriction and proneuromast formation by phosphorylating NMII motor.

1.3.4 Notch signaling pathway regulates lateral line cell fate switch and neuromast morphogenesis

Notch signaling is an evolutionally conserved pathway that mediates an immense amount of processes from sensory bristle specification in *Drosophila* to neurogenesis, somite formation, angiogenesis and eye development in vertebrates (Artavanis-Tsakonas et al., 1999; Bray, 1998; Lewis, 1998; Morgan, 1917). The classic function of Notch signaling was described by *Drosophila* 'neurogenic' phenotype where the loss of Notch results in the failure of a field of cells to properly segregate into two lineages that ultimately form either cuticle (dermis) or nervous system cells (Guruharsha et al., 2012; Lehmann et al., 1983). The lateral inhibition mechanism ensures that cells in the same proneural cluster are driven towards different fates by stochastic acquisition of proneural genes in some cells and induction of proneural inhibitors in their immediate neighbors. This feedback loop driven lateral inhibition mechanism is employed in many different organ systems and is a well-conserved metazoan invention (Artavanis-Tsakonas et al., 1999). The lateral inhibition process defines which cells adopt sensory fate and which remain as a supporting cell population. During zebrafish nervous system development, cells in proneural clusters first acquire a potential to adopt a neural fate by expressing proneural genes, such as basic helix-loop-helix (bHLH) transcription factors. The proneural genes drive expression of Delta, a membrane-bound receptor, which activates its receptor, Notch, in the neighboring cells and then through the series of cleavage events Notch intracellular domain (NICD) is released from the cell membrane (Guruharsha et al., 2012; Itoh and Chitnis, 2001). This allows the translocation of NICD into cell nucleus, where it forms a transcriptional complex with the DNA-binding protein Supressor of Hairless (SuH, Rbp-J in mammals) and the nuclear effector Mastermind (MAM), thereby activating transcription of target genes (Bray, 2006; Kopan and Ilagan, 2009). This Delta-Notch interaction defines a canonical Notch signaling that leads to

the expression of bHLH factors of the Enhancer-of-split family, which have an antagonising proneural gene function (Appel and Eisen, 1998; Chitnis, 1999; Haddon et al., 1998; Meinhardt and Gierer, 1974; Takke et al., 1999). However, recently it has been shown that Notch signaling can also function independently of ligand and transcription ('non-canonically') and post-translationally regulate Wnt/β-catenin signaling in multiple organisms and tissues (Andersen et al., 2012).

During zebrafish lateral line development, Notch signaling mediates several processes: 1) the segregation between posterior lateral line ganglion (pLLG) and the primordium, 2) hair cell fate determination and 3) proneuromast morphogenesis (Itoh and Chitnis, 2001; Matsuda and Chitnis, 2010; Mizoguchi et al., 2011). At an early stage when the posterior lateral line placode is segmenting into the pLLG and the primordium, Notch signaling favors the primordium fate over the neuronal fate. Thus, the loss of Notch signaling in *mib1* mutants (described below) causes the increase in pLLG cell number at the expense of the primordium cells (Mizoguchi et al., 2011). Later, when the primordium is already established, Notch mediates the specification of sensory hair cells. The progenitors of hair cells are singled out in the primordium by the expression of the bHLH gene *atoh1a*, which drives the expression of *deltad*, that in turn activates Notch in the neighboring cells (Itoh and Chitnis, 2001). Notch signaling activates the expression of Hairy Enhancer-of-split-related genes, such as *her4*, which inhibit *atoh1a* and prevent Notch expressing cells from differentiating into hair cells (Itoh and Chitnis, 2001; Sarrazin et al., 2006). Simultaneously, when hair cell specification occurs, the primordium cells are also organized into proneuromasts. It was demonstrated that as *atoh1a* expression becomes established in the central cells, it drives not only Notch ligand *deltad*, but also the expression of *fgf10*, while it inhibits expression of *fgfr1* (Matsuda and Chitnis, 2010). This source of Fgf in the central cells ensures proneuromast formation and their stability (see above). Therefore, Notch

restriction of *atoh1a* expression determines Fgf activity pattern and proneuromast formation (Figure 1-1H; (Matsuda and Chitnis, 2010)).

1.3.5 Hippo signaling pathway elements regulate primordium size

Cell proliferation and its regulation is critical during organogenesis; failure to tightly control cell renewal can lead to organ overgrowth and tumor formation. In the past two decades, the Hippo signaling pathway emerged as a major regulator of organ size during development and homeostasis (Yu and Guan, 2013). Hippo signaling promotes cell death and differentiation and inhibits proliferation in various species ranging from *Drosophila* to vertebrates (Lu et al., 2010; Pan, 2007). Upon increase in cell density, the canonical Hippo pathway is activated and its effectors YAP1 (Yes-associated protein 1) and TAZ (transcriptional co-activator with a PDZ domain) are phosphorylated by a cascade of kinases thereby promoting their cytoplasmic retention and/or degradation (Yu and Guan, 2013). However, when the Hippo pathway is inhibited, YAP/TAZ can translocate into the nucleus where they promote cell proliferation, survival, differentiation, tissue regeneration and organ size determination (Figure 1-2X; (Barry and Camargo, 2013; Bossuyt et al., 2014; Yu and Guan, 2013; Zhao et al., 2011b)). Recent studies showed that in addition to cell density, YAP/TAZ responds to cell shape changes, which is independent of canonical Hippo cascade but rather regulated through cell-cell junction associated proteins, such as Motin family (Yu and Guan, 2013; Zhao et al., 2011a). Motin proteins mediate an increase in cell surface tension by inducing cytoplasmic retention of YAP/TAZ similar to, but independent of the canonical Hippo pathway (Agarwala et al., 2015).

In the posterior lateral line, loss of the Motin protein Angiomotin-like 2a (Amotl2a; Figure 1-1I) function results in cell overproliferation and significant increase in primordium size, which is rescued back to the wildtype level by inhibition of Yap1 (Figure 1-1I; (Agarwala

et al., 2015)). Interestingly, an additional factor which mediates hyperplasia in *amotl2a* mutant primordia is a Wnt/β-catenin effector gene *lef1*. Inhibition of *lef1* in the *amotl2a* deficient embryos also restores the primordia cell number (Agarwala et al., 2015). Altogether, these results demonstrate that Amotl2a regulates primordium cell renewal by repressing both, Yap1 and Lef1 proliferation-promoting activities. However, unlike the profound effect on primordium size neither Amotl2a or Yap1 regulate neuromast size (Agarwala et al., 2015).

1.4 Epithelial apical junctional complex and tissue remodeling

The epithelial apical junctional complex (AJC) is located at the apex of the lateral membrane of polarized epithelial cells (Figure 1-3A) and is a key regulator of multiple cellular functions, such as cell-cell adhesion, integrity of epithelial barrier, contractile forces during morphogenesis and wound healing (Rodriguez-Boulan and Macara, 2014). Also, AJC is a hub for signaling pathways controlling cell proliferation, cell differentiation and cell polarity (Knust and Bossinger, 2002). Using electron microscopy (EM), the organization of AJC revealed two structures: the zonula occludens (tight junction, TJ) and the zonula adherens (adherens junction, AJ) (Farquhar and Palade, 1963). The tight junction is defined by location of the Claudin and Occludin family proteins whereas Cadherins are located at the adherens junction (Knust and Bossinger, 2002; Nelson, 2003; Tsukita et al., 2001). Claudins and Cadherins interact homophilically with the same family of proteins on the neighboring cell to form AJC structure (Takai and Nakanishi, 2003; Vogelmann and Nelson, 2005).

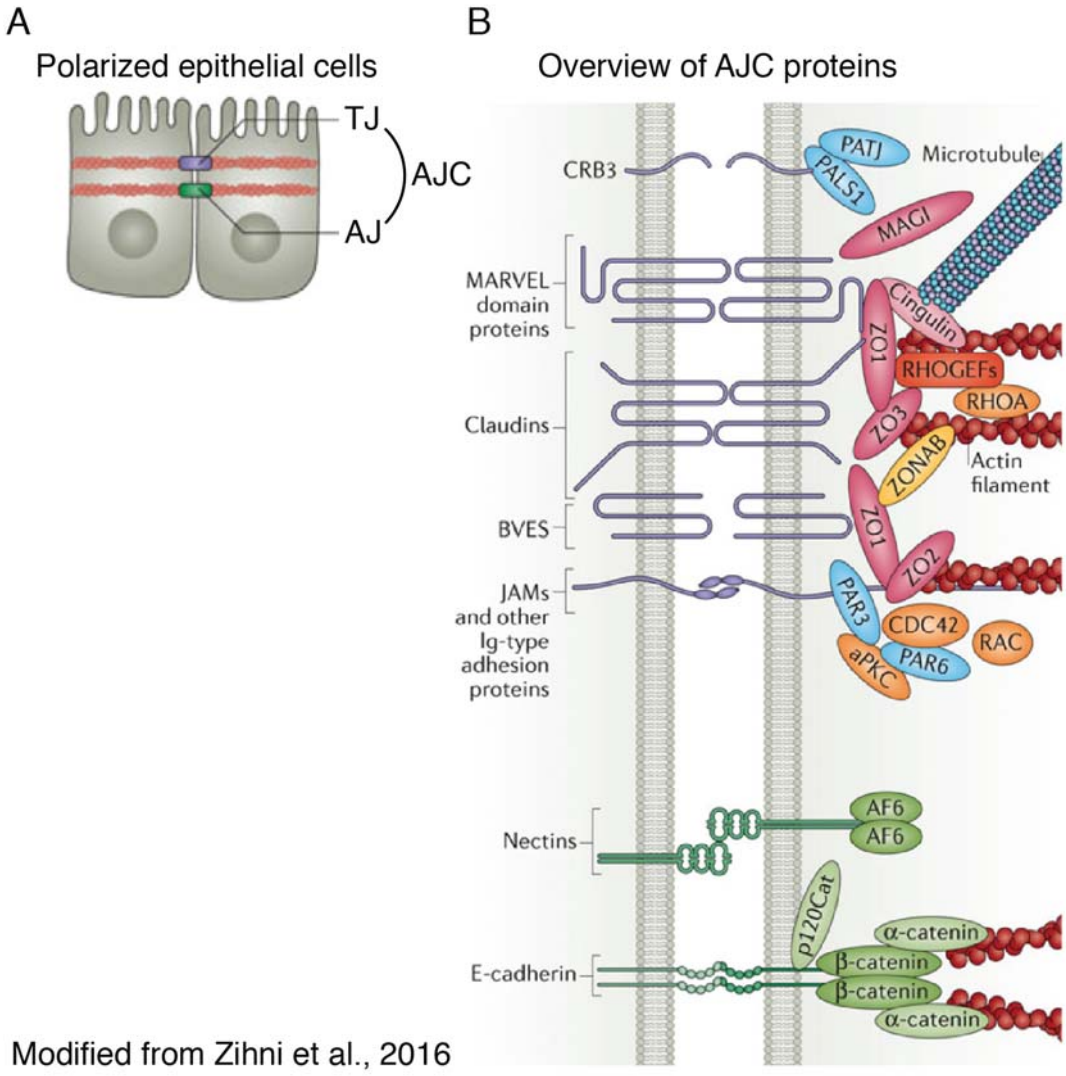

Figure 1-3. The epithelial apical junctional complex (AJC)
(A) Tight junctions (TJ) (purple) are apically located in the polarized epithelial cells. The adherens junctions (AJ) (green) form just below the TJ. The actin belt (pink) encircles the individual cells. (B) Brief overview of the types of AJC proteins with only representatives of the main groups shown (Zihni et al., 2016).

Cadherins and Claudins as well as other transmembrane proteins of the AJC are linked to scaffolding proteins (Catenins and PDZ domain-containing proteins) which connect them to the actin cytoskeleton and thereby all actin-associated proteins (Anderson et al., 2004; Nelson, 2003; Takai and Nakanishi, 2003; Tsukita et al., 2001). In addition, each of these scaffolding proteins have binding motifs that link together different AJC subcomplexes into higher order protein complexes (Vogelmann and Nelson, 2005). Tight junctions hold cells together, block the passage of ions and molecules between neighboring

cells and inhibit transportation of integral membrane proteins between apical and basal surfaces in the cell (Gonzalez-Mariscal et al., 2003). Cadherins accumulate along the actin belt and form AJs with the neighboring cell (Figure 1-2A,A'; (Nagafuchi and Takeichi, 1988)). The actin belt is critical for tissue integrity and it organizes itself when F-actin bundle encircles the individual cells (Figure 1-3A; (Takeichi, 2014)). In mature epithelial sheets, the bundle of F-actin stretches parallel to the cell borders. At cell-cell boundaries, Cadherins interact through their amino-terminal EC1 domains homophilicaly, which results in an adhesive dimer that produces a primary force that attaches cells together (Nagafuchi and Takeichi, 1988). Inside the cell, Cadherins bind to Catenins, forming the cadherin-catenin complex that firmly 'zips up' plasma membranes (Hirano et al., 1992).

Another important function regulated by the AJC is the establishment of an apically localized actin meshwork that constricts and leads to tissue remodeling, such as multicellular rosette formation (discussed above). E-cadherin, which constitutes the AJ, acts as a scaffold for cytoskeleton-associated protein complexes, such as N-WASP (neural Wiscott-Aldrich Syndrome protein) and Arp2/3 that regulate de novo actin filament polymerization at the cell junctions (Ehrlich et al., 2002; Kovacs, 2003). The Arp2/3 complex gives rise to an extensive network of branched actin filaments. In addition, N-WASP promotes actin filament incorporation into the apical actin belt that supports AJ integrity (Kovacs et al., 2011). Besides the function of TJ in cell barrier maintenance, it is also structurally and functionally linked to actin cytoskeleton, mainly through ZO, occludin and cingulin proteins (Figure 1-3B; (D'atri and Citi, 2001; Fanning et al., 1998; Wittchen et al., 1999)). Depletion of ZO-1 and ZO-2 proteins lead to a dramatic expansion of the AJ associated actin belt and destabilized TJ formation (Fanning et al., 2012). Occludin is a membrane protein that directly interacts with ZO proteins and attaches them to the cell membrane (Feldman et al., 2005). Cingulin, localizes at TJ and is an actin cross-linking

protein that also binds myosin and regulates actin-bundling, which provides structural support to F-actin meshwork (D'atri and Citi, 2001). In summary, the AJC is a critical site that anchors and organizes F-actin and other cytoskeletal filaments, through specific adaptor and regulatory proteins (Citi et al., 2014).

Cell junction proteins and cell polarity determinants act together whereby the same proteins that control polarity dictate the location of AJC. The establishment of cell polarity is initiated by an extracellular cue, such as cell signaling or cell-cell contact that creates asymmetry in the cell membrane (Bryant and Mostov, 2008; Mellman and Nelson, 2008). This asymmetry triggers the formation of polarity complexes that promote the establishment of distinct apical and basolateral membrane domains (Figure 1-3B). For instance, the Crumbs and Par complexes (composed of Par-6, Par-3 and atypical protein kinase C (aPKC)) are localized to the apical side of the AJC and are required for its formation. However, in return, TJ components, such as Junctional adhesion molecules (JAMs), contribute to cell polarity by interacting with Par3/Par6/aPKC complexes, thereby maintaining these proteins within the apical domain and ensuring correct AJC establishment (Ebnet et al., 2004). Another important component acting below the AJC is the Scribble complex (Scrib, Dlg and Lgl) that modulates the expansion of the basolateral membrane domain (Bilder and Perrimon, 2000). This assymetric distribution of polarity and AJC proteins facilitates the maintenance of polarized state in the cell required for it to function and integrate into the tissue.

Chapter 2

Constitutive activation of Notch or Wnt/β-catenin induces larger lateral line organs

2.1 Introduction

2.1.1 Strategies for Notch and Wnt/β-catenin manipulations in the zebrafish embryo

To investigate Notch signaling function in zebrafish posterior lateral line development we used two genetic systems. For Notch gain-of-function analyses, embryos were obtained from a mating between *Tg(cldnB:lynGFP);Tg(cldnB:gal4)* and *Tg(UAS:myc-Notch1a-intra)* carriers (Scheer et al., 2002). Notch1aICD (ICD, intra-cellular domain) expression is induced by Gal4 protein binding to the UAS:NICD effector. The promoter for the tight junction protein ClaudinB, which is highly expressed in the lateral line and the skin, is driving Gal4 activation. Thus, NICD overexpression is specific to ClaudinB positive cells. The NICD transgene is myc-tagged and antibody staining against c-Myc confirms widespread expression in the lateral line and the skin of the embryo (Figure 2-1C,D). Notch target gene *her4* expression is elevated in the NICD embryos at 13 hpf, showing that expression is induced at a time-point when lateral line is starting to form (Appendix Figure 1).

To investigate the Notch-loss-of function phenotype we used the *mind bomb 1* (*mib1*^{ta52b}) mutant (Itoh et al., 2003; Matsuda and Chitnis, 2010). Mib is a RING ubiquitin ligase, which interacts with the intracellular domain of the Notch ligand Delta to promote its ubiqutinilation and internalization (Itoh and Chitnis, 2001). When Mib is absent, Notch signaling cannot be efficiently activated. Specifically, Mib is required for Delta endocytosis and Notch extracellular domain (NECD) transendocytosis in the signaling cell, which is an

inductive signal for Notch intracellular domain (NICD) propagation in the receiving cell and consequent Notch activation ((Itoh et al., 2003); see Chapter 1).

In addition, we also used pharmacological Notch signaling inhibitors, such as γ-secretase inhibitors DAPT or LY411575. These drugs directly interfere with the cleavage of the NICD receptor and prevent its propogation into the cell nucleus (Olsauskas-Kuprys et al., 2013).

To study the role of Wnt/β-catenin signaling in posterior lateral line formation and development we used a recessive zebrafish mutation in *apc (adenomatous polyposis coli)* (*apc*^{mcr}) (Aman and Piotrowski, 2008; Hurlstone et al., 2003). APC is a scaffolding protein known to inhibit Wnt/β-catenin signaling by being a part of a destruction complex that targets β-catenin to proteosomes in the absence of active Wnt resultin in increased Wnt signaling (Bienz, 2002; Rubinfeld et al., 1996). We performed additional Wnt overexpression experiments by using the GSK3-β inhibitor BIO, which, similarly to *apc* mutants, impedes the β-catenin destruction in the cell (Tseng et al., 2006). Conversely, to reduce Wnt/β-catenin signaling, we overexpressed the Wnt inhibitor *dkk1b* by using a heat-shock inducible transgenic line (Tg(*hs:dkk1b*);(Stoick-Cooper et al., 2007)). Dkk1 is a diffusible inhibitor of Wnt/β-catenin pathway acting upstream of β-catenin and is activated by the Fgf signaling in the trailing domain of the primordium (Aman and Piotrowski, 2008; Niehrs, 2006).

2.2 Results

2.2.1 Constitutive activation of Notch or Wnt regulates posterior lateral line organ size

The constitutive activation of Notch intracellular domain (NICD) in the lateral line greatly increases neuromast size compared to siblings (Figure 2-1A-B', Figure 2-2A,A'). The increase in neuromast size also occurs in Wnt overexpressing *apc* mutants (Figure 2-1F-F';(Wada et al., 2013)). In contrast, a reduction of Notch in *mib1* mutants leads to

fragmentation of the primordium and deposited neuromasts (Figure 2-1E-E';(Matsuda and Chitnis,2010)).

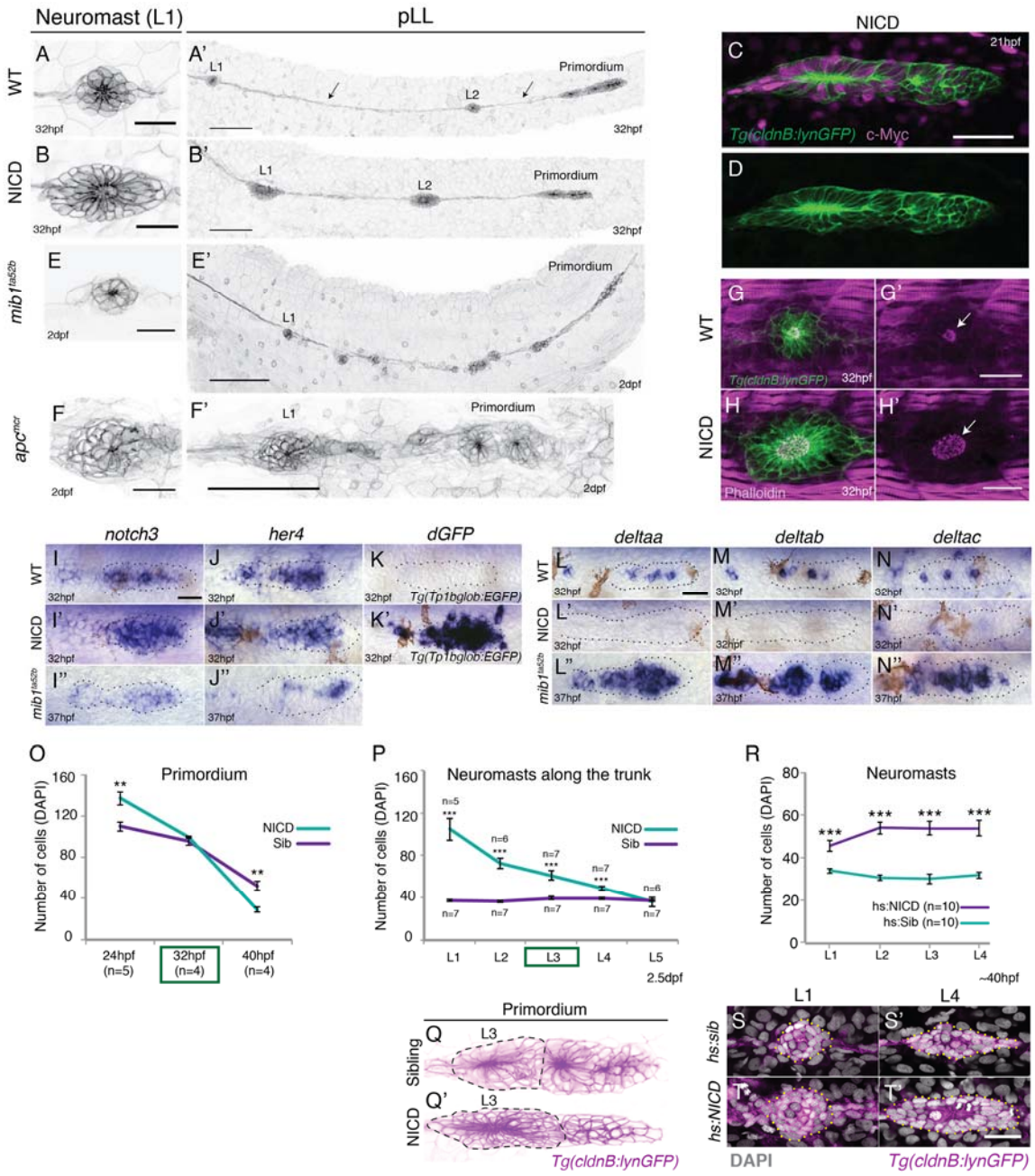

Figure 2-1. Induction of Notch signaling increases lateral line organ size

(A and B and E and F) First deposited trunk neuromasts (L1) in *Tg(cldnB:lynGFP).* (B) NICD and (F) *apc*^{mcr} neuromasts are larger than (A) WT and (E) *mib1*^{ta52b} neuromasts. Scale bar is 25µm. (A' and B' and E' and F') Posterior lateral line in *Tg(cldnB:lynGFP).* (A') WT, (B') NICD, (E') *mib1*^{ta52b} and (F') *apc*^{mcr}. Scale bar is 100µm. (C and D) NICD transgenic embryos are labeled by a Myc-tag. The c-Myc antibody in magenta. Scale bar is 50µm. (G-H') L1 neuromasts stained with Phalloidin at 32hpf. In NICD neuromasts (H and H') the apical F-actin meshwork (arrow) is larger compared to wildtype (WT) (G and G'), suggesting that NICD neuromasts are composed of more apically constricted cells. Scale bar is 25µm. (I-N'') Expression of Notch pathway genes in the primordium.

(I') *notch3*, (J') *her4* and *dgfp* in the Notch reporter *Tg(Tp1bglob:EGFP)* (K') are upregulated in NICD primordia compared to WT (I and J and K) and *mib1*^{ta52b} (I'' and J'') primordia. The Notch reporter only seems to be activated by high levels of Notch signaling, as it is not active in wildtype primordia (K), even though the Notch target *her4* is expressed (J). Scale bar is 25µm. (L-N'') Expression of *delta* ligands in the primordium. (L') *deltaa*, (M') *deltab* and *deltac* (N') are largely downregulated in NICD compared to WT (L and M and N) and *mib1*^{ta52b} (L'' and M'' and N'') primordia. Scale bar is 25µm. (O) NICD and sibling primordia sizes decrease overtime. NICD primordia start out (24hpf) with significantly more cells compared to sibling primordia, but after the second deposition cycle at ~32hpf NICD and sibling primordia have a similar amount of cells. By 40hpf NICD primordia are composed of significantly less cells. Error bars represent standard error (p<0.01=** Student's *t* test). (P) NICD neuromasts (L1-5) along the trunk of the embryo at 2.5dpf consist of significantly more cells compared to siblings. NICD primordia deposit big neuromasts, even at 32hpf when NICD and sibling primordia possess the same cell number (time point (32hpf) is marked in the (O) green box). (Q, Q') NICD primordium forms larger L3 proneuromast (Q'). Error bars indicate standard error (p<0.001=*** Student's *t* test). (R-T') Notch activation in *hs:NICD* embryos after the primordium and ganglion have separated still significantly increases neuromast sizes (R, T') compared to a (S') sibling. These results indicate that the number of cells in neuromasts is independent of primordium size. Notch overexpression was induced by a 39°C heat-shock for 45min starting at 25hpf (L1 was still a part of the primordium). Embryos were fixed after L4, L5 deposition (~40hpf). Error bars indicate standard error (p<0.001=*** Student's *t* test). Scale bar is 25µm. This figure is modified from Kozlovskaja-Gumbrienė et al. (2017).

The analysis of filamentous actin (F-actin) composition in the first trunk neuromast (L1) by phalloidin staining suggested that NICD neuromasts are composed of many more apically constricted cells compared to siblings (Figure 2-1G-H'). NICD induction was evidenced by strong expression of Notch targets *notch3*, *her4* and activation of Notch signaling reporter- *Tp1bglob:EGFP* in the primordium (Figure 2-1I-K'). On the other hand, *delta* ligands are absent from NICD primordia (Figure 2-1L-N'). To the contrary, *mib1* mutant primordia lack strong *notch3* and *her4* expression, but have abundant *delta* ligand expression (Figure 2-1I'',J'' and L''-N'';(Matsuda and Chitnis, 2010)). Additionally, NICD primordia migrate more slowly, deposit less neuromasts and by two days only 20% of primordia reach the tail tip (Figure 2-2A-C). NICD primordia form and deposit enlarged neuromasts, which results in a prominent depletion of primordia cells prior to depositing the terminal clusters (Figure 2-1O).

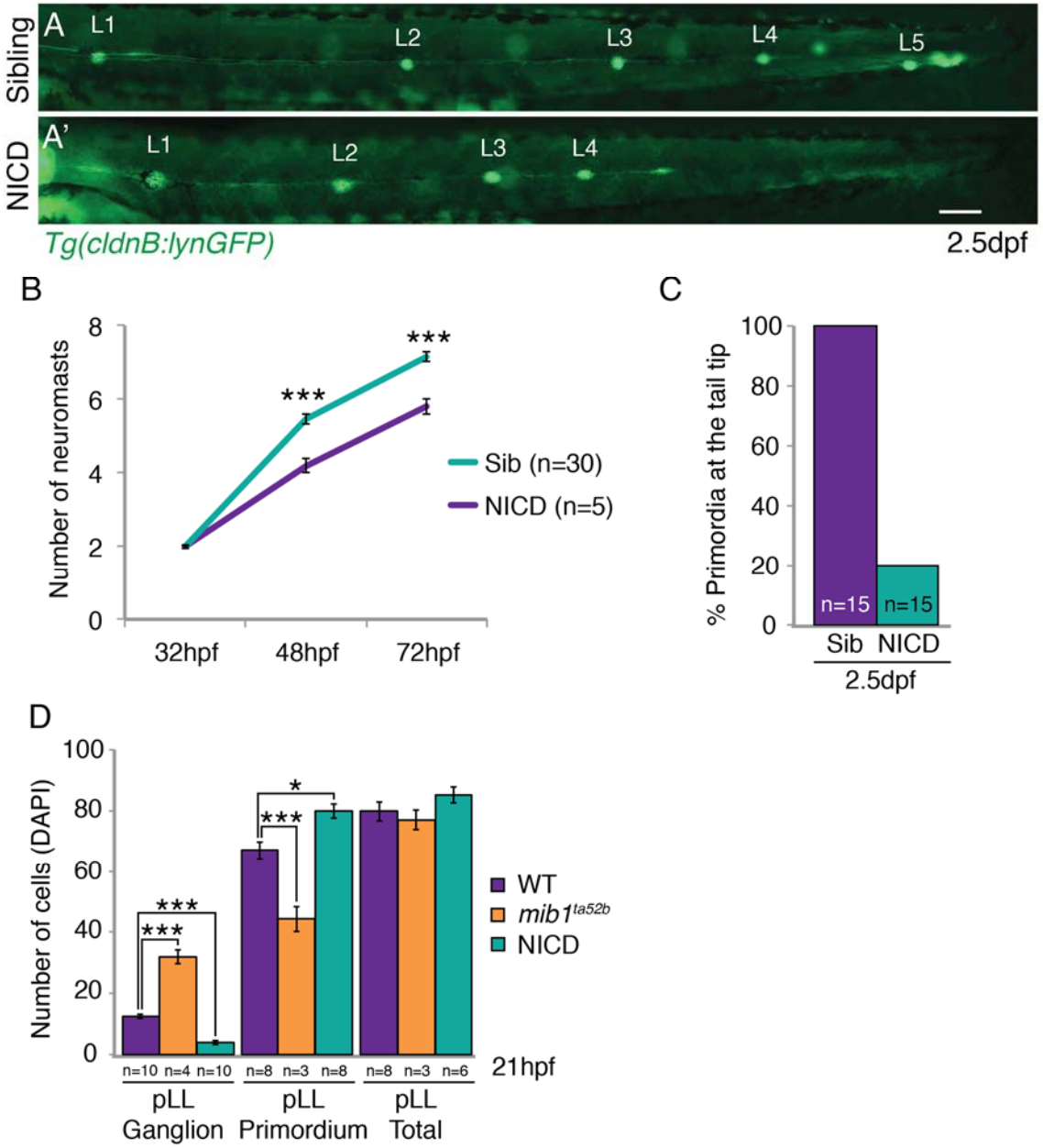

Figure 2-2. NICD primordia do not migrate to the tail tip and deposit fewer neuromasts
(A and A') posterior lateral line in 2.5dpf *Tg(cldnB:lynGFP)* larvae. Scale bar is 100µm. (A' and B) NICD primordia deposit fewer neuromasts. Error bars represent standard error ($p<0.001$=*** Student's *t* test). (C) 80% of NICD primordia stall and fail to reach the tail tip. (D) Notch signaling regulates posterior lateral line primordium fate versus ganglion fate (also in (Mizoguchi et al., 2011)). The NICD posterior lateral line (pLL) primordium has significantly more cells compared to wildtype at the expense of ganglion cells. In contrast, in *mib1*^{ta52b} mutants more cells are specified towards the ganglion fate and less cells contribute to the primordium. Error bars represent one-way ANOVA with Tukey pairwise comparison test ($p<0.05$=*, $p<0.001$=***). This figure is modified from Kozlovskaja-Gumbrienė et al. (2017).

In the developing lateral line placode Notch signaling regulates primordium and posterior lateral line ganglion segregation (Mizoguchi et al., 2011). Specifically, Notch

conditions more cells towards the primordium fate at the expense of the number of ganglion cells (Figure 2-2D;(Mizoguchi et al., 2011)). Consequently, the initial increase in the number of primordium cells could regulate neuromast enlargement in NICD embryos (Figure 2-1O). To test this hypothesis, we first calculated the number of cells in the primordium at different time-points during its development. Although, NICD neuromast and primordium sizes are initially larger than in the sibling (at 24 hpf), they progressively decrease along the trunk of the embryo. At 32 hpf when sibling and NICD primordia are not significantly different in size, NICD L3 neuromasts are still larger than their sibling counterparts (Figure 2-1O,P-Q'). Second, we heat-shock activated Notch in the lateral line after ganglion and primordium separation and observed an increase in neuromast size (Figure 2-1R-T'). These results demonstrate that although the primordium size is limiting the pool of available cells for proneuromast generation, it is not directly regulating the forming neuromast size.

2.2.2 Notch and Wnt/β-catenin regulate neuromast size independent of yap1

Organ size regulation in many tissues has been attributed to the Hippo pathway (see Chapter 1). It was shown that some known Hippo pathway genes, such as Hippo regulator *amotl2a* (a tight junction-associated scaffolding protein) and transcriptional effector *yap1* are controling posterior lateral line primordium size. Specifically, in *amotl2a* mutants primordium cells overproliferate, which causes a significant increase in primordium cell number. The effect of *amotl2a* loss can be reverted by the simultaneous *yap1* function disruption (Agarwala et al., 2015). These results strongly argue for the Hippo signaling involvement in posterior lateral line organ size regulation. Therefore, to test if Hippo is regulating larger neuromast formation in NICD and *apc* mutants we tested Hippo gene expression in Notch and Wnt perturbations, as well as the effect of *yap1* loss in NICD and

apc backgrounds. *yap1* is expressed in the leading 2/3 of the wildtype primordium (Figure 2-3A') and upregulated in the NICD primordia as well as in the *apc* primordia where it correlates with the observed increase in cell proliferation ((Aman et al., 2011); Figure 2-3B',D'). Consistently, *yap1* is downregulated in *mib1* and in Wnt depleted *hs:dkk1* primordia (Figure 2-3C',E'). However, *yap1* is not expressed in deposited wildtype, NICD, *mib1*, *apc* or *hs:dkk1* neuromasts, suggesting that proliferation regulation cannot be attributed to Yap1 function in the forming lateral line organs (Figure 2-3A-E). We also analyzed the expression of the canonical Hippo pathway inhibitor *stk3* (the ortholog of *hippo* kinase in *Drosophila*) in the posterior lateral line organs. *stk3* is downregulated both in NICD neuromasts and the primordia, with some expression remaining in the most central cells (Figure 2-4A-B'). Contrary, *stk3* is greatly upregulated in *mib1* primordium and the neuromast (Figure 2-4C,C'). Surprisingly, the *stk3* expression is positively regulated by Wnt, as it is higher in *apc* mutants and downregulated in *hs:dkk1b* primordia and neuromasts compared to the wildtype situation (Figure 2-4D-E'), suggesting that canonical Hippo signaling is activated differently by Notch and Wnt perturbations. We also tested *amotl2a* expression and again the highly proliferative *apc* primordia shows increased expression in the neuromast and primordia (Figure 2-4F,F' and Figure 2-4I,I'), whereas, *amotl2a* is abrogated in the *hs:dkk1b* lateral line organs (Figure 2-4J,J'). On the other hand, NICD largely inhibits *amotl2a*, but it is not changed in the *mib1* background (Figure 2-4G,G' and Figure 2-4H,H'). These data suggest that the expression of Hippo signaling genes does not always match the proliferative status of lateral line organs in different Wnt or Notch manipulations, which indicates that functions of these genes remain to be investigated in the future.

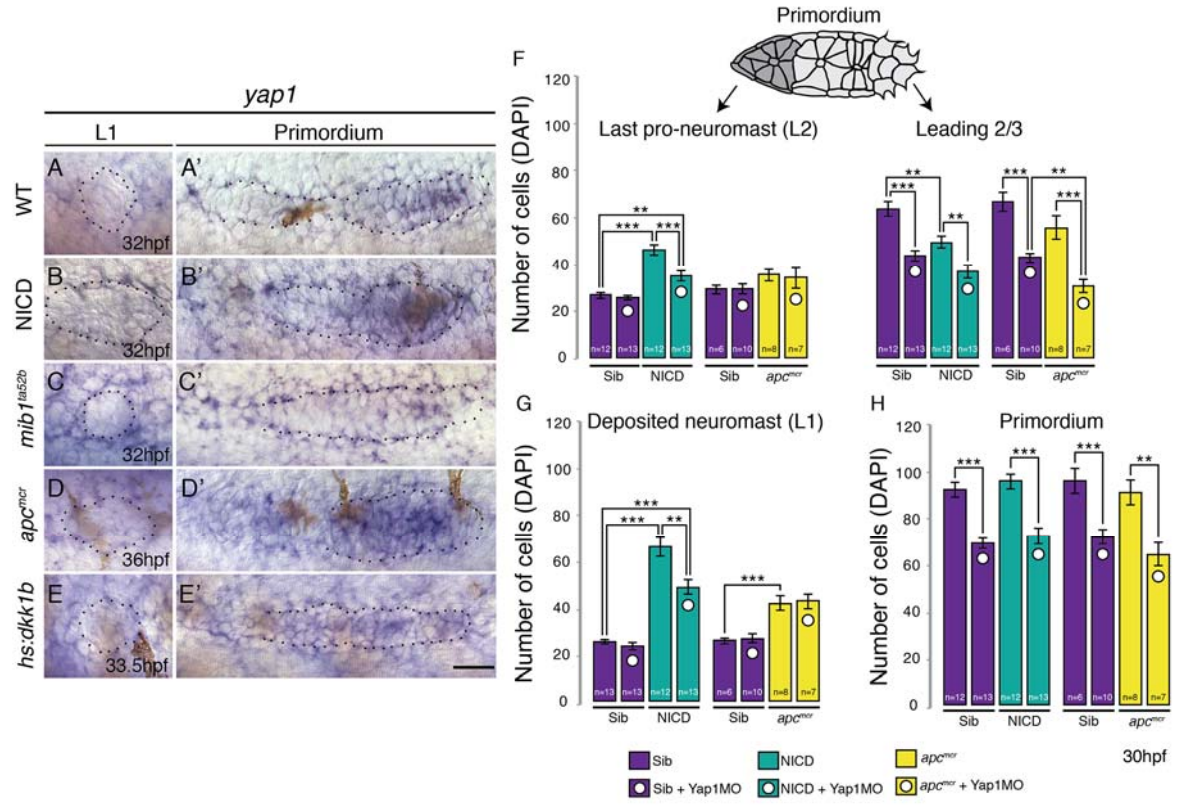

Figure 2-3. The Hippo pathway member *yap1* regulates primordium size but not neuromast size

(A-E) *yap1* is not expressed in WT neuromasts (A) or neuromasts in which Notch (B and C) or Wnt signaling (D and E) are manipulated. (A'-E') *yap1* is upregulated in the primordium after (B') Notch and (D') Wnt overexpression compared to (A') wildtype siblings and Wnt downregulation (E'). (C') Notch loss in *mib1*^{ta52b} mutants leads to downregulation of *yap1*. (F) Loss of *yap1* by morpholino injections significantly reduces the number of cells in the leading 2/3 of WT, NICD and *apc*^{mcr} primordia, as well as the overall primordium size (H). (G) Notch and Wnt signaling significantly increases the number of cells in deposited L1 neuromasts, which is not rescued to a wildtype level by *yap1* morpholino injections. Even though the size of NICD L1 and L2 pro-neuromasts is significantly reduced in *yap1* morphants, they are still significantly larger than the corresponding WT neuromasts (F and G). Error bars represent standard error from one independent experiment ($p<0.05$=*, $p<0.01$=**, $p<0.001$=*** Student's *t* test). Scale bar is 25µm. This figure is reprinted from Kozlovskaja-Gumbrienė et al. (2017).

However, the *yap1* upregulation in the primordia is consistent with an increased cell number in NICD and *apc* neuromasts. Importantly, *yap1* morpholino knockdown rescues the overproliferation phenotype in *amotl2a* mutant primordia (Agarwala et al., 2015). We therefore tested the effect of *yap1* loss on NICD and *apc* lateral line organ size. The cell number is significantly decreased in the *yap1* expression domain of the NICD and *apc*

primordia when *yap1* morpholino is introduced, similar to what is shown in the wildtype primordia (Figure 2-3F;(Agarwala et al., 2015)). We also injected *yap1* morpholino into homozygous *p53* mutant embryos to test for toxicity (Aman et al., 2011). Our results show similar decrease in the primordium cell number from aproximatelly 100 to 80 cells as in the wildtype embryos (Figure 2-4K, Figure 2-3F), suggesting that decrease in cell number is not caused by morpholino-induced *p53* activation (Kok et al., 2015). Even though the primordium size is significantly decreased in the morphant embryos, the neuromast cell number is not rescued to a wildtype level in NICD or *apc* L1 and soon-to-be deposited L2 neuromasts (Figure 2-3F,G). The reduction in NICD neuromast size in the *yap1* morphants may be a result of primordium size decrease, since primordium size limits the number of cells available for allocation into the neuromast (Figure 2-1O,P). To conclude, the above experiments demonstrate that the increase in NICD and *apc* neuromast size is not regulated by *yap1* function.

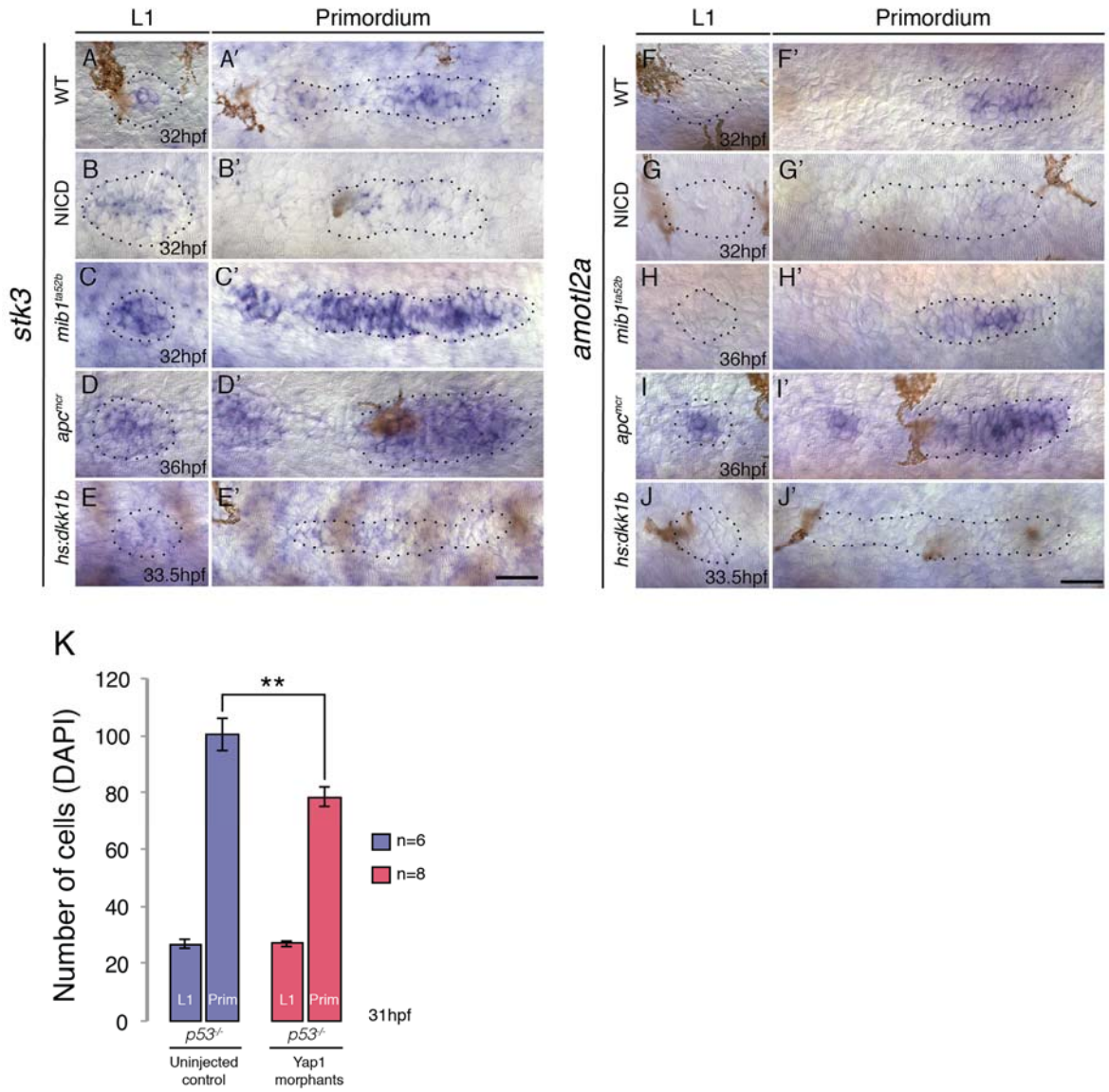

Figure 2-4. Hippo signaling components in the lateral line

(A-A') In the wildtype lateral line the canonical Hippo pathway inhibitor *stk3* (the ortholog of *hippo* kinase in Drosophila) is expressed in central cells of the primordium, as well as in central cells of deposited neuromasts. (B-B') *stk3* is downregulated in NICD and *hs:dkk1b* (E-E') primordia and neuromasts. (C-C') *stk3* is strongly upregulated in *mib1*^{ta52b} and *apc*^{mcr} (D and D') neuromasts and primordia. This suggests that the activation status of canonical Hippo pathway is different in NICD and *apc* mutants. (F) *amotl2a*, which inhibits Wnt-induced proliferation is not expressed in the deposited neuromast, but in the central region of the wildtype primordium (F'). (G and G') *amotl2a* expression is downregulated in NICD primordia and in *hs:dkk1b* primordia where Wnt signaling is disrupted (J and J'). (H and H') *amotl2a* expression is not affected in the *mib1*^{ta52b} primordium, whereas it is induced after Wnt upregulation (I and I'), even though proliferation is reduced *hs:dkk1b embryos* and upregulated in *apc* mutants. Scale bars are 25µm. (K) *yap1* morpholino injections do not affect primordium size via the activation of *p53*. Injection of *yap1* morpholino into *p53* homozygous embryos still leads to a significant reduction in primordium cell number. Error bar represents standard error from four independent experiments ($p<0.01$=** Student's *t* test). This figure is reprinted from Kozlovskaja-Gumbrienė et al. (2017).

2.2.3 Notch regulates organ size independent of proliferation unlike Wnt/β-catenin

Wnt activation causes neuromast growth through increased cell renewal, therefore we wanted to test if proliferation is also driving NICD neuromast growth independent of *yap1* function (Wada et al., 2013). Interestigly, in contrast to overproliferating *apc* neuromasts, the NICD neuromasts are almost absent of dividing cells (Figure 2-5A-D). Accordingly, *apc* neuromasts grow significantly between 32-56 hpf, while NICD neuromast size remains similar over the same period (Figure 2-5E). The BrdU index, which shows the number of cells in the S-phase, is not significantly changed in *apc* primordia at 31 hpf, or in NICD primordia at 35 hpf (Figure 2-5F-H). Accordingly, the number of cells in the *apc* and NICD primordia is not different from the wildtype siblings (Figure 2-5I).

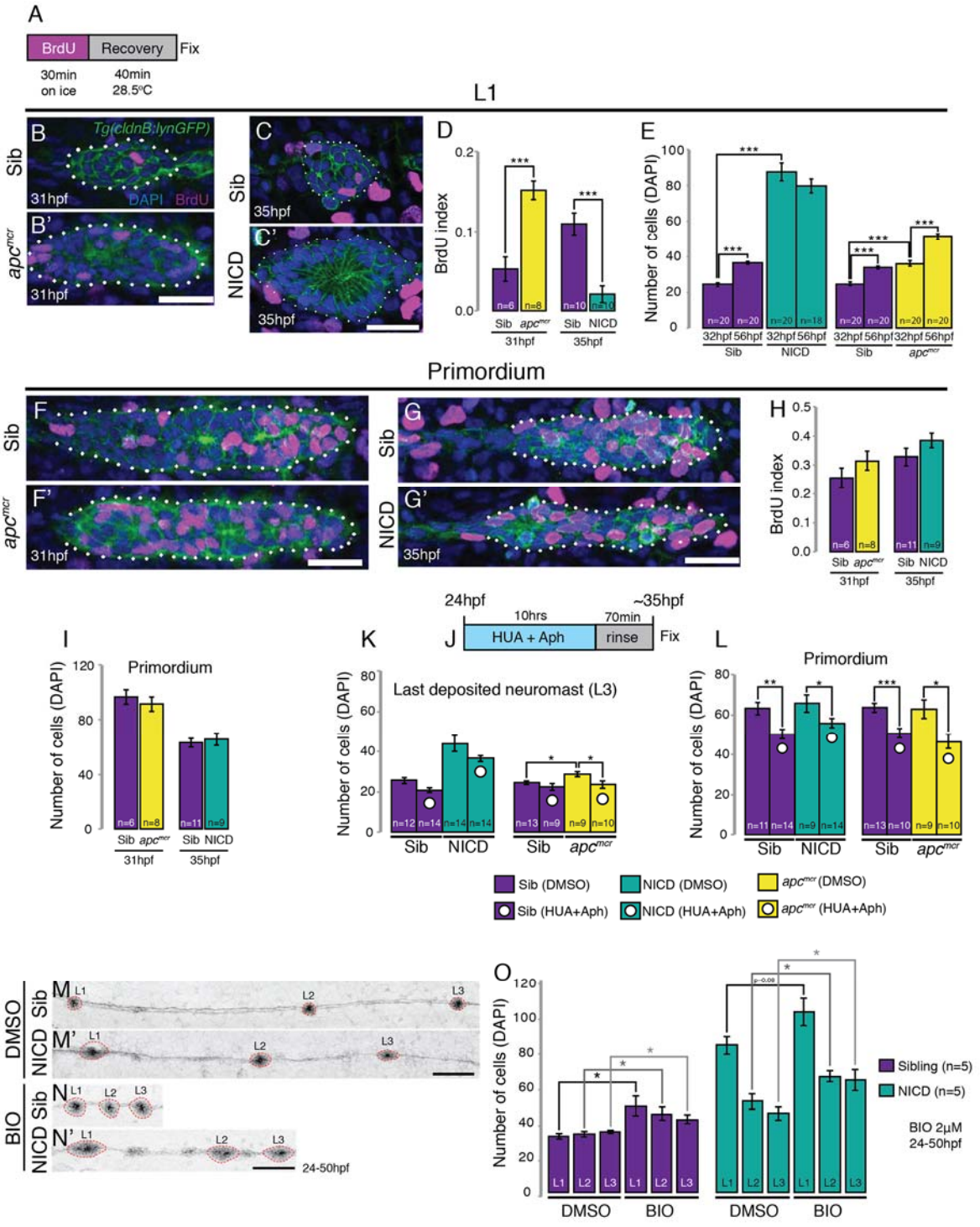

Figure 2-5. Proliferation is not responsible for large neuromasts in NICD embryos
(A) BrdU treatment strategy. (B-C') Representative images of BrdU-positive nuclei in L1 *apc*^{mcr} (B') and NICD neuromasts (C'). (B and B' and D) The BrdU index is increased in *apc*^{mcr} L1 neuromasts and significantly reduced in NICD L1 neuromasts (C and C' and D). (E) Nevertheless, the number of cells is significantly higher in the *apc*^{mcr} and NICD L1 neuromasts. While the *apc*^{mcr} neuromast grows overtime, the NICD neuromast size does not significantly change from 32hpf to 56hpf.

(F-G') Representative images of BrdU positive nuclei in *apc*^{mcr} (F') and (G') NICD primordia. (F-H) There is no significant difference in the BrdU index (H) or the number of cells (I) between sibling and *apc*^{mcr} or sibling and NICD primordia. (J) Hydroxyurea and aphidicolin treatment strategy. (K) Cell cycle inhibition with hydroxyurea and aphidicolin significantly reduces the number of DAPI- positive cells in the last deposited neuromasts in *apc*^{mcr} embryos. There is no significant reduction in sibling or NICD neuromast sizes after cell cycle inhibition. (L) Cell cycle inhibition significantly reduces the number of cells in sibling, *apc*^{mcr} and NICD primordia. Scale bars are 25µm. Treatment of sibling and NICD embryos with the GSK3β inhibitor BIO causes significant enlargement of neuromasts (L1-3). Scale bar is 100µm. Error bars represent standard error from one independent experiment ($p<0.05$=*, $p<0.01$=**, $p<0.001$=*** Student's *t* test). This figure is reprinted from Kozlovskaja-Gumbrienė et al. (2017).

The striking increase in BrdU index in deposited *apc* neuromasts compared to primordia suggests that in these mutant neuromasts grow only after the deposition, whereas, formation of enlarged NICD neuromasts is regulated within the primordium by a proliferation independent mechanism. We soaked embryos in the DNA replication inhibitors, hydroxyurea and aphidicolin (HUA and Aph) to verify cell proliferation contribution during proneuromast formation process (Figure 2-5J-L). Indeed, the last deposited NICD neuromast size is not significantly affected even though primordium cell number is largely decreased after the drug treatment. On the other hand, HUA and Aph application rescues *apc* neuromast size to a wildtype level, also it reduces primordium cell number (Figure 2-5K-L). To verify that Notch and Wnt are regulating neuromast size by independent mechanisms we applied pharmacological Wnt activator BIO on NICD embryos. Indeed, even larger neuromasts were formed upon the induction of Wnt in NICD embryos, suggesting an additive effect of Wnt and Notch signaling (Figure 2-5M-O). To conclude, Wnt regulates neuromast size by proliferation in deposited neuromasts, while the effect of Notch is intrinsinc to the primordium and independent of cell proliferation.

2.2.4 Notch regulates organ size independent of a cell fate function

As we already established that cell proliferation does not regulate neuromast size in NICD embryos, we next wanted to test if another well known function of Notch- cell fate

specification could govern lateral line organ size. We analysed in detail the number of four different cell types present in NICD and sibling lateral line primordium: 1) mesenchymal, unpatterned cells in the leading domain, 2) hair cell progenitors, 3) support cells and 4) interneuromast cell (INC) progenitors that are deposited in between neuromasts (Figure 2-1A',arrows).

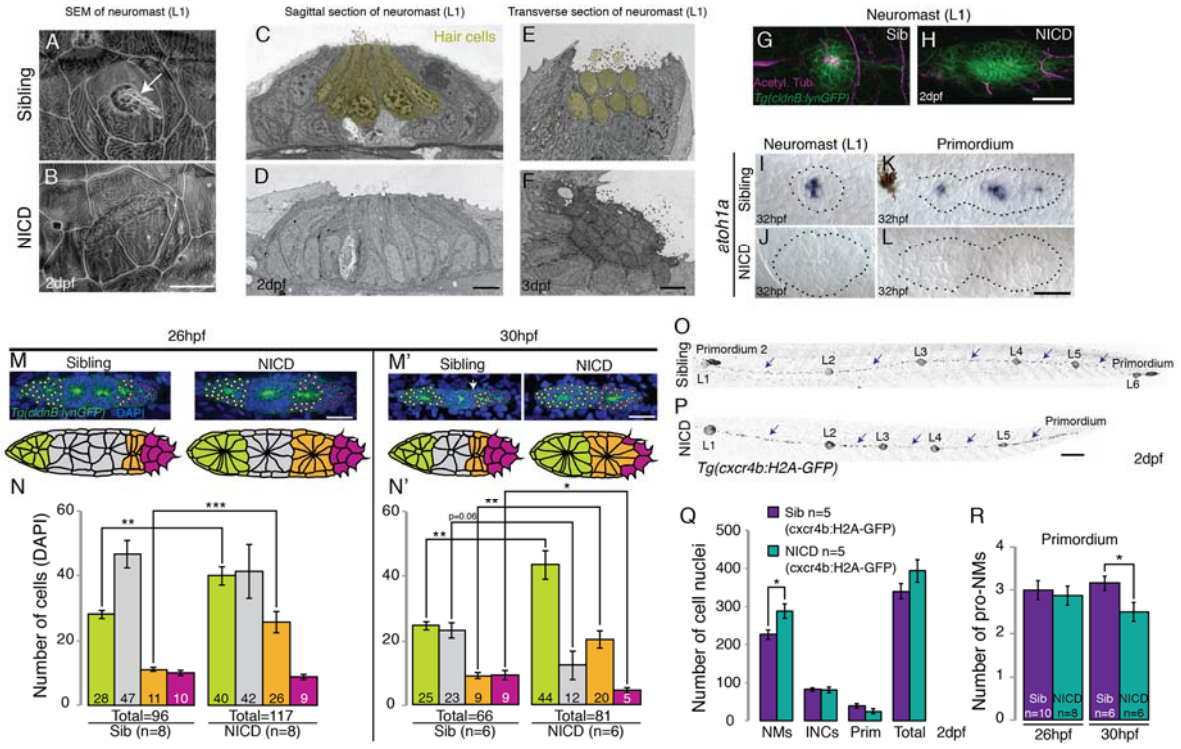

Figure 2-6. NICD neuromasts are not larger because of a switch in cell fate.
Scanning electron micrograph of a 2dpf sibling (A) and NICD neuromast (B) shows that no hair cells (white arrow in WT) are present in the NICD neuromast. Scale bar is 10μm. (C-F) Transmission electron sections though sibling (C,E) and NICD neuromasts (D,F). (C,E) Hair cells are false colored in yellow. (D,F) No hair cells are present in NICD neuromasts. (C-F) Scale bars are 5μm. (G and H) Acetylated tubulin antibody stains hair cells in a sibling neuromast (G), but staining is absent in a NICD neuromast (H). (G and H) Scale bar is 25μm. (I and L) The proneural gene *atoh1a* is not expressed in NICD neuromasts (J) and the primordium (L). (I-L) Scale bar is 25μm. (M-N') Cell number (DAPI counts) in the different parts of the primordium. Magenta indicates mesenchymal tip cells, orange indicates the first proneuromast and green indicates the about to be deposited proneuromast. The gray cells are calculated by subtracting mesenchymal, first pro-neuromast and last pro-neuromast cell numbers from the total number of cells in the primordium. (M and M') Scale bar equals 25μm. (O,P) *Tg(cxcr4b:H2A-GFP)* labels all lateral line nuclei.

(Q) NICD neuromasts consist of significantly more cells compared to sibling neuromasts, but there is no difference between the number of interneuromast cells (INCs) or the primordium cells at 2dpf. (O and P) Scale bar equals 100μm. (R) Significantly fewer proneuromasts are formed in a NICD primordium at 30hpf. Error bars represent standard error from one independent experiment ($p<0.05$=*, $p<0.01$=**, $p<0.001$=*** Student's *t* test). This figure is reprinted from Kozlovskaja-Gumbrienė et al. (2017).

In the zebrafish ear and lateral line, Delta/Notch signaling specifies sensory hair cells and support cells during development (Haddon et al., 1999; Itoh and Chitnis, 2001; Millimaki et al., 2007; Riley et al., 1999). The Notch receptor specifies support cells and the Notch inducing *deltad*- (and *atoh1a*) – expressing cells differentiate into hair cells in the center of proneuromast ((Matsuda and Chitnis, 2010); see Chapter 1). Notch signaling inhibits *atoh1a*, therefore there are no hair cells generated in the NICD primordia (Figure 2-6A-L;(Matsuda and Chitnis, 2010)). However, even within the wildtype primordium only few *atoh1a*-labeled hair cell precursors exist per proneuromast (Figure 2-6K), thus, their cell fate switch into support cells cannot account for an increase of an average of 15 or 11 cells in the first NICD proneuromast (orange, Figure 2-6M-N') and an increase of 12 to 19 cells in the last NICD proneuromast at 26 hpf and 30 hpf (green, Figure 2-6M-N'). Nevertheless, we tested if ectopic induction of hair cells could normalize NICD neuromast size. To activate hair cell production we heat-shock induced *atoh1a* using a transgenic line (Figure 2-7A-E''). Hair cell specification in *Tg(hs:atoh1a;NICD)* larvae did not alter neuromast size significantly, as NICD neuromasts with hair cells were similar in size to the regular NICD neuromasts. This suggests that NICD neuromasts are enlarged not due to a switch in cell fates. Notably, *hs:atoh1a* alone significantly increases neuromast size (Figure 2-7C'' and F, light green bar). The elevation of *her4* expression in response to *atoh1a* activation suggests that Atoh1a induces larger neuromasts possibly through activation of Notch signaling in the primordium (Figure 2-7B-E).

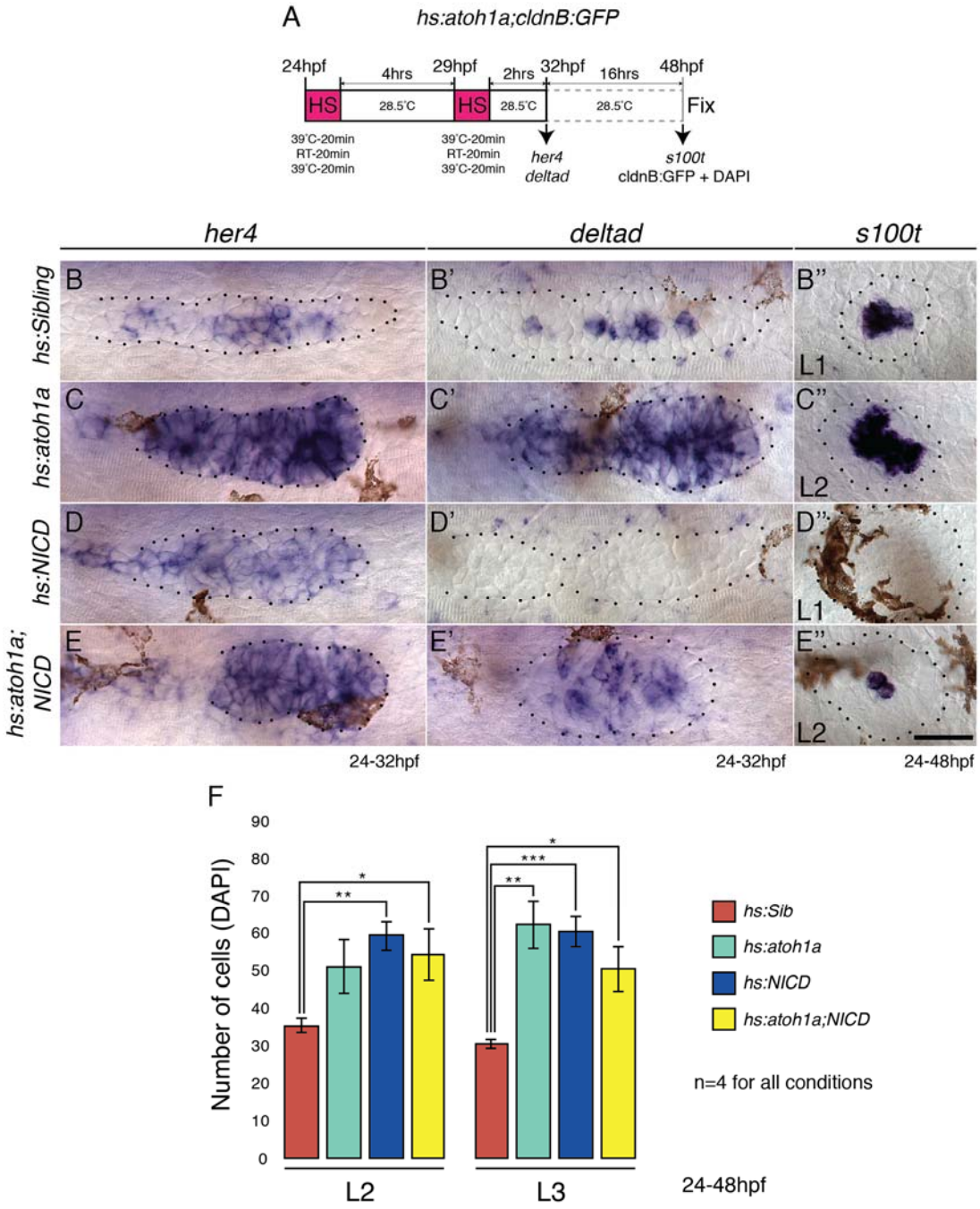

Figure 2-7. Overexpression of *atoh1a* induces neuromast size through activation of Notch signaling

(A) Heat-shock strategy to activate *atoh1a* in the lateral line. (B, C, D, E) *her4* expression in the primordium. RT-room temperature. (C) The expression of *her4* is even more highly elevated in *hs:atoh1a* primordia than in NICD primordia (D). (B'-E'') Expression of the *atoh1a* target *deltad* in the lateral line. (C') *deltad* expression is upregulated and expanded in the *hs:atoh1a* primordia, completely absent in NICD primordia (D') and re-established in some cells in the *hs:atoh1a;NICD* primordia (E'). (C'') Activation of *atoh1a* upregulates *s100t* (hair cell marker) expression in 48 hpf WT neuromasts and induces *s100t* in several cells in NICD neuromasts (E''). (B-E'') Scale bar is 25μm. (F) *atoh1a* overexpression induces L3 neuromast size by itself (light green). Error bars represent standard error from one independent experiment ($p<0.05$=*, $p<0.01$=**, $p<0.001$=*** Student's *t* test). This figure is reprinted from Kozlovskaja-Gumbrienė et al. (2017).

We then tested if cell fate switch in the leading mesenchymal cells contributes to larger neuromast formation. Our quantifications demonstrate an equal number of mesenchymal cells in the sibling and NICD primordia at 26 hpf. However, the leading region is reduced from 9 to 5 cells at 30 hpf in NICD primordia (Figure 2-6M-N'). Accordingly, this reduction in the mesenchymal cells is not sufficient to explain the increase in NICD neuromast size. The last potential switch that could contribute to lateral line organ enlargement is the incorporation of future interneuromast cells (INCs) into forming proneuromasts (Figure 2-6M', arrow, see Chapter 1) and subsequent loss of INCs in between the formed neuromasts. However, INC number is not affected in NICD embryos (Figure 2-6O-P arrows, 2-6Q). Notably, the only significant difference between sibling and NICD is the number of proneuromasts per primordia. The NICD primordia contain on average fewer, larger proneuromasts at the expense of one normal-sized wildtype proneuromast (Figure 2-6M and M', grey cells, and 2-6R). Therefore, cell fate changes do not contribute to lateral line organ enlargement in NICD embryos, but rather more support cells are allocated into fewer proneuromasts.

2.3 Discussion and Future directions

2.3.1 Notch induces larger neuromasts independent of yap1 or cell proliferation

Wnt and Notch signaling regulate neuromast size by two independent mechanisms. Wnt increases neuromast cell proliferation after deposition, whereas Notch signaling induces organ size as it forms within the primordium in a proliferation-independent manner. Accordingly, cell cycle inhibition in the NICD embryos does not significantly alter the neuromast size, similarly to wildtype phenotype (Aman et al., 2011). Likewise, although *amotl2a* reduction causes cell overproliferation in the trailing domain in the primordium

and a consequent increase in the primordium size, which can be reverted by simultaneous disruption of *yap1* function (Agarwala et al., 2015), neither *amotl2a* or *yap1* reduction affect the forming neuromast size in wildtype, *apc* or NICD embryos (Figure 2-3G-H;(Agarwala et al., 2015)). Therefore, primordium and neuromast size control relies on separate molecular mechanisms. However, hyperplastic *amotl2a* deficient primordia generate one additional neuromast (Agarwala et al., 2015). Similarly, smaller primordia in *lef1* mutants (Wnt signaling loss) produce fewer, but normal size neuromasts (McGraw et al., 2011; Valdivia et al., 2011). Thus, primordium size does not regulate neuromast size, but rather the number of sensory organs. Therefore, an increase in deposited organ number is probably not specific to *amotl2a* loss, but rather to an elevated primordium cell proliferation. Notably, the primordium deposits sensory organs in closer intervals also in the embryos treated with BIO, which demonstrates an additional cell proliferation control from Wnt signaling (Aman et al., 2011). In the future, it would be interesting to dissect how proliferation in distinct primordium domains affects deposited organ number. For example, by injecting *yap1* morpholino into embryos treated with BIO we could suppress cell proliferation in the trailing domain in the primordium and test if it is sufficient to restore normal neuromast number when Wnt is elevated in the leading part.

2.3.2 Disecting potential Hippo pathway regulation and function in lateral line development

yap1 is upregulated and *amotl2a* is reduced in the NICD lateral line without affecting primordium cell number, suggesting that these Hippo signaling elements also posses proliferation-independent functions that need to be futher explored (Figures 2-5H-I, Figure 5-4A). Previous studies have reported physical interaction between NICD and Yap1 and that NICD requires Yap1 to activate its transcriptional program in smooth muscle development

(Manderfield et al., 2015). Also, genome-wide Chip-seq for Rbp-J (a DNA binding mediator of Notch signaling) from neuronal stem cells has demonstrated Rbp-J binding throughout the *yap* locus and that transgenic NICD overexpression leads to increased Yap levels (Li et al., 2012). To further dissect protential cross talk between Yap1 and Notch we need to assess Yap1 protein levels and expression location within the primordia cells by immunohistochemistry. First, we must determine if elevated Yap1 levels are retained in the NICD cell cytoplasm, or if Yap1 is translocated into the nucleus to elicit its function. It has been previously shown that E-cadherin can sequester and thereby inactivate Yap1 in the cytoplasm (Kim et al., 2011). Thus, even though NICD induces *yap* transcription, it also known to augment E-cadherin expression (see below), which might block Yap1 propagation into the nucleus, making it inactive.

In addition, cortical cell tension is a well-known negative regulator of Yap activity (Mo et al., 2014). Possibly, *yap* overexpression is triggered by an increasing mechanical tension in the NICD primordia cells. One way to indirectly assess tension is to measure how crowded NICD primordia are compared to their siblings by counting cell number per area, or measuring the distance between cell nuclei in the primordium. However, we would have to correlate these measurements with possibly independently regulated cell volume changes. Our data did show that NICD and wildtype primordia are composed of similar amount of cells at 32 hpf, but it is still unclear if there are differences between primordia dimensions. Another likely source for increased mechanical tension in NICD embryos is the formation of less proneuromasts within NICD primordium (see below), which forces cells to stretch towards the middle of the forming organ. Our data shows that *stk3* (Hippo kinase) expression is supressed in NICD primordia (Figure 2-4A'-E'). Molecularly, this result might indicate NICD interferance with the Hippo signaling function to restrain Yap in the cytoplasm in response to an increasing mechanical tension within the NICD primordium.

Yap1 is also shown to interact with Wnt/β-catenin signaling. Interestingly, Yap1 has a dual role in relation to Wnt/β-catenin, whereby cytoplasmic Yap1 inhibits β-catenin propagation into the nucleus, but once inside, both transcription factors often act synergistically (reviewed in Kim and Jho (2014)). Thus, if Yap1 protein is overexpressed, but withheld in the NICD cell cytoplasm by E-cadherin or other junctional proteins (see above), it could potentially inhibit β-catenin in the cytoplasm and suggest a mechanism by which Notch is suppressing Wnt/β-catenin signaling in the primordium (Figure 5-2I-I',J-J',K-K').

2.3.3 The increase in organ size is not due to cell fate changes in NICD embryos

Notch signaling specifies support cells by inhibiting the proneural gene *atoh1a* expression in the primordium, which is required for neurogenic cell fate acquisition ((Bermingham et al., 1999); Figure 2-6J,L and Figure 5-4C). Accordingly, Notch overexpression leads to the loss of *atoh1a*-positive hair cell progenitors, whereas the loss of Notch signaling in the *mib1* mutant primordia leads to expansion of *atoh1a* and *delta*-positive hair cell precursors (Figure 2-1L''-N'';(Itoh and Chitnis, 2001)). Downregulation of *atoh1a* in *mib1* mutants slightly restores *e-cadherin* expression (Matsuda and Chitnis, 2010). In *Drosphila* many neurogenic mutants show abnormalities in different epithelial structures whereby they lose their epithelial phenotype and cells dissociate (Hartenstein et al., 1992). Nevertheless, it is unlikely that the NICD phenotype is caused by the loss of *atoh1a* positive hair cell precursors due to several reasons: 1) re-expression of Atoh1a in NICD primordia does not rescue the neuromast size (Figure 2-7E'',F), 2) *apc* and *hs:atoh1a* primordia, which both have increased levels of *atoh1a*, are inducing *e-cadherin* expression, arguing against previously suggested function for *atoh1a* being a negative *e-cadherin* regulator (Figures 4-1CC, 5-1CC'', Figure 4-2A,B), 3) inhibition of *atoh1a/b* function with morpholinos does not affect *e-cadherin* expression or make rosettes bigger (Matsuda and

Chitnis, 2010; Nechiporuk and Raible, 2008). On the contrary, our data shows that *atoh1a* overexpression induces neuromast size and upregulates Notch target *her4* expression (Figure 2-7B,C,F). This interesting finding suggests that neuromast size in *hs:atoh1a* embryos is likely regulated by Notch signaling acting downstream of Atoh1a dependent Delta ligand expression. Atoh1b is a primary *her4* signaling activator in the developing zebrafish ear, and is also expressed in the primordium (Matsuda and Chitnis, 2010; Radosevic et al., 2014). The molecular mechanism behind Notch regulation by Atoh1a in the lateral line still needs to be investigated. First, it is important to establish if Atoh1a is acting through DeltaD to activate Notch signaling or whether it is a direct regulation. We need to assess if *her4* expression is maintained at high levels in the embryos obtained from a mating between *hs:atoh1* transgenics and *deltaD* mutants, or if DeltaD is indeed required to enhance Notch signaling. Next, even though Atoh1a upregulates Notch signaling, it is still unclear how neuromasts get enlarged in the *hs:atoh1a* embryos. Specifically, are proneuromasts enlarged through the cell allocation mechanism we described in this thesis, or whether Atoh1a regulates cell proliferation similar to Wnt overexpression phenotype.

Importantly, our data demonstrates that, even though NICD primordia loose the hair cell population, which could introduce signaling changes in the neighboring cells, the loss of hair cells is not the cause of enlarged neuromast formation in the NICD embryos.

Chapter 3

Notch is sufficient to induce lateral line organ morphogenesis

3.1 Introduction

Fgf signaling is absolutely required for proneuromast formation in the lateral line (Lecaudey et al., 2008; Nechiporuk and Raible, 2008). It has been proposed that Fgf signals from cells in the middle of proneuromast induce peripheral cell constriction, which organizes primordia cells into stable rosettes. The following molecular mechanism regulating constriction at the cellular level has also been proposed. The Fgf receptor 1 (Fgfr1) acts through the Ras-MAPK pathway and induces scaffolding protein *shroom3* transcription in the support cells. Shroom3 brings Rock2a kinase to the apical surface of the cell where it activates non-myosin motor (pNMII) to exert actin constriction and thereby induces apical narrowing of the cell (Harding and Nechiporuk, 2012). Additionally, Fgf signaling is required for Notch activation in the primordium. Notch target gene *her4* and *notch3* receptor expression is abrogated in the primordia treated with Fgf inhibitors (Nechiporuk and Raible, 2008).

3.2 Results

3.2.1 Notch regulates neuromast formation independent of Fgf

As it has already been established that Fgf pathway regulates neuromast formation in the lateral line, we immediately hypothesized that Fgf signaling is probably increased in the NICD primordia, which forms enlarged rosettes. Surprisingly, even though *fgfr1* is expressed at a normal level, Fgf ligands (*fgf3* and *fgf10*) and Fgf targets (*pea3* and *dkk1b*) are substantially inhibited in NICD primordia (Figure 3-1A, A', B, B', C, C', D, D', Figure 5-1L, L'). The loss of Fgf signaling in the NICD primordia can be attributed to several reasons. First,

Notch inhibits *atoh1a*, which is required for *fgf10a* expression in the more mature proneuromasts (Figure 2-6J,L and Figure 3-1C,C', arrows; (Matsuda and Chitnis, 2010)). Second, Notch inhibits Wnt signaling, which normally induces Fgf signaling in the trailing part of the primordium (see below, Figure 5-1I'-K';(Aman and Piotrowski, 2008)). Therefore, elevated Notch signaling disrupts Fgf signaling through inhibition of *atoh1a* and Wnt signaling in the primordium. Counterintuitively, the loss of Notch, similar to NICD overexpression, also supresses Fgf signaling in the lateral line. Namely, *fgf10a* is expanded in the central proneuromast cells in *mib1* primordia, but *fgfr1* and *pea3* are largely suppressed with only some expression maintained in the most peripheral cells in the primordium (Figure 3-1A'',D''). The main reason why the Fgf signal is reduced in the Notch depleted central *mib1* primordia cells is due to uncontrolled *atoh1a* expansion, which is known to inhibit *fgfr1* in the lateral line (Figure 3-1A''-D'';(Matsuda and Chitnis, 2010)).

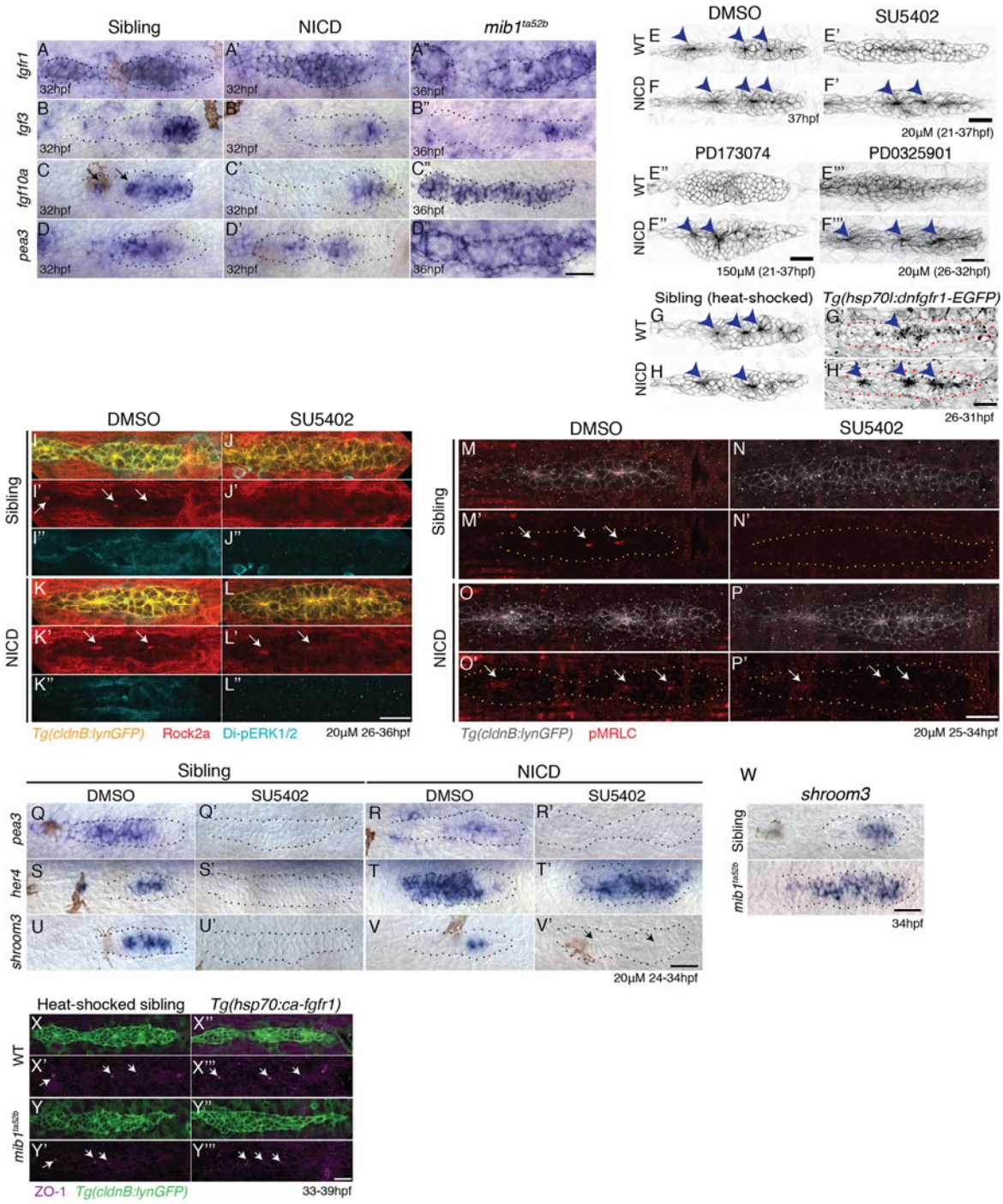

Figure 3-1. Notch induces proneuromast (rosette) formation independent of Fgf-MAPK-Shroom3 signaling

(A-D'') The expression of Fgf pathway members in the primordium is altered by Notch signaling. Fgf ligand (B' and C') and target gene expression (D') is largely downregulated in NICD primordia compared to siblings (B-D). (B'') *fgf3* and (D'') *pea3* expression is downregulated in *mib1*^{ta52b} primordia, but *fgf10* expression (C'') is largely expanded. *fgfr1* expression remains normal in NICD (A') but is downregulated in the center of the *mib1*^{ta52b} primordia (A''). (E-H') Notch induces proneuromast formation independent of Fgf-MAPK signaling. NICD primordia form proneuromasts in the presence of Fgfr1 and MAPK inhibitors (F' and F'' and F''') as well as after the induction of dominant-negative Fgfr1 (H'), while sibling proneuromast formation fails after these manipulations (E'-E''' and G').

(G-H') Embryos were heat-shocked 2 times at 39°C for 20min with 20min incubation at a room temperature in between, starting at 26 hpf and fixed 4 hrs later. (I-L'') Notch regulates apical Rock2a accumulation independent of Fgf signaling. Contrary to sibling primordia (J'), the Rock2a expression is maintained in the apices of the forming proneuromasts in NICD primordia treated with the Fgfr1 inhibitor SU5402 (L'). (J'' and L'') Fgf downregulation is confirmed by the loss of di-pERK1/2 expression in the primordium. (M-P') Notch regulates Phosphorylated Myosin Regulatory Light Chain (pMRLC) expression independent of Fgf signaling. (N') Sibling primordia lose the pMRLC expression after Fgfr1 inhibitor treatment, but pMRLC expression is maintained in the apices of treated (P') NICD proneuromasts. (Q-V') NICD primordia form proneuromasts (black arrows) in the absence of *shroom3* expression (V'). Treatment with the Fgfr1 inhibitor SU5402 depletes *pea3* (Q' and R'), *her4* (S') and *shroom3* (U' and V') expression in control and NICD primordia. (T') *her4* expression is maintained in NICD primordia after Fgfr1 inhibition. (W) *shroom3* is upregulated in *mib1*^{ta52b} primordia, although Fgf signaling is downregulated. (X-Y''') Constitutive activation of Fgf signaling by heat-shock induction of Fgfr1 does not rescue rosette formation in *mib1*^{ta52b} primordia (Y''') suggesting that Fgf signaling is not sufficient for rosette formation in the absence of Notch signaling. (X-Y''') Embryos were heat-shocked at 39°C for 40min, starting at 33hpf and fixed 4hrs later. Scale bar in all panels is 25µm. This figure is reprinted from Kozlovskaja-Gumbrienė et al. (2017).

As the expression of Fgf signaling is not completely abrogated in the NICD primordia and therefore might still regulate proneuromast formation, we fully inhibited Fgf signaling and tested if it is sufficient to rescue NICD phenotype. We used pharmacological Fgfr1 inhibitors SU5402 and PD173074 (Figure 3-1E-F''), treated NICD embryos with MAPKK/Di-pErk inhibitor (PD0325901) (Figure 3-1E-F'', Figure 3-2A-B'), and used a heat-shock inducible dominant-negative *fgfr1* transgenic in the NICD background (Figure 3-1G-H'). Even though the primordia eventualy stalled, none of these Fgf signaling perturbations disrupted rosette formation in the presence of Notch overexpression (Figure 3-1F',F'',F''',H'). In addition, cellular components required for apical constriction, such as Rock2a and pMRLC are still present and properly localized to the cell apices in the NICD primordia in the absence of Fgf target- Di-pErk expression (Figure 3-1J'',L'' and L'-P). These results indicate that Notch is sufficient to properly localize apical constriction machinery and thereby regulate proneuromast formation in the absence of Fgf signaling (Figure 3-1I-P).

3.2.2 Notch acts downstream of Fgf-Ras/MAPK pathway

To confirm that Notch signaling is regulated by Fgf signaling in the primordium we performed an *in situ hybridization* analyses for Notch target *her4* expression in embryos treated with Fgf inhibitor (Figure 3-1Q-V'). Indeed, *her4* is largely reduced in the siblings, however Fgf inhibitor had no effect on Notch target gene expression in NICD primordia (Figure 3-1Q-S';(Nechiporuk and Raible, 2008)). In addition, Notch acts downstream of the Ras/MAPK pathway, since MAPKK inhibitor PD0325901 does not only inhibit Fgf targets Di-pERK1/2, *pea3* and *fgfr1*, but also *notch3* and *her4* expression (Figure 3-2A-F').

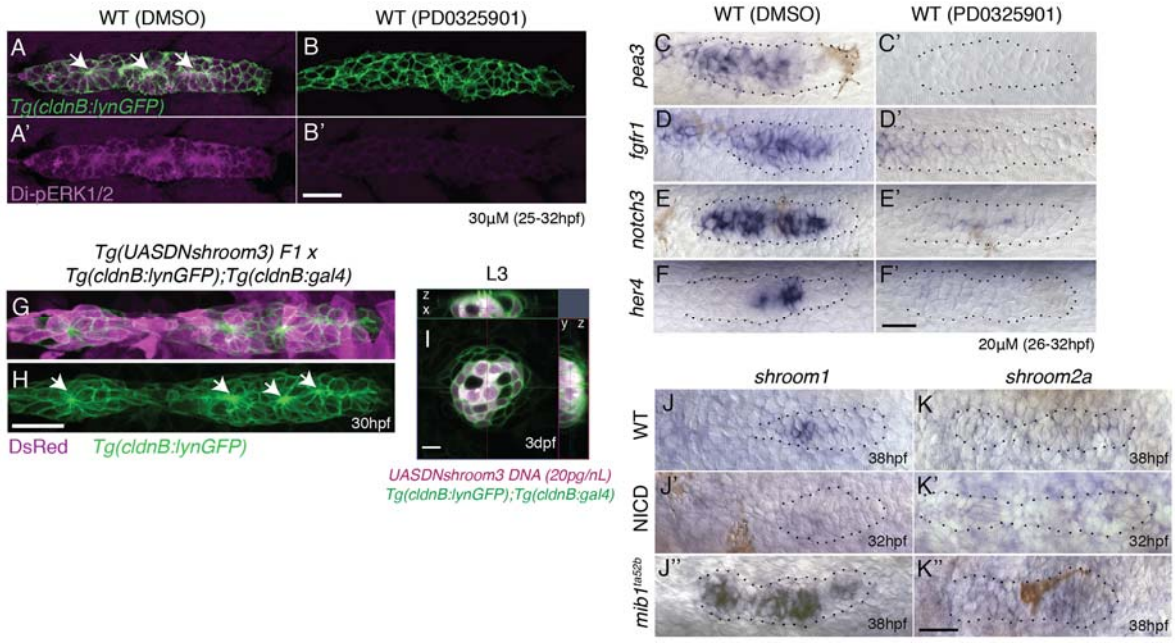

Figure 3-2. Notch signaling regulates proneuromast formation downstream of the MAPK pathway and shroom3 is dispensable for rosette formation
(A-B') MAPK is required to maintain di-pERK1/2 expression in the primordium. (B') The MAPK inhibitor PD0325901 leads to a strong reduction of di-pERK1/2 expression. PD0325901 downregulates the Fgf targets *pea3* (C-C'), *fgfr1* (D-D'), *notch3* (E-E') and the Notch target *her4* (F-F'). (G-I) Loss of *shroom3* by induction of *DNshroom3* using the *cldnb* promoter does not disrupt proneuromast formation (H) or maintenance of deposited neuromasts (I). (J) *shroom1* is expressed in the trailing region of the wildtype primordium, is downregulated in NICD (J') and highly upregulated in *mib1*^{ta52b} primordia (J'') showing that *shroom1* is inhibited by Notch signaling. *shroom2a* expression is also inhibited by Notch signaling. *shroom2a* expression is barely detectable in wildtype (K) and NICD (K) primordia but upregulated in *mib1*^{ta52b} primordia. We currently do not understand why *shroom* genes are upregulated in *mib1* primordia, as at least *shroom3* is regulated by Fgf. All scale bars are 25µm. This figure is reprinted from Kozlovskaja-Gumbrienė et al. (2017).

To test if Notch signaling regulates proneuromast formation downstream of Fgf, we crossed Notch-depleted *mib1* mutants to a heat-shock inducible constitutively-active *fgfr1* tansgenic line (*Tg(hs:cafgfr1)*, Figure 3-1X-Y'''). The resulting *mib1;ca:fgfr1* embryos still have a fragmented primordium with reduced localization of the tight junction marker ZO1, similar to *mib1* mutants alone (Figure 3-1Y-Y''', arrows). This data confirms that Fgf signaling is unable to induce rosette formation in the absence of Notch signaling. To conclude, our results show that Fgfr acts through the Ras-MAPK pathway to activate Notch signaling which regulates apical constriction and rosette formation in the wildtype primordia.

3.2.3 Shroom3 role is dispensable in neuromast formation

Next, we wanted to assess *shroom3*, an Fgf-dependent scaffolding protein that places Rock2a kinase apically, function in NICD rosette formation (Figure 3-1W;(Ernst et al., 2012)). *shroom3* is inhibited in Fgf-depleted primordia, reduced in NICD primordia, completely lost from NICD primordia treated with Fgf inhibitor and upregulated in *mib1* primordia (Figure 3-1U, V, V', W). Notably, Fgf-depleted NICD primordia are forming proneuromasts (Figure 3-1V', arrows) in the absence of *shroom3*, which argues that the latter is not required for rosette formation in the presence of Notch. We also tested *shroom3* requirement by expressing a *dominant negative shroom3* (*DNshroom3*) in the wildtype primordia. Surprisingly, we did not observe any defect during proneuromast formation or in the already deposited lateral line organ maintenance (Figure 3-2G-I). Likewise, in contrast to a previously published data (Durdu et al., 2014; Ernst et al., 2012) we did not witness any delay in proneuromast formation in *shroom3* morphants, which had significantly reduced *shroom3* levels (Appendix Figure 2).

To investigate if other *shroom* genes could act redundantly in NICD primordia, we tested *shroom1*, *shroom2a*, *shroom2b* and *shroom4* expression in the lateral line (Figure 3-

2J-K''). We found that *shroom2b* and *shroom4* are not expressed in the primordium or neuromasts. However, *shroom1* is present in the central cells in the trailing domain and *shroom2a* is only weakly expressed in wildtype primordia (Figure 3-2J-K). Importantly, *shroom1* and *shroom2a* are absent from NICD primordia and therefore cannot substitute for Shroom3 function in proneuromast formation (Figure 3-2J'-K'). Surprisingly, *shroom1* and *shroom2a* expression is elevated in the *mib1* mutants, where Fgf signaling is decreased and at least *shroom3* was shown to be an Fgf target in the primordium (Figure 3-1U';(Ernst et al., 2012)). These data demonstrate that Notch regulates apical constriction and proneuromast formation in a *shroom*-independent manner.

3.2.4 A reduction of Notch leads to cell constriction loss and proneuromast fragmentation

Our findings revealed a novel function of Notch signaling in generating apical constrictions, which are required to form stable proneuromasts. Nevertheless, we wanted to test if apical constrictions are affected in the Notch mutant primordia and if so, what is the influence on the proneuromast structure compared to wildtype and NICD primordia. Cells in NICD proneuromasts constrict similar to wildtype proneuromasts, as the ratio of cell constriction area to the largest cell area is not significantly different (Figure 3-3A,B,E). However, in 36 hpf old *mib1* mutant primordia, cells in the most mature proneuromast (R3) lose their apical constrictions, which disrupts the connection between cell apices and leads to proneuromast fragmentation (Figure 3-3C-E). We also defined and measured apical constriction volumes in primordia by coloring in magenta the area where proneuromast cell apices meet using Imaris (Bitplane) software (Figure 3-3F). Subtracting the younger rosette (R2) apical constriction volume from a more mature proneuromast (R3) constriction volume results in a positive value for wildtype proneuromasts, however, in the *mib1* mutants this

difference is negative. Therefore, this data indicates that in Notch mutants, unlike in wildtype primordia, the apical constriction volume decreases as a rosette matures, suggesting that *mib1* primordia cannot maintain rosette structure, which ultimately leads to primordia fragmentation, a phenotype described by Matsuda and Chitnis (2010). Apical constriction volume disintegration becomes more evident after 32 hpf in *mib1* mutants, as the loss of Notch signaling becomes progressively more severe due to depleted maternal contribution (Matsuda and Chitnis, 2010).

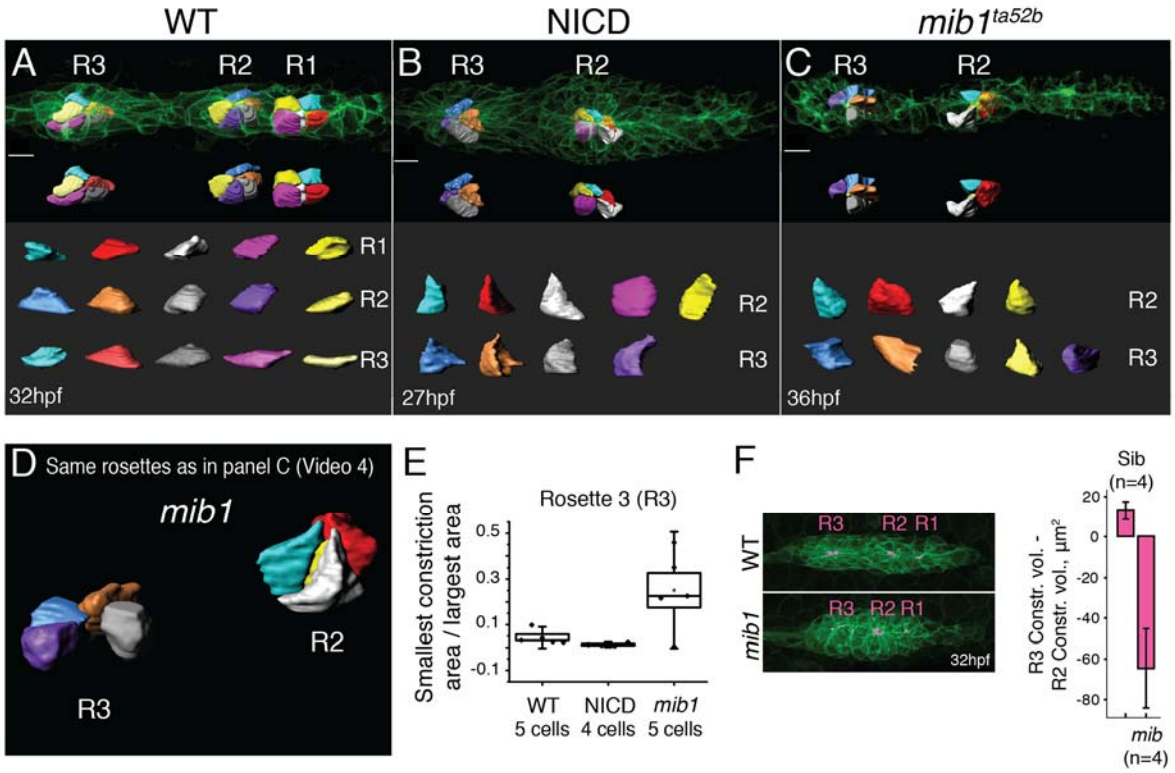

Figure 3-3. Loss of Notch signaling disrupts apical constrictions
(A-E) Analysis of cell shapes using Imaris software. R1-R3 indicate proneuromast numbers. (A) In wildtype and (B) NICD primordia all analyzed proneuromast cells in all rosettes constrict apically. Cells in a *mib1*^{ta52b} primordium (C) constrict in the more immature rosette (R2) but are lacking constricted apices in the last proneuromast (R3) at 36hpf. The scalebars equal 10µm. The individual cells are scaled differently. While the individual cells within one graph are scaled the same with respect to each other, no comparison can be made between different samples. This is due to the limitations of the Imaris scale bar function, rooted in the complexity of displaying 3D data. (D) Still image of an animation of the same primrodium as in (C) demonstrating the shape changes in R3. (E) Quantification of apical constrictions (area). Cells from the most mature proneuromasts (R3) were selected for analysis. Boxplot defines standard error and the ends of the whiskers show standard deviation between different cells.

(F) The bar graph shows the apical constriction volume value when the R2 volumes are subtracted from R3 volumes. Constriction volumes gradually diminish in maturing proneuromasts in *mib1*^{ta52b} primordia, therefore, the last proneuromast (R3) in *mib* mutants has a significantly smaller constriction volume in comparison to R2, whereas, in the siblings R3 is larger than R2, which results in a positive value. This figure is reprinted from Kozlovskaja-Gumbrienė et al. (2017).

3.3 Discussion and Future directions

3.3.1 Notch cell-autonomously induces neuromast formation downstream of Fgf

The current understanding about neuromast formation relies on Fgf signaling acting from the central cells towards the Fgf receptor containing peripheral cells, which once activated are apically constricting and forming lateral line organs (Harding and Nechiporuk, 2012; Lecaudey et al., 2008; Nechiporuk and Raible, 2008). Indeed, loss of Fgf signaling causes proneuromast disintegration and failure to form new rosettes (Lecaudey et al., 2008; Nechiporuk and Raible, 2008). Additionally, a current report suggested an interesting mechanism to maintain cells in the proneuromast, whereby Fgf signaling in the most mature rosettes depends on a dorsal lumen that serves as an Fgf ligand source for the cells that are apically in contact with the lumen to activate Fgf target *pea3* (Durdu et al., 2014). However, lumina only form in the trailing proneuromasts and therefore are not required for Fgf-mediated formation of the more nascent rosettes (Figure 5-4B). Our data shows that Fgf signaling is unnecessary for proneuromast formation in the presence of Notch overexpression. However, this finding questions the basic principle of proneuromast formation, whereby in NICD primordia the Fgf ligand that must be restricted to a central cell and organize surrounding cells into rosette is absent. Likely, this stereotypic pattern of Fgf ligand expression regulates the forming organ size by limiting the number of cells responding to Notch signaling. It would be interesting to test if in the larger primordia with more cells, such as *amotl2a* mutants, we could also form larger proneuromasts by expanding the pool of Fgf ligand producing cells and presumably in this way create more

cells that respond to Notch signaling.

Another interesting question is why NICD primordia form two rosettes instead of three as in the wildtype situation. Moreover, we still do not understand why cells cluster into a rosette at all when there is no organizing center left in the NICD primordia. We hypothesize that the Notch-driven changes in cell adhesion and cortical cell tension modify the morphology of the organ to achive minimal surface tension (Heisenberg and Bellaiche, 2013). To test this hypothesis we need to find the means to alter cell adhesion properties between the primordia cells and see how and if it affects rosettogenesis. Presumably, NICD primordia with weakened cell adhesion would break down into more, smaller and randomly organized rosettes, but this remains to be tested.

3.3.2 Shroom3 is not required for cell constriction in the presence of Notch signaling

Shroom3 is a scaffolding protein that brings Rock kinase to the apical surface of the cell where it activates acto-myosin meshwork contraction which is driving cell apical constriction in multiple organisms and tissues (see Chapter 1). The Shroom3 requirement was also demonstrated in the proneuromast formation process, however, our results do not support this finding ((Durdu et al., 2014; Ernst et al., 2012); Figure 3-2G-I, Appendix Figure 2, arrows). Most importantly, proneuromast cells apically constrict normally in the absence of *shroom3* in NICD embryos (Figure 3-3V-V', arrows). During chicken otocyst invagination apical constriction occurs independent of Shroom3 function but through the apically recruited atypical cadherin Celsr1, suggesting that apical constriction can be achieved via diverse mechanisms (Sai et al., 2014). Next it would be interesting to address the role of Celsr in proneuromast formation by injecting celsr1a/b morpholinos into *celsr2* mutant zebrafish embryos, which by themselves have no defect in rosette formation (not shown).

Chapter 4

Notch increases organ size by regulating cell-cell adhesion

4.1 Introduction

It is widely established that tissue or cell segregation results from binding specificities between different adhesion molecules (Duguay et al., 2003). Interestingly, the strength of adhesion between the cells that express the adherens junction protein Epithelial cadherin (E-cadherin, cdh1) is proportional to the level of E-cadherin expression. Moreover, cells that maintain high levels of E-cadherin expression sort out from cells with low levels of E-cadherin (Angres et al., 1996).

Previous studies in the lateral line have shown that changes in primordium cohesion correlate with changes in *e-cadherin (cdh1)* and *n-cadherin (neural cadherin, cdh2)* gene expression (Matsuda and Chitnis, 2010). In the wildtype primordia *e-cadherin* is expressed at low levels in the leading domain of the primordium, while expression becomes progressively higher in the rosette formation area and is strongest in about to be deposited proneuromasts. However, *e-cadherin* expression is relatively low in the *atoh1a*-positive hair cell precursors (Figure 4-1C;(Matsuda and Chitnis, 2010)). In the Notch mutant *mib1* primordia, loss of *e-cadherin* expression progressively spreads from the central cells into the support cells and its expression is almost completely absent in all the cells when the primordium fragments. Conversly, *atoh1a* expression is expanded in the *e-cadherin* negative cells. Consistent with *atoh1* being associated with reduced *e-cadherin*, *atoh1a/b* morpholino injection restored some of the initial *e-cadherin* expression and improved the *mib1* primordium fragmentation phenotype (Matsuda and Chitnis, 2010).

n-cadherin is broadly expressed at the leading domain of primordium, and its expression becomes restricted to the central cells in mature proneuromasts as they prepare

for deposition. Although *n-cadherin* expression overlaps with the central cells, it is also induced in the surrounding support cells (Figure 4-2G;(Matsuda and Chitnis, 2010)). However, decreased Notch signaling in *mib1* mutants does not alter *n-cadherin* expression in the primordium. Taken together, it has been proposed that effective adhesive junctions are formed between the support cells that express both types of cadherins and then hair cells are held together solely by *n-cadherin*. These authors claim that in the *mib1* mutant, primordia fragmentation occurs due to *atoh1a* expansion (see above) and consequent loss of *e-cadherin* from the support cells, which leads to disabled cell adherence between the hair and support cell populations (Matsuda and Chitnis, 2010).

Besides classical cadherins, such as E- and N-cadherin, there are multiple other adhesion molecules that may also contribute to primordium integrity and proneuromast formation. For example, Epithelial cell adhesion molecule (Epcam) is a calcium-independent, cell junction molecule that changes cell adhesiveness by distorting normal AJC organization when mutated in zebrafish embryos (Slanchev et al., 2009). As it has been described above (see Chapter 1), adherens junction molecules regulate cell polarity and tight junction proteins through multiple feedback interactions. Therefore, it is not surprising that *epcam* was shown to regulate tight junctions, specifically, expression of claudins (Wu et al., 2013).

Claudins are tight junction molecules that besides controlling permeability in epithelia, also affect cell-cell adhesion as demonstrated in *Xenopus* blastomeres and cell culture (Brizuela et al., 2001; Kubota et al., 1999). In addition, loss of claudins leads to an epithelial to mesenchymal transition, while their overexpression causes cells to adhere more tightly (Bhat et al., 2015). *claudin-6* morphants fail to accumulate apical actin due to defective cell adhesions and apical-basal polarity in *Xenopus* pronephros development (Sun et al., 2015). Again, claudins encompass only a small part of tight junction proteins.

Interestingly, occludins act as organizing centers and as anchoring docks for multiple other tight junction proteins as well as for tight junction accessory proteins (Feldman et al., 2005). In addition, occludin was also demonstrated to induce cell-cell adhesion through interaction with the ZO1 protein in fibroblasts that lack cadherins (Van Itallie and Anderson, 1997).

4.2 Results

4.2.1 Notch-positive cells self-organize to form larger neuromasts

As the signaling center hypothesis prevails for proneuromast formation, we wanted to test if NICD expressing cells recruit surrounding wildtype cells into rosettes, or if they act cell-autonomously and form enlarged proneuromasts solely through attachments to other NICD cells. We created mosaic neuromasts by transplanting cells (magenta color) from NICD transgenic embryos or wildtype embryos (as a control) into wildtype *Tg(cldnb:lynGFP)* embryos and compared neuromast size and cell composition between these two conditions (Figure 4-1A-B'). Our experiment demonstrates that neuromasts (green color) become larger than an average wildtype neuromast (grey line) only when they include NICD clones, but not if they contain wildtype clones (Figure 4-1B,B'). Moreover, our analysis shows that mosaic neuromasts always contain a similar amount of the host wildtype cells (black) irrespective of the type of transplant (Figure 4-1B'). Thus, NICD transducing cells are not acting as signaling centers as they do not recruit any extra wildtype cells (Figure 4-1B'). An increase in organ size occurs only due to cell-autonomous incorporation of an excessive number of NICD cells by other NICD cells.

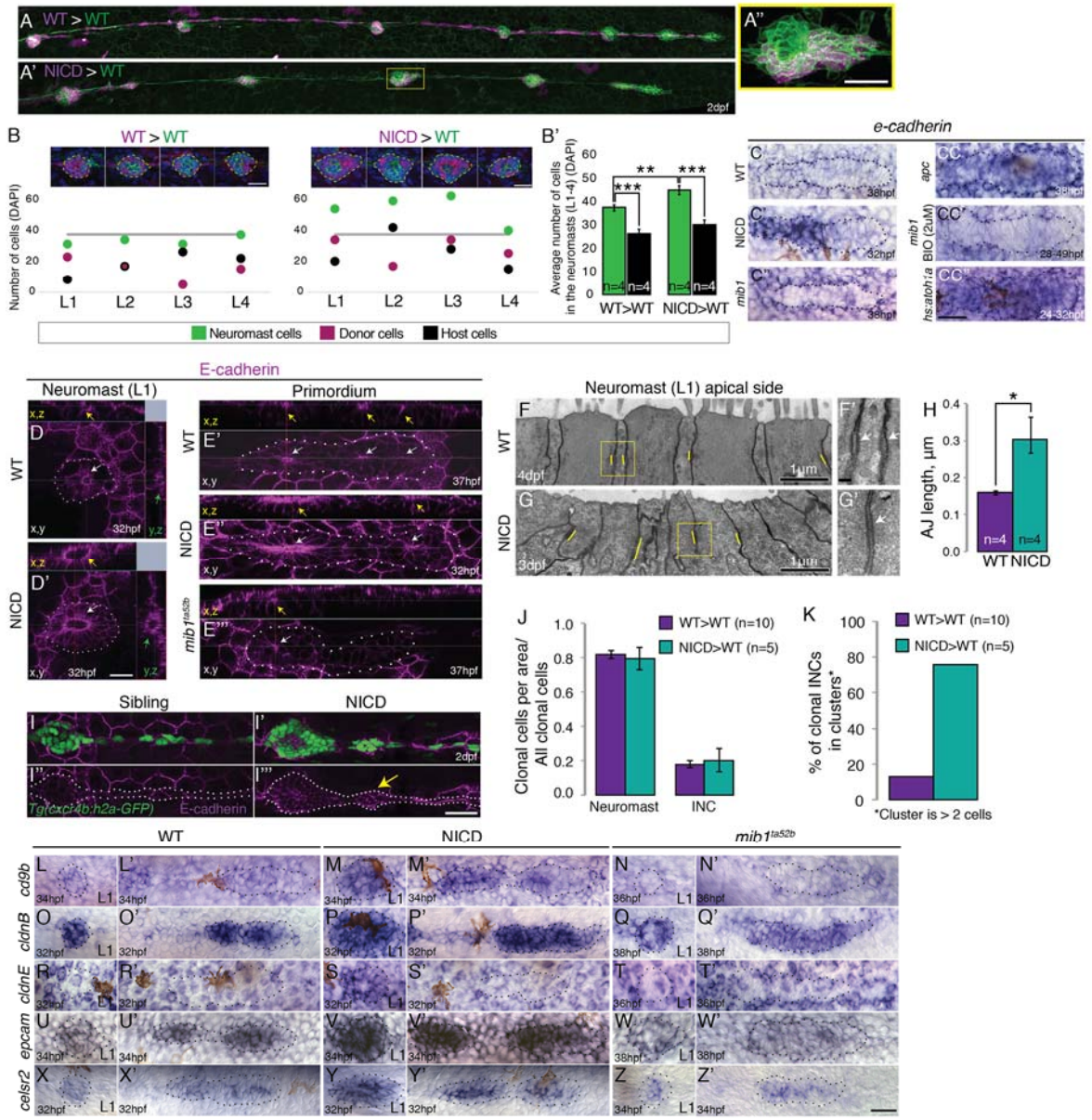

Figure 4-1. Notch cell-autonomously induces cell clustering

(A,B and B') Wildtype cells transplanted into a wildtype embryo do not cause larger neuromasts. (A'-B') Mosaic, NICD-positive cells that are transplanted into a wildtype embryo are clumping together and form bigger neuromasts. (A'') Mosaic L3 neuromast from panel (A') where NICD positive cells cluster together to form an enlarged neuromast. (B) Images at the top of the graph show 2 examples of L1-L4 neuromasts with clone cell numbers measured below. Left: WT cells transplanted into WT lateral line and right: NICD cells transplanted into WT lateral line. Colored dots below indicate three values measured for each neuromast: green- total number of cells in the neuromast, magenta- number of transplanted cells, black- number of host cells (a calculated value of magenta cells subtracted from the number of green cells). The grey line indicates the average neuromast size of all WT neuromasts containing WT clones. (B') Quantification of cell transplantation experiments. The significant increase in the neuromast size (green bars; 38 versus 45 cells) in NICD>WT experiments compared to WT>WT situation is only due to addition of transplanted NICD cells, since the number of host cells (black bar) is not significantly changed between two types of cell transplantation strategies (26 versus 30 cells).

(C-CC'') *e-cadherin* expression in the primordium is upregulated by Notch (C') and by Wnt signaling (CC) compared to a wildtype primordium (C). (C'') *e-cadherin* is downregulated in *mib1*^{ta52b} primordia and in *mib1*^{ta52b} in which Wnt is activated with BIO (CC') suggesting that Wnt requires Notch signaling to induce *e-cadherin.* (CC'') *e-cadherin* is upregulated in *hs:atoh1a* primordia in which *her4* (Notch target) is also expanded (see Figure 4—figure supplement 1C). (D-I''') Notch upregulates E-cadherin protein expression in neuromasts (D'), proneuromasts in the primordium (E'') and in interneuromast (INCs) cells (yellow arrow) (I''') compared to a wildtype sibling (D, E' and I-I''). In *mib1*^{ta52b} embryos *e-cadherin* is downregulated (E'''). Strongest E-cadherin expression is marked by the yellow arrows in the x,z plane, white arrows in the x,y plane and green arrows in the y,z plane. (F-H) NICD causes a significant increase in apical adherens junction lengths (AJ). (F' and G') Magnification of the areas in yellow boxes in F and G. AJs are marked by the white arrows. Error bar indicates standard error (p<0.05=* Student's *t* test). (I-I''') E-cadherin expression in the NICD interneuromast cells, which tend to form clusters (arrow), quantified in (K). (J) Transplanted NICD cells contribute in similar proportions to neuromasts and interneuromast cells as transplanted wildtype cells. (K) Transplanted NICD cells form significantly more clusters, as defined by groups of cells that contain 2 or more cells. (L-Z') Apical junction genes, such as adherens junction genes and tight junction components are upregulated by NICD. (L-N') *cd9b* is upregulated in NICD neuromasts and the primordium (M and M') compared to siblings (L and L'), and is downregulated in *mib1*^{ta52b} embryos (N and N'). (O-Q') *cldnB* is upregulated in NICD neuromasts and the primordium (P and P) compared to a sibling (O and O') and slightly reduced in *mib1*^{ta52b} embryos (Q and Q'). The *cldnB* signal is especially low in the center of *mib1*^{ta52b} neuromasts (Q). (R-T') *cldnE* is upregulated in NICD neuromasts (S) compared to a sibling (R). *cldnE* is unchanged in *mib1*^{ta52b} neuromasts (T). (R', S' and T') No change in *cldnE* expression is seen in wildtype, NICD and *mib1*^{ta52b} primordia. (U-W') *epcam* is overexpressed in NICD neuromasts and the primordium (V and V') compared to siblings (U and U') but *epcam* is downregulated in *mib1*^{ta52b} embryos (W and W'). (X-Z') *celsr2* is overexpressed in NICD neuromasts and the primordium (Y and Y') compared to siblings (X and X') and *mib1*^{ta52b} embryos (Z and Z'). All scale bars are 25µm, unless stated otherwise. Error bars represent standard error (p<0.05=*, p<0.01=**, p<0.001=*** Student's *t* test). This figure is reprinted from Kozlovskaja-Gumbrienė et al. (2017).

4.2.2 Notch signaling regulates e-cadherin expression

Previously it was hypothesized that proneuromast formation could depend on cell-cell adhesion that is conveyed through molecules such as *e-cadherin* and *n-cadherin* (see above;(Matsuda and Chitnis, 2010)). Consistent with this, we found that NICD upregulates *e-cadherin* mRNA and E-cadherin protein expression in the primordium and deposited neuromasts (Figure 4-1C-C', D-E''). Additionally, NICD neuromasts have lengthened

adherens junctions (Figure 4-1F-H).

To better understand *e-cadherin* regulation interplay between different signaling pathways that are known to act in the primordium, we analyzed *e-cadherin* expression after Atoh1a, Wnt, Fgf and Notch signaling manipulations (Figure 4-1C-CC''). Importantly, our data discredited the hypothesis that Atoh1a negatively regulates *e-cadherin* (see Chapter 2) and therefore the upregulation of *e-cadherin* cannot be attributed to the loss of *atoh1a* in the NICD primordia. Notably, we demonstrate that ectopic *atoh1a* expression in wildtype primordia causes an increase in *e-cadherin* expression and neuromast size (Figure 4-1CC'', Figure 2-7F), which could argue that Atoh1a positively regulates *e-cadherin* expression. However, induction of *atoh1a* also largely increases *her4* expression in the primordium (Figure 2-7C,F). These data suggest that *atoh1a* indirectly raises *e-cadherin* levels through regulation of Notch in the primordium.

e-cadherin expression is also elevated in the Wnt overexpressing *apc* mutant primordia, suggesting that *e-cadherin* is regulated by Wnt as in many other cell types (Figure 4-1CC;(Heuberger and Birchmeier, 2010)). However, our analyses show that similar to Atoh1a, Wnt regulates induction of *e-cadherin* via the initiation of Notch signaling, as *e-cadherin* is downregulated in *mib1* primordia and elevation of Wnt by BIO treatment is not sufficient to rescue *e-cadherin* levels in the Notch-depleted *mib1* primordium (Figure 4-1C'' and CC'). Similarly, Fgf signaling is activating *e-cadherin* through Notch signaling. *e-cadherin* expression is largely depleted in wildtype primordia treated with an Fgf inhibitor, but *e-cadherin* is still expressed in the presence of NICD overexpression (Figure 4-2C-F'). *n-cadherin*, on the other hand, is regulated only by Wnt signaling as its expression is elevated in the *apc* mutants, but there is no significant change in the Notch perturbed primordia (Figure 4-2G-J;(Matsuda and Chitnis, 2010)). However, we did not observe any proneuromast formation or maintenance defects in the *n-cadherin* mutants (pac^{tm101b},

cdh2^{hi3644}, data not shown;(Durdu et al., 2014)). Together, these experiments show that *e-cadherin* is regulated by Notch signaling downstream of Atoh1a, Fgf and Wnt in the primordium.

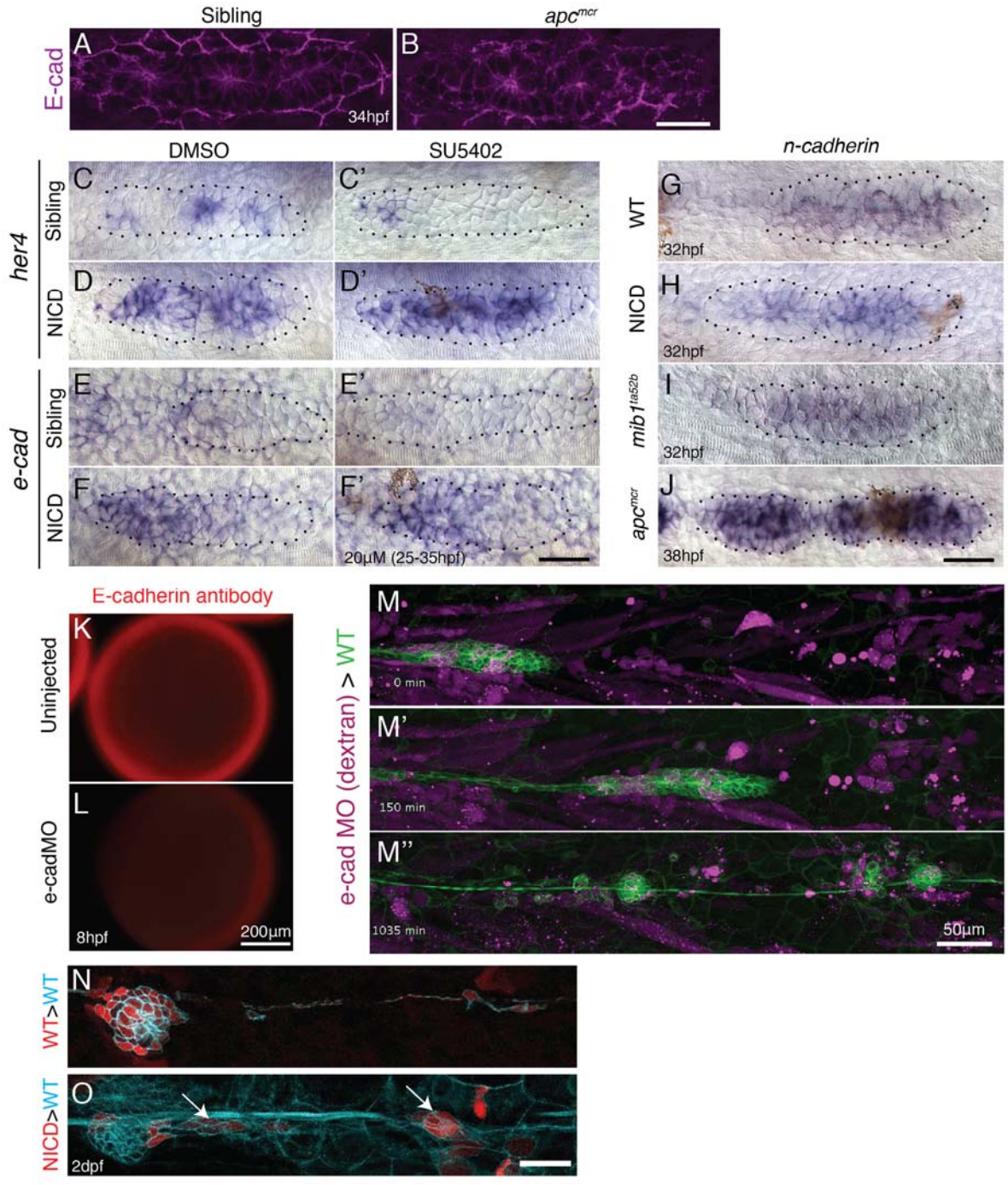

Figure 4-2. E-cadherin deficiency does not disrupt proneuromast formation
(A and B) Wnt signaling upregulates E-cadherin antibody expression in the posterior lateral line primordium. Scale bar is 50μm. (C-F') Notch regulates *e-cadherin* expression downstream of Fgf signaling. (C and C') The Fgfr1 inhibitor SU5402 depletes the expression of the Notch target gene *her4* in the primordium.

(D and D') NICD induces *her4* in the absence of Fgf signaling. (E and E') Fgf is required to induce *e-cadherin* in the primordium. (F and F') (F) In NICD primordia, *e-cadherin* is upregulated, even in the absence of Fgf signaling (F'), therefore, *e-cadherin* is a Notch target downstream of Fgf signaling. (G-J) *n-cadherin* expression is unchanged in NICD and *mib1*^{ta52b} primordia (I). *n-cadherin* is induced by Wnt signaling (J).
(K-L) Injection of the translation blocking *e-cadherin* morpholino significantly reduces E-cadherin antibody expression in a 8hpf embryo (L). (M-M'') Still images taken at different time points of a timelapse recording of a wildtype primordium in green that contains transplanted e-cadherin morpholino injected cells. Transplantation of e-cadherin morpholino injected cells into a wildtype host does not disrupt proneuromast formation. (O) Transplanted NICD cells form clusters (marked with the white arrows), which is not observed when wildtype cells (N) are transplanted into a wildtype host (quantification in Figure 7K). All scale bars are 25µm, unless stated otherwise. This figure is reprinted from Kozlovskaja-Gumbrienė et al. (2017).

To determine *e-cadherin* function in proneuromast formation, we transplanted *e-cadherin* morphant cells into wildtype embryos, as *e-cadherin* mutants die during epiboly (Figure 4-2K-M'';(Kane et al., 2005)). Evidently, *e-cadherin* deficient cells do not affect neuromast formation even when almost the entire neuromast consists of morphant cells, which is most likely due to functional redundancy with other cell adhesion molecules (Figure 4-2M-M'').

In order to test if NICD affects cell adhesion and sorting themselves out, we analysed transplanted NICD cell behavior in wildtype host. First, we quantified if NICD cells preferentially contribute to proneuromast or interneuromast population. Our analysis revealed that NICD and wildtype cells have equal preference to either lateral line cell type, again demonstrating that Notch does not exert its function in lateral line organogenesis through a cell fate switch (Figure 4-1J). Nonetheless, NICD cells that contributed to the interneuromast cell population were more prone to form clusters of 2 or more cells, whereas wildtype cells usually align into a string (Figure 4-1I-I''', arrow and Figure 4-1K; Figure 4-2N,O). Nearly 76% of NICD cells formed clusters compared to 13% of wildtype cells. Together with the finding that NICD cells contribute to larger neuromast formation in wildtype hosts, we conclude that Notch overexpression regulates cell adhesion.

4.2.3 Notch signaling upregulates apical junction complex molecules

To identify genes that are transcriptionally regulated by Notch signaling during proneuromast formation we isolated GFP positive cells from dissected 36 hpf tails of *Tg(cldnB;lynGFP);Tg(cldnB:gal4)* x *Tg(UAS:nicd)* and sibling *Tg(cldnB;lynGFP);Tg(cldnB:gal4)* embryos by FACS sorting and performed RNASeq analysis. We determined 187 genes that were upregulated in the NICD lateral line compared to wildtype controls (not shown). The most enriched cellular component revealed by GO term analysis is 'apical junction complex', containing the tight junction components *claudinb (cldn)*, *claudina (cldna)*, *claudine (cldne)* and *cingulinb (cgnb)* (Figure 4-1O-P and R-S', Appendix Figure 3). Also, high enrichment was evident for 'actin cytoskeleton' genes, such as *formin1 (fmn1)*, *myo5c*, *baiap2b* and *cgnb* (not shown). Cgnb is a junctional adaptor that links F-actin to tight junctions and inhibits RhoA signaling (Aijaz et al., 2005; Terry et al., 2011; Van Itallie and Anderson, 2014). Other molecules that interact with apical junction complex are also upregulated, such as *rab25a*, a Rab11 GTPase family member, as is *celsr2*, an atypical cadherin (Figure 4-1X-Y'). As was mentioned above, Celsr1, if reduced, disrupts otic vesicle formation in chicken embryos because of the loss of cell apical constrictions due to perturbed actomyosin recruitment to the apical junctional complex (Sai et al., 2014). RNASeq analysis also revealed that *cd9b*, a Tetraspanin family member implicated in cell-matrix adhesion and Sdf1 (Cxcl12a) mediated migration is also upregulated by Notch signaling (Figure 4-1L-M';(Arnaud et al., 2015; Leung et al., 2011)). Our in situ analyses with a number of candidate adhesion molecules also demonstrated that *epcam* is strongly upregulated by Notch signaling (Figure 4-1U-V'). Conversly, multiple cell adhesion related genes were downregulated in *mib1* mutants, supporting the finding that Notch regulates apical junction complex molecules (Figure 4-1N-Z').

To test if apical junction associated genes are responsible for large lateral organ

formation, we injected *cldnb* morpholino into wildtype embryos, and also tested *celsr2*^{rw71} mutants for lateral line phenotype (Kwong and Perry, 2013; Wada et al., 2006). However, similar to *e-cadherin* morphant cells, there was no defect in rosettogenesis, likely due to the presence of other *claudins* and *celsr1a/1b* in the primordium (data not shown). Likewise, *epcam* mutants do not have a lateral line phenotype (Slanchev et al., 2009). The *cd9b* function has been previously disrupted by morpholino injection, but as this knockdown strategy can be toxic, it is currently unclear if the observed neuromast formation defect is real and therefore requires further investigation (Aman et al., 2011; Gallardo et al., 2010).

Our analysis has revealed that (a) cell adhesion is upregulated in NICD cells, as transplanted cells form clusters and (b) cell adhesion molecules act redundantly as their individual knockdown does not cause a neuromast malformation phenotype. Since, apical junctional complex was the most highly enriched GO term in NICD primordia, and NICD-positive cells cluster together, we conclude that Notch signaling induces proneuromast formation by regulating a combination of cell-cell adhesion proteins and their accessory proteins.

4.3 Discussion and Future directions

4.3.1 Notch signaling regulates apical junctional complex genes

RNASeq and GO term analyses of FACS isolated primordium cells revealed that members of the epithelial apical junctional complex (AJC) were upregulated in NICD embryos. Taking into consideration that Notch also upregulates E-cadherin expression and transplanted NICD cells coalesce (Figure 4-1D-E'',K and Figure 4-2O), we hypothesize that an increase in cell adhesion is driving proneuromast enlargement. However, transplanted E-cadherin morphant cells do not disrupt lateral line rosettogenesis likely due to a redundancy with other adhesion molecules, such as *epcam* and *claudins*. The *epcam*

(*tacstg*) mutant displays compromised epithelial morphogenesis during zebrafish gastrulation movements, and its loss does not disrupt neuromast formation suggesting that epcam acts redundantly with other adhesion molecules in the primordium (Slanchev et al., 2009). Along these lines, Claudin-7 upregulation was shown to induce epithelial characteristics in the mouse colon (Bhat et al., 2015), however the lateral line formation remained normal in the *claudinb* morphants (not shown). The finding that the knockdown of individual cell adhesion or tight junction elements does not disrupt proneuromast formation is reminiscent to the collectively migrating *Drosophila* boarder cells, which lose their cohesiveness only when JNK signaling is inhibited, which is an upstream regulator of multiple downstream targets (Llense and Martin-Blanco, 2008).

Interestingly, basolateral genes *lgl1* and *lgl2* were also implicated in proneuromast formation. Their combined downregulation was sufficient to disrupt most nascent rosette generation in the primordium (Hava et al., 2009). Lgl proteins act upstream of Notch signaling, as the loss of *lgl1* in the zebrafish retina induces Notch expression, and in the mouse brain *lgl1* positively regulates Notch inhibitor Numb (Clark et al., 2012; Klezovitch et al., 2004). In NICD primordia *lgl2* expression is normal (data not shown), which suggests that possibly *lgl2* acts upstream of Notch in the lateral line as well. It is important to investigate whether *lgl1/2* is regulated by Fgf signaling, which could possibly be a link between Fgf and Notch signaling (see above). If Notch signaling is indeed regulated by cell polarity genes and then acts on cell adhesion genes, this establishes an interesting Notch signaling function in cell polarity regulation.

Redundancy is a limiting factor in studying the loss of cell adhesion phenotype. However, it would be interesting to understand how cell adhesion disruption affects primordium morphology. Do cells apically constrict, but cannot organize into rosettes, or whether the apical-basal cell polarity is also disrupted when cell adhesion proteins are

limited and, thus, primordium fragments similar to lateral line phenotype in *mib1* mutants. To overcome the cell adhesion protein redundancy problem, we could try removing several core adherens and tight junction members simultaneously, such as E-cadherin and Occludin. However, even though occludins anchor multiple tigh junction proteins to the cell membrane, our strategy might still be insufficient to disrupt cell-cell adhesion since some molecules, such as claudins do not interact with occludins.

Chapter 5

Notch signaling is an integral part of the Wnt/Fgf network that regulates posterior lateral line morphogenesis

5.1 Introduction

Collective cell migration and primordium morphogenesis relies on interaction between Wnt/β-catenin and Fgf signaling (Aman and Piotrowski, 2008; Chitnis et al., 2012). It is therefore important to understand how Notch signaling fits into this gene interaction network. Wnt/β-catenin signaling is activated in the leading region of the primordium and it induces Fgf in the trailing part. However, both pathways repress each other by activating inhibitors in their respective expression domains (*dkk1b* and *sef/dusp6*) (Aman and Piotrowski, 2008; Matsuda et al., 2013). Fgf signaling transcriptionally activates *notch3* receptor in the support cells and *deltaa* and *atoh1a* in the hair cell progenitors in the forming proneuromasts in the primordium, however if Notch signaling also acts downstream of Wnt signaling has not been investigated (Nechiporuk and Raible, 2008). From the recent studies in the mature neuromasts, we know that Notch negatively feeds back on Wnt signaling, however this interaction has not been tested in the primordium context (Romero-Carvajal et al., 2015).

The Wnt/β-catenin/Fgf feedback system is not only critical for primordium subdivision into morphologicaly distinct domains, but also maintains a proneuromast deposition zone at a defined distance from the leading part of the primordium (Aman et al., 2011). As the primordium grows through cell proliferation, existing proneuromasts are progressively displaced into the deposition zone where they slow down and ultimately get deposited. The deposition zone is marked by chemokine receptor *cxcr7b* expression and cells begin expressing this gene only when they are displaced into the trailing domain

behind the inhibitory influence of Wnt/β-catenin signaling in the leading domain (Aman et al., 2011). It is important to determine how Notch signaling fits into this interplay and whether besides regulating proneuromast formation it also affects deposition downstream of Fgf signaling in the primordium.

Another important aspect, which regulates proneuromast deposition rate is the speed at which the primordium travels along the trunk of the embryo. It has been hypothesized that reducing the primordium migration speed without affecting cell proliferation rate, which already by itself regulates neuromast deposition, would increase the number of deposited proneuromasts by prolonging the time primordia have to complete deposition cycles (Aman et al., 2011). Again, primordium speed has never been addressed in respect to Notch manipulations in the lateral line, and therefore it is important to understand how Notch signaling functions in regards to proneuromast deposition regulation.

Cell adhesion governs the internal organization of primordia cells into sensory organs, however adhesion molecules also couple the primordium internal mechanics with the microenvironment through which it migrates and deposits sensory organs. Specifically, extracellular domains of adhesion molecules, such as integrins which coalesce and form focal adhesions, bind to components of extracellular matrix (ECM), while cytoplasmic tails interact with the cytoskeleton and signaling proteins (Breau and Schneider-Maunoury, 2015; Burridge and Chrzanowska-Wodnicka, 1996). Cell-matrix adhesion provides anchoring sites for pulling forces required for primordium movement forward and probably neuromast deposition, however recently it has been also recognized that these cell anchoring sites transduce mechanical cues and crosstalk with signaling pathways that regulate cytoskeleton dynamics, proliferation, survival and differentiation (Hynes, 2002; Schwartz and DeSimone, 2008; Stepniak et al., 2009). In the future it will be important to

understand if and how Wnt/Fgf and Notch signaling interplay regulates primordium migration and neuromast deposition through cell-matrix contact regulation.

5.2 Results

5.2.1 Notch acts downstream of Wnt signaling

Up until now, we only knew a few aspects of how the Notch signaling pathway integrates into a signaling network that governs primordium development. First, Fgf signaling is required for transcriptional regulation of Notch in the primordium (Figure 3-1S'; (Nechiporuk and Raible, 2008) and second, Notch inhibits *atoh1a* positive cells within the support cells and thereby exerts its lateral inhibition function by restricting hair cell fate to the central cells in the proneuromast (Matsuda and Chitnis, 2010). However, it is important to determine the interaction between Wnt and Notch signaling and how their interplay affects proneuromast formation.

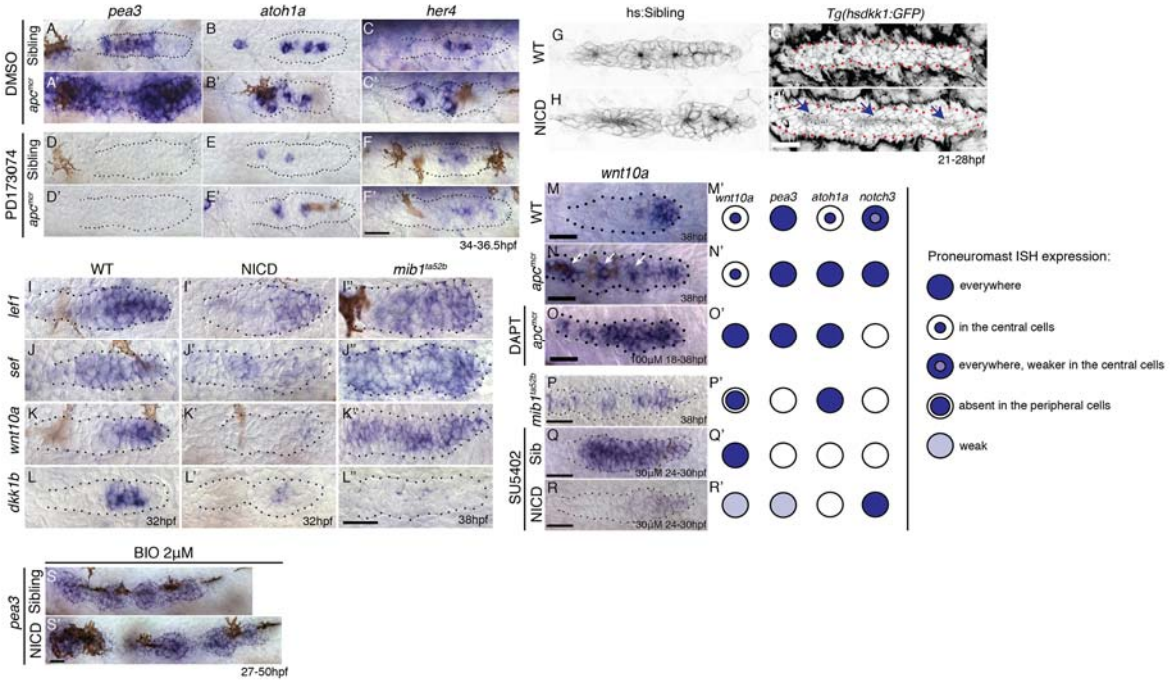

Figure 5-1. Wnt induces Notch signaling in the primordium via Fgf
(A and A') The expression of the Fgf target *pea3* is strongly increased in *apc*^{mcr} primordia at 36.5hpf. (B and B') In *apc*^{mcr} primordia (B') *atoh1a* expression is increased compared to a sibling (B), but it still is restricted to individual cells. (C and C') *her4* expression is slightly expanded in the primordium after Wnt upregulation by *apc*^{mcr} (C'). (D-F') The Fgf inhibitor PD173074 inhibits the expression of *pea3* (D') and prevents the upregulation of *atoh1a* (E'). The expression of *atoh1a* is lost in the first proneuromast, as *atoh1a* is Fgf dependent. The more trailing central cells express *atoh1a* because it becomes self-regulatory. The Fgf inhibitor downregulates *her4* in sibling (F) and *apc*^{mcr} mutant primordia (F'). (G-H') Loss of Wnt signaling in the primordium by heat-shock induction of *dkk1b* does not disrupt proneuromast formation in NICD (H') compared to heat-shocked sibling primordia (G') suggesting that Notch acts downstream of Wnt and Fgf in proneuromast formation. (I-L'') Notch inhibits Wnt signaling in the primordium. The expression of Wnt targets *lef1* (I'), *sef* (J'), *wnt10a* (K') and *dkk1b* (L') expression is downregulated in NICD primordia. Conversely, in *mib1*^{ta52b} primordia *lef1* (I''), *sef* (J'') and *wnt10a* (K'') are upregulated. (L'') *dkk1b* is downregulated in *mib1*^{ta52b} primordia, because Fgf signaling is secondarily lost (see text). (M-R') *wnt10a* expression expands only in the absence of Notch signaling in the primordium. (M-N') In *apc*^{mcr} primordia *wnt10a* expands towards the trailing region but is restricted to more central cells (arrows) (N,N'). (O,O') Downregulation of Notch with the γ-secretase inhibitor DAPT, causes a much more complete expansion of *wnt10a* in the trailing region of *apc*^{mcr} primordia, demonstrating that Notch signaling inhibits *wnt10a* in the primordium. (Q-R') *wnt10a* expression is expanded in the absence of Notch signaling when primordia are treated with Fgf inhibitor (Q,Q') but is once again restricted to the leading region of the primordium if NICD is activated in the absence of Fgf (R,R'). (S) Treatment of sibling embryos with the GSK3β inhibitor and Wnt activator BIO causes the upregulation of *pea3*. (S') BIO treatment of NICD embryos rescues the loss of *pea3* in NICD primordia demonstrating that Wnt activates Fgf signaling upstream of Notch and that the loss of Fgf signaling in NICD is secondary to the loss of Wnt signaling. Wnt signaling is lost because Notch negatively feeds back to Wnt downstream of Fgf. All scale bars are 25μm. This figure is reprinted from Kozlovskaja-Gumbrienė et al. (2017).

In the Wnt overexpressing *apc* mutants and embryos treated with GSK3-β inhibitor BIO, the Fgf genes *pea3* and *atoh1a* are upregulated as well as the Notch target *her4* (Figure 5-1A-A', B-B', C-C' and Figure 5-2A-D). Also, Notch reporter expression is greatly elevated in the *apc* mutant L1 neuromast and primordia (Figure 5-2E-H'). To determine if Wnt regulates Notch signaling through Fgf or whether it directly affects Notch, we treated sibling and *apc* mutants with the Fgfr1 inhibitor PD173074. The loss of Fgf impedes *pea3*, *atoh1a* and *her4* in sibling and *apc* mutants, especially in the youngest, leading proneuromasts (Figure 5-1D-F'), which shows that Wnt is not sufficient to induce *atoh1a* or *her4* without the presence of Fgf (Figure 5-1E,E' and F,F'). Also, proneuromast formation is not impeded in the primordia that lack Wnt signaling in the presence of NICD, demonstrating that Notch signaling acts downstream of Wnt signaling (Figure 5-1G-H'). To conclude, Wnt activates Fgf signaling which then regulates *atoh1a*, *delta* ligands and Notch signaling in the primordium (Figure 5-4).

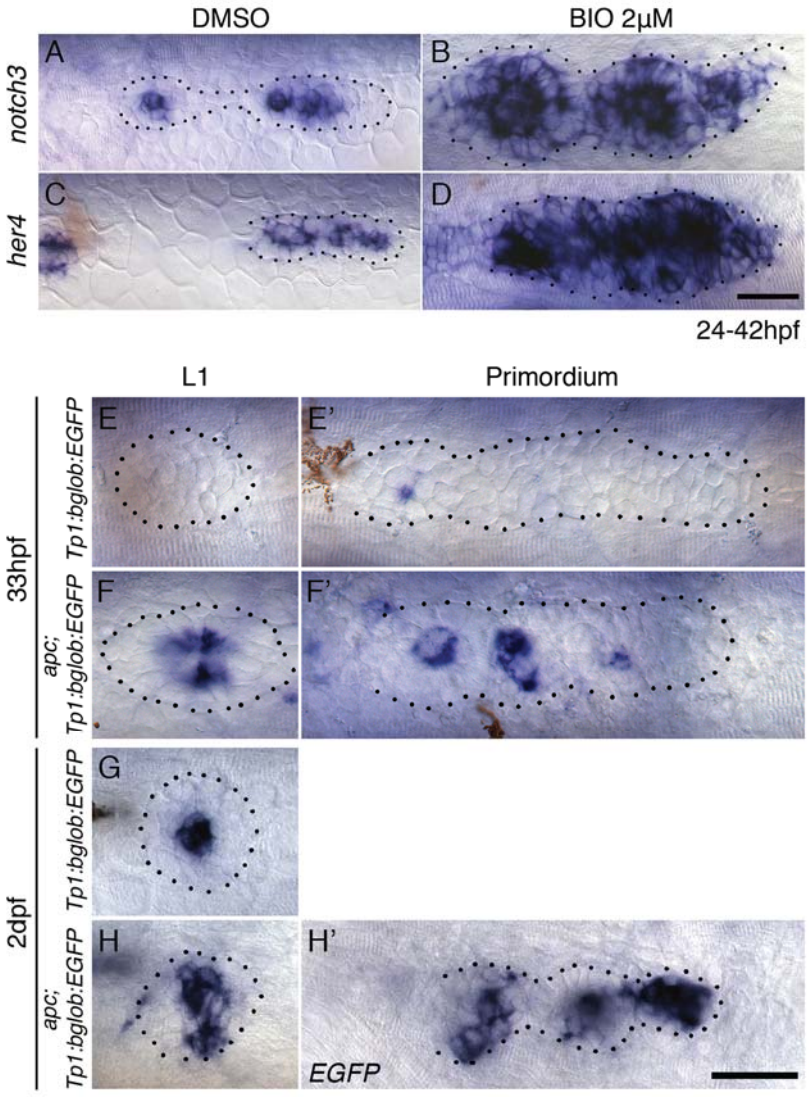

Figure 5-2. Wnt signaling induces Notch signaling
(A-B) The upregulation of Wnt signaling by exposure to the GSK3β inhibitor BIO leads to strong upregulation of the Notch target *notch3* and *her4* (C-D). Scale bar is 25µm. (E-H') The *egfp* expression of the Notch reporter *Tg(Tp1bglob:EGFP)* is upregulated in *apc* primordia and neuromast (F,F') compared to a wildtype sibling (E,E') at 33hpf and 2dpf (G-H').
This figure is modified from Kozlovskaja-Gumbrienė et al. (2017).

5.2.2 Notch inhibits Wnt signaling in the primordium

Next we wanted to assess if Notch regulates Wnt signaling in the primordium. In NICD primordia Wnt target genes *lef1*, *wnt10a* and *sef* are largely suppressed, whereas in *mib1* mutants these genes expand into the trailing domain of the primordium (Figure 5-1I-K'',P). Interestingly, the Fgf target and Wnt inhibitor *dkk1b* is also strongly reduced in the NICD primordia (as well as in *mib1*), but this reduction is not sufficient to enable *wnt10a*

expansion (Figure 5-1L-L''). This result suggests that Notch supresses *wnt10a* by a feedback interaction which has not been previously described in the primordium. Accordingly, *wnt10a* does not expand into all primordia cells, but rather is constricted to the central cells in the *apc* proneuromasts (Figure 5-1M and N, arrows). To test if this restriction occurs due to the presence of Notch we treated *apc* primordia with the γ-secretase inhibitor DAPT, which indeed alleviates *wnt10a* repression from the central cells and allows its expansion into the periphery of the primordium (Figure 5-1O and O'). Additionaly, we showed that *wnt10a* expression is still suppressed in the NICD primordia treated with Fgf inhibitor, whereas in the wildtype primordia *wnt10a* expands in the absence of Fgf signaling (Figure 5-1Q-R). This experiment rules out the possibility that Fgf directly inhibits *wnt10a*. Most likely, Fgf induces Notch, which in turn inhibits *wnt10a* expression in the trailing part of the primordium. In conclusion, as illustrated by the schematic representation of proneuromast signaling, *wnt10a* expression correlates only with changes in Wnt and Notch signaling (*notch3*, Figure 5-1M'-R'), as *wnt10a* is expands irrespective of the presence of *pea3* and *atoh1a* expression (Figure 5-1O, O' and Q, Q'). Thus, the analysis of Wnt/Fgf/Notch signaling in NICD primordia reveals an Fgf/dkk1b independent strategy for Wnt regulation in the primordium.

5.2.3 Notch represses Fgf by inhibiting Wnt signaling

Our finding that Notch negatively feeds back on Wnt signaling also explains Fgf repression in the NICD primordia. Fgf signaling in the most nascent proneuromast region relies on activation by Wnt signaling in the leading part of the primordium. Later, in the more mature proneuromasts, *atoh1*a signaling takes the lead in regulating Fgf expression and Wnt is not required anymore (Aman and Piotrowski, 2008; Matsuda and Chitnis, 2010). Therefore, the loss of Fgf in the NICD primordia can be attributed to both Notch functions:

inhibition of Wnt signaling and inhibition of *atoh1a* in the trailing region of the primordium. We treated NICD embryos with the GSK3-β inhibitor BIO, which resurrected *pea3* expression in the lateral line (Figure 5-1S,S'). This finding demonstrates that Notch regulates Fgf through Wnt inhibition in the primordium.

5.2.4 Notch signaling regulates proneuromast deposition rate

The analysis of neuromast spacing reveals that NICD primordia deposit sensory organs closer to each other starting with L2 neuromasts (Figure 5-3A,B). As the average distance from the ear to the tail tip between the NICD and widtype sibling embryos is not significantly different, our data suggest that Notch signaling increases the neuromast deposition rate. It is already established that primordium cell proliferation rate and chemokine signaling regulated by Wnt and Fgf systems are the main neuromast deposition regulators. However, such factors as primordium migration speed and differential cell adhesion must be also considered. We wanted to investigate how the NICD phenotype contributes to our current understanding about neuromast deposition.

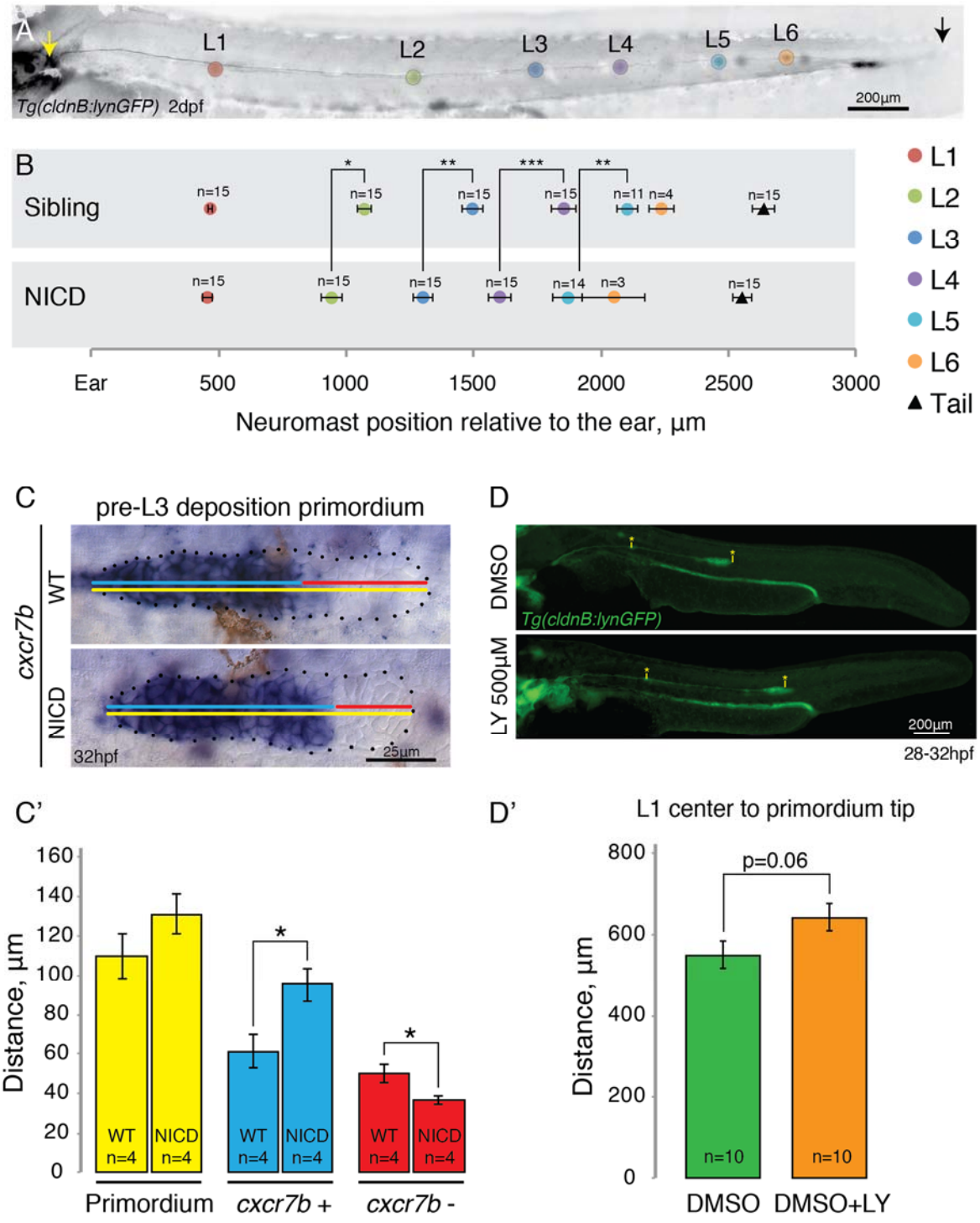

Figure 5-3. Notch signaling regulates proneuromast deposition rate

(A-B) Neuromasts are deposited closer to each other in the NICD posterior lateral line. (C and C') *cxcr7b* expression domain (blue) is expanded in the NICD primordium at the expense of the *cxcr7b*-free zone in the leading domain (red). The total length is not significantly different between wildtype and NICD primordia (yellow) at 32hpf. (D and D') The wildtype primordia treated with the Notch inhibitor LY411575 migrate further than control primordia. (D') The average distance from the middle of L1 neuromast to the primordium tip. Distance was measured by using the Freehand line tool in Fiji software.

To determine the effet of Notch on neuromast spacing we first analysed if chemokine gene expression patterns are changed in the primordium. The expression of the chemokine ligand *cxcl12a* and the receptor *cxcr4b* is not changed in NICD primordia (not shown), as they are still restricted to a narrow stripe along the myoseptum and the leading domain of the primordium, respectively (Aman et al., 2011). However, the *cxcr7b* expression domain is significantly larger in the Notch overexpressing primordia at 32 hpf (Figure 5-3C,C'). As primordia size at 32 hpf are similar between NICD and wildtype embryos, we hypothesize that the expanded *cxcr7b* expression invades into the Wnt signaling domain. This result is expected as Wnt is a negative regulator of *cxcr7b* expression and that Notch inhibits Wnt signaling in the primordium (Figure 5-1I'-K'; (Aman and Piotrowski, 2008)). It is hypothesized that *cxcr7b* expressing cells are predisposed for sooner deposition as they are masked from sensing *cxcl12a* (Aman et al., 2011). Our data shows that cells transition into the *cxcr7b* domain sooner in the NICD primordia than in the wildtype primordia, which could explain why NICD primordia deposit neuromasts in shorter intervals. In conclusion, Notch signaling likely controls lateral line organ spacing by upregulating *cxcr7b* expression through a negative feed back on Wnt signaling in the primordium, however this needs to be further investigated.

Previously, it has been hypothesized that slower migrating primordia with no change in cell proliferation would deposit neuromasts closer to each other (Aman et al., 2011). We demonstrate that Notch overexpressing cells proliferate similarly to wildtype cells in the primordium (Figure 2-5H). Therefore, we wanted test if Notch the primordium migration speed. Indeed, the primordia migration in NICD embryos is slower (not shown). Conversly, our preliminary data suggests that wildtype primordia treated with the Notch inhibitor LY411575 tend to migrate further during the same period of time than the control sibling primordia (Figure 5-3D,D'). However, we need further investigation to conclude that the

altered primordium speed affects neuromast deposition rate.

These data demonstrate that Notch signaling potentially regulates neuromast deposition rates by two different mechanisms: 1) by increasing the number of cells exposed to the presumed neuromast deposition factor *cxcr7b* and 2) by regulating the speed at which the primordium migrates.

5.3 Discussion and Future directions

5.3.1 Notch regulates neuromast formation downstream of Wnt/Fgf signaling

Our results suggest that cell signaling between central hair cell precursors and surrounding support cells is slightly different between the most nascent and more mature rosettes (Figure 5-4B,C; (Matsuda and Chitnis, 2010)). In the first forming proneuromast *fgf3/10a* is induced by Wnt in all cells, whereas in trailing, more mature rosettes *fgf10a* ligand is restricted to a central cell. This restriction occurs due to Notch signaling that inhibits *atoh1a* expression in the supporting cells (Figure 5-4C). Interestingly, even though Fgf ligands are initially expressed in a broader domain, the downstream targets *atoh1a* and *delta* ligands are imediately restricted to a central hair cell progenitor. Similarly, *wnt10a* is only expressed in one central cell in the proneuromast. This immediate restriction of *atoh1a* differs from findings in *Drosphila* where *atoh1* is first broadly expressed marking prosensory domain and only later, at cell specification stage becomes gradually restricted (Jarman et al., 1995; Millimaki et al., 2007). We still do not understand how this restriction occurs so quickly in the primordium. Another difference between signaling in the nascent and more mature rosette have previously been described, whereby in the trailing proneuromasts Fgf is no longer regulated by Wnt signaling, but rather through the induction by Atoh1a (Figure 5-4C; (Matsuda and Chitnis, 2010)). Intriguingly, *atoh1a* expression is independent of Fgf and becomes self-regulatory in the mature proneuromasts (Matsuda and Chitnis, 2010;

Millimaki et al., 2007). Even though Fgf and Notch signaling are highly expressed in the supporting cells, some expression is still maintained in the central cells, as evidenced by *pea3*, *her4* and *notch3* expression, albeit at lower levels (Figure 3-1Q,S and Figure 2-1I). Presumably, this low level of Notch signaling is sufficient to maintain central cell integrity in proneuromasts through the apical constriction and cell adhesion regulation.

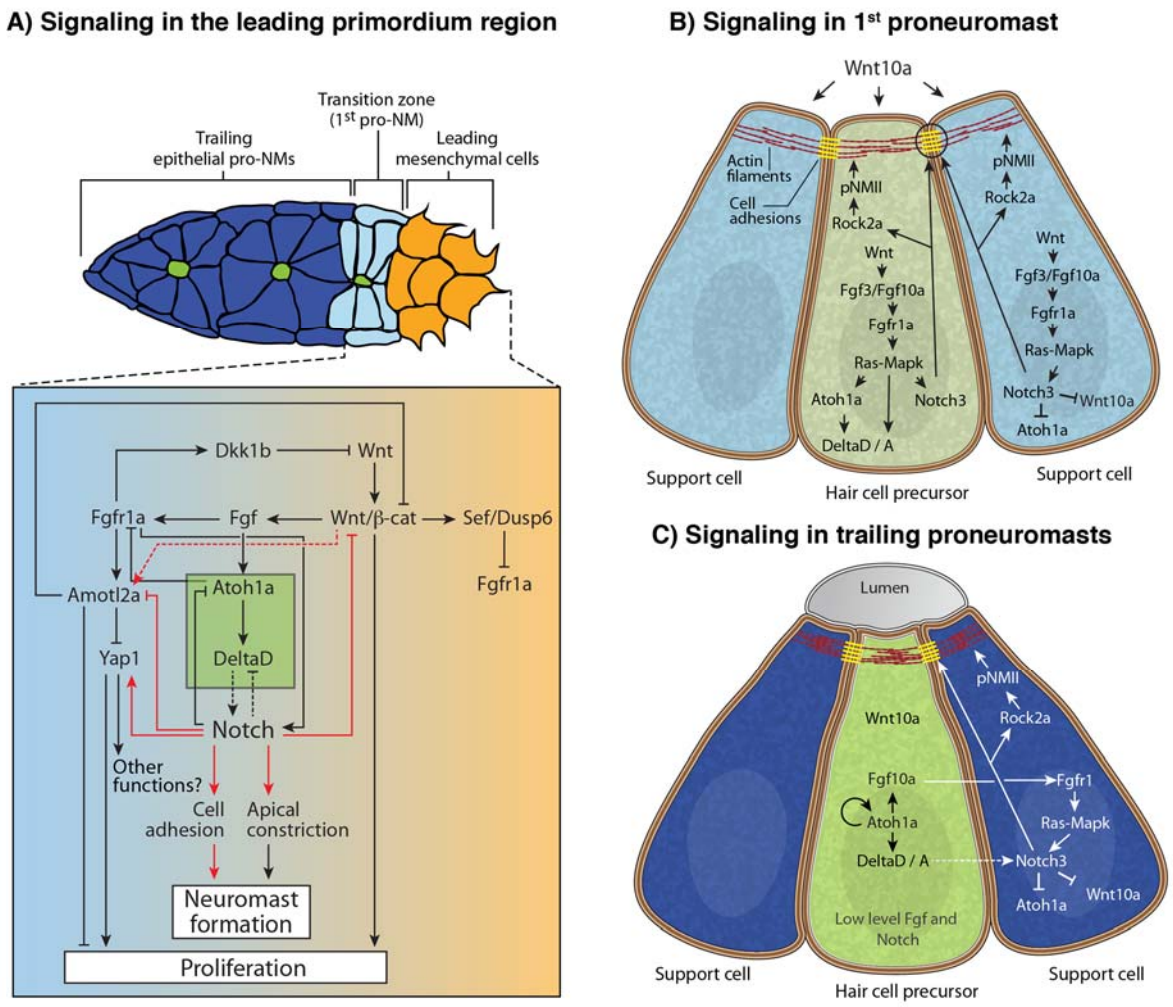

Figure 5-4. Model of the signaling interactions between Wnt, Fgf and Notch
Arrows in red indicate interactions described in this study. Other interactions are described in (Agarwala et al., 2015; Chitnis et al., 2012; Matsuda and Chitnis, 2010). Notch acts downstream of Wnt and Fgf signaling to form proneuromasts in the posterior lateral line via the upregulation of cell adhesion or/and cell apical constriction. Notch signaling also inhibits *amotl2a* and promotes *yap1* transcription, which induces some of the proliferation observed in the primordium. However, *yap1* does not affect neuromast size. Notch also negatively feeds back to restrict Wnt signaling, thus being an essential component of the signaling interactions that coordinate migration with organ formation.

(B) Signaling in the most nascent proneuromast. Fgf signaling (*fgf3/10a* and *fgfr1*) is induced by Wnt ligands in all proneuromast cells where it then induces *atoh1a* and Notch signaling (Chitnis et al., 2012). As a result, Notch regulates apical constriction and cell adhesion in all proneuromast cells. (C) Signaling in the trailing proneuromasts. Fgf and Delta ligand expression now depends on Atoh1a and not Wnt anymore in central hair cell precursors (green). Fgf signaling is activated through Fgfr1 in the peripheral cells where it also induces Notch signaling (Matsuda and Chitnis, 2010). Notch signaling activates apical constriction and cell adhesion machinery in the support cells. This figure is reprinted from Kozlovskaja-Gumbrienė et al. (2017).

5.3.2 Non-canonical Notch signaling in the posterior lateral line

Although Notch signaling mediates a number of biological processes through the canonical pathway, a ligand- or transcription independent (non-canonical) function has also been reported in cell culture and *in vivo* (reviewed in Andersen et al. (2012)). However, non-canonical Notch signaling has never been addressed in the posterior lateral line. We could test if disrupting the canonical, Suppressor of Hairless (SuH)-dependent Notch transcriptional function is sufficient to rescue the NICD enlarged rosette phenotype. For example, we could generate transgenic lines that are missing the NICD nuclear localization sequence or mate NICD transgenic fish to SuH mutants and analyze their offsprings. Interestingly, a novel non-canonical role for Notch in antagonizing Wnt/β-catenin is seen in multiple species (Acosta et al., 2011; Endo et al., 2002; Kwon et al., 2011; Muñoz-Descalzo et al., 2011). *Drosophila*, membrane bound NICD inhibits β-catenin by sequestering it in the cytoplasm and targeting it for proteasome-mediated degradation (Logan and Nusse, 2004; Winston et al., 1999). Thus, as NICD overexpression suppresses Wnt/β-catenin target gene expression in the primordium (Figure 5-1I-K'), it is important to test if this inhibition is only transcriptional or if NICD possibly antagonizes Wnt/β-catenin signaling also in a non-canonical manner. Intriguingly, Notch inhibits active β-catenin independent of GSK3-β function (Muñoz-Descalzo et al., 2011). Therefore, it would be interesting to test if Wnt/β-catenin targets, such as *lef1* and *wnt10a* are still inhibited in the NICD overexpressing primordia treated with a GSK3-β inhibitor BIO.

5.3.3 Notch signaling and proneuromast deposition rate

We showed that Notch signaling does not regulate proneuromast deposition rate by changing cell proliferation in the primordium (Figure 2-5H), however another possibility is primordium migration speed regulation through Notch effect on Fgf signaling. Primordia deposit neuromasts further away form each other upon Fgf signaling reduction and, conversely, the distance between neuromasts is decreased when Fgf is overexpressed in the lateral line (Durdu et al., 2014). However, our study has demonstrated that the distance between NICD neuromasts is diminished, even though Fgf signaling is largely reduced in NICD primordia. As we now know that Notch elicits its proneuromast formation function downstream of Fgf signaling, it is possible that the neuromast deposition rate is also regulated by Notch signaling through the *cxcr7b* domain expansion in the primordium (Figure 5-3C,C').

Primordium migration speed is another important parameter that regulates the neuromast deposition rate. Presumably, a slower migrating primordium deposits more neuromasts, if primordium cell proliferation is not altered. Our preliminary data suggest that Notch signaling has a negative impact on primordium movement (Figure 5-3D,D'). Thus, it would be intesting to investigate how Notch regulates primordium migration speed. Possibly, as the primordium moves along the embryo's trunk it maintains transient attachments to the basal lamina and the skin. Therefore, we could test if Notch signaling modulates cell-to-substrate adhesion genes, such as integrins, which would presumably make the primordium migrate slower. We have already performed an antibody staining in the wildtype primordia against the Focal adhesion kinase (FAK), which localizes to junctions and acts downstream of integrins to regulate organization of the actin cytoskeleton (Arnold et al., 2013). FAK is expressed in the apical constrictions (Appendix Figure 4, arrows) of proneuromasts in the primordium and in between the somites (Appendix Figure 4).

Interestingly, this suggests that primordium maintains contacts with the skin through the cell apical area, which is much larger in the NICD embryos (Figure 2-1G-H') and therefore could explain why NICD primordia migrate slower, however this needs further investigation. Alternatively, it is possible that the primordium attachment to the substrate contribution to migration is minor and primordium tends to migrate along the myoseptum just because of its groove, which provides more space between the skin and the muscle and makes movement less restricted compared to other places along the trunk of the embryo. However, we would need to knock-down integrin function in the lateral line to test if cell-matrix adhesion regulates primordia migration and/or proneuromast deposition.

Chapter 6

Summary

Together, our experiments demonstrate that Notch signaling is an essential part of the feedback loop between Wnt/β-catenin and Fgf signaling that coordinates cell migration with sensory cell specification and organ morphogenesis. Importantly, we show that Notch signaling acts cell-autonomously and downstream of Fgf signaling in lateral line organ formation via the regulation of cell adhesion and tight junction molecules. Therefore, Notch is involved in sensory organ rosette self-organization that is analogous to rosettes and that precede lumen formation in pre-implantation mouse embryos (Bedzhov and Zernicka-Goetz, 2014). Similarly, rosette formations occur during *C. elegans* gastrulation but are also characteristic for some brain tumors (Pohl et al., 2012; Wippold and Perry, 2006). We speculate that Notch signaling might be involved in these other biological contexts as well. Therefore, our results do not only inform lateral line biology but also contribute to our understanding of morphogenesis of other organs and tissues and how rosettes form in certain brain tumors.

Chapter 7

Materials and methods

7.1 Chemicals and reagents

Reagent name	Catalog number	Company
Acetic acid	A6283	Sigma-Aldrich
BCIP (150mg/3mL)	11383221001	Roche
Bouin's fixative	16045	Polysciences
BSA	A7906	Sigma-Aldrich
Ethanol (EtOH), 200 proof	DSP-MD-43	Koptec
Formamide (dionized)	606	VWR
Glyo-Fixx	6764262	Shandon
LiCl	L9650	Sigma
LMP	V3841	Promega
Methanol (MeOH)	BD1135	VWR
$MgCl_2$	2444-01	VWR
NaCl	BP358-212	Fisher
NBT (300mg/3mL)	11383213001	Roche
PBS	AM9625	Ambion
PFA (4%)	J542	VWR
Phenol Red	P0290	Sigma-Aldrich
Proteinase K	3115828001	Roche
Torula RNA	R6625	Sigma-Aldrich
Tricaine (MS-222)	No Catalog #	Western Chemical
Tris	0497	VWR
Triton X-100	T9284	Sigma-Aldrich
Tween 20	P2287	Sigma-Aldrich

7.2 Solutions and media

0.5X E2 medium: 7.5mM NaCl, 0.25mM KCL, 0.5mM $MgSO_4$, 0.075mM KH_2PO_4, 0.025mM Na_2HPO_4, 0.5mM $CaCl_2$, 0.35mM $NaHCO_3$.

PBST: 0.1% Tween 20 in 1x PBS

HYB^+ solution: 50% Formamide, 5x SSC, 0.1% Tween 20, 5mg/mL Torula RNA.

NBT/BCIP staining solution: 50mM $MgCl_2$, 0.1M NaCl, 0.1M Tris, 1% Tween 20, NBT (3.4µL/mL), BCIP (3.5µL/mL).

7.3 Fish maintenance and fish strains

The following fish strains were used: *Tg(cldnb:lynGFP)*^{zf106} (Haas and Gilmour, 2006), *Tg(Tp1bglob:eGFP)*^{um13} (Parsons et al., 2009), *Tg(UAS:myc-Notch1a-intra)*^{kca3} (Scheer and Campos-Ortega, 1999), *Tg(hsp70l:Gal4-VP16)*^{VU22} (Shin et al., 2007), *apc*^{mcr} (Hurlstone et al., 2003), *mindbomb, mib1*^{ta52b} (Itoh and Chitnis, 2001), *Tg(hsp70l:dkk1b-GFP)*^{w32} (Stoick-Cooper et al., 2007), *Tg(hsp70l:dnfgfr1-EGFP)*^{pd1} (Lee et al., 2005), *Tg(hsp70:ca-fgfr1)*^{pd3} (Marques et al., 2008), *Tg(hsp70:atoh1a)*^{x20} (Millimaki et al., 2010), *Tg(UASDNshroom3)* (created by injecting plasmid: pT2dest(bidirectional UAS)-dsred-shrm3DN(520-874)) received from B. Link (Clark et al., 2012; Kwan et al., 2007), *Tg(ubi:Zebrabow)* (Pan et al., 2013), *p53*^{zdf1}, *pac*^{tm101b}, *cdh2*^{hi3644} kind gift from Anand Chandrasekhar. *Tg(-8.0cldnB:gal4vp16)*^{psi8} transgenic line was generated in the Piotrowski laboratory by Mark Lush (Kozlovskaja-Gumbrienė et al., 2017). *TgBAC(cxcr4b:H2A-GFP)p2* transgenic line was generated in the Knaut laboratory (Kozlovskaja-Gumbrienė et al., 2017). All experiments were performed according to guidelines established by the Stowers Institute IACUC review board.

7.4 Immunohistochemistry and Phalloidin staining

Embryos for Phalloidin staining were fixed for 30min in 4% paraformaldehyde (PFA), washed 3 times for 5min with 0.8% TritonX in PBS (PBT) and incubated for 2hr at room temperature (RT) with Phalloidin (Invitrogen, 1:40 in 2% PBT). For immunohistochemistry embryos were fixed in 4%PFA at 4°C for the following antibodies: c-Myc (9E10) Santa Cruz Biotechnology (sc-40) (1:500), Anti-Acetylated Tubulin (T679) Sigma-Aldrich (1:500), mouse anti-ZO1 (Zymed; 61-7300) (1:200). Glyo-fixx (Thermo Scientific, UK) at 4°C was used as a fixative for these antibodies: Di-pERK1/2 (Diphosphorylated ERK-1&2 antibody-mouse (M8159) Sigma-Aldrich) (1:500), Anti - ROCK - 2a (CT), Z - FISH- rabbit (AS-55431) (1:50), Mouse Anti-E-Cadherin (610182) BD-Biosciences (1:500), Bouin's fixative (Polysciences) was

used for Phospho-Myosin Light Chain 2 (Ser19) Antibody (#3671 Cell Signaling (1:20)), and 95% MeOH and 5% Acetic acid fixative was used for FAK (C-20) Santa Cruz Biotechnology (sc-558) (1:100).

7.5 BrdU and Pharamacological inhibitors

BrdU incorporation, Hydroxyurea and Aphidicolin treatment (inhibition of proliferation) was performed as described in (Aman et al., 2011). Rat anti-BrdU (Accurate; OBT0030G) was used at a dilution of 1:500. To visualize nuclei embryos were placed into 0.1ng/mL DAPI (Invitrogen). All chemical inhibitors were diluted in E2 medium containing 1% DMSO to concentrations as indicated in the text. Dechorionated embryos were incubated in the drug solution for different times as indicated in the text. The γ-secretase inhibitor LY411575 was purchased from Selleckchem. Other drugs were purchased from Tocris: Fgfr1a inhibitors PD173074 and SU5402, MAPK/ERK inhibitor PD0325901, GSK-3β inhibitor BIO and γ-secretase inhibitor DAPT.

7.6 Morpholinos

Morpholino antisense oligos (Morpholinos) were purchased from Gene Tools (OR, US). Morpholinos were diluted in the dionized water and Phenol Red solution (0.1% final concentration) and injected into the one cell stage embryos. The splice-blocking *yap1* morpholino (5'-AGCAACATTAACAACTCACTTTAGG-3') was injected at a concentration of 10ng/2nL (Skouloudaki et al., 2009). Translation blocking E-cadherin morpholino (5'-ATCCCACAGTTGTTACACAAGCCAT-3') was injected at a concentration of 8.4ng/2nL (Babb and Marrs, 2004).

7.7 In situ hybridization (ISH)

In situ hybridization procedures were performed as described in Kopinke et al. (2006). Briefly, RNA-probes were prepared by PCR-based technique. To generate RNA-probe template we used published primers or created primer sequences by inputting the FASTA

sequence of a gene into a Primer3 program (see below for a list of primers). *In situ* hybridization was performed on the whole-mount embryos fixed in PFA 4% for overnight at 4°C and dehydrated in MeOH (4-steps: 25%MeOH/75%PBST, 50%MeOH/50%PBST, 75%MeOH/25%PBST, 100%MeOH). Embryos were kept in MeOH in -20°C until the re-hydration (4-steps: 75%MeOH/25%PBST, 50%MeOH/50%PBST, 25%MeOH/75%PBST, PBST) just before the beginning of the *in situ* hybridization procedure. For permeabilization, embryos were incubated with Proteinase K (10µg/mL in PBST) for 1min at RT and refixed in 4% PFA for 30min at RT. Subsequently, embryos were washed 3 x 5min in PBST at RT, transferred into HYB^+ solution, and prehybridized for 14 hr at 65°C. The remaining steps were performed in the InsituPro (Intavis) robot, based on the procedures described in Piotrowski and Nüsslein-Volhard (2000). For detection, embryos were incubated in the NBT and BCIP solution. To stop the color reaction, PBST was added, followed by fixation in 4% PFA. For flat mounting, the yolk was dissected away, the embryos placed facing the myoseptum up on a microscope slide and covered with a cover slip. Specimens were photographed on a Zeiss Axio Imager 2 using AxioCam camera.

The following probes were used: *lef1*, *pea3*, *sef*, *axin2*, *fgf3*, *fgf10*, *fgfr1*, *dkk1b* (Aman and Piotrowski, 2008), *wnt10a* (Lush and Piotrowski, 2014), ***deltaa***, ***deltab***, ***deltac, deltad*** (Itoh and Chitnis, 2001), *dGFP*, *notch3*, *her4.1, atoh1a* (Jiang et al., 2014), *cxcr7b* (Dambly-Chaudière et al., 2007), *s100t* (Galanternik et al., 2015), *shroom3* (Ernst et al., 2012), *epcam* (probe cb6 from ZIRC), *celsr2* (Siddiqui et al., 2010; Wada et al., 2006), *cldne* kind gift from Ashley Bruce. The following primers were used to clone other probes: *yap1* (Fw 5'-CGACTTTCCTTGAAAACGGT-3' and Rv 5'-AAGGTGTAGTGCTGGGTTCG-3'), *stk3* (Fw 5'-GCAGTGCTTCCTTAAACTCCAAAC-3' and Rv 5'-GCAGGAATCTAGAGTAAGATGCAG-3'), *amotl2a* (Fw 5'-TGGAGAAGGTGGAAAGGATG-3' and Rv 5'-GCTGGGCTCTTCTGAATCAC-3'), *shroom1* (Fw 5'-CGTCTATGATGGGCAAACCT-3' and Rv 5'-GGCAGGTCGTATGAGATGGT-3'),

shroom2a (Fw 5'-AACAAGCAAACCCAATGGAG-3' and Rv 5'-CTTTGGAGGCGAGTTGTAGC-3'), *cdh1* (Fw 5'-TGGAAGAACAAGGACGCTCT-3' and Rv 5'-TCTCAGGGACAGATGCAGTG-3'). The following probes were cloned into pPR-T4P vector using AA18 and PR244 primers: *cldnb* (Fw 5'-CATTACCATCCCGAAACGAAAAAGCATGGCATC-3' and Rv 5'- CCAATTCTACCCGAGAGGCT GTTTCAAACGTGG-3'), *cd9b* (Fw 5'-CATTACCATCCCGTTGTGTTCACACACTCGCTG-3' and Rv 5'- CCAATTCTACCCGACAACAGGACAACCACTCGC-3').

7.8 Genotyping

Fish strain	Forward primer	Reverse primer	Product size, bp
Tg(hsp70:ca-fgfr1)^{pd3}	5'-GCAGCCTGACAGGACTTTTC-3'	5'-GATCCGACAGGTCCTTTTCA-3'	2075
Tg(hsp70:atoh1a)^{x20}	5'-GCAGCCTGACAGGACTTTTC-3'	5'-GCTGCTCTTCCTGAAGTTGG-3'	750
Tg(hsp70l:Gal4-VP16)^{VU22}	5'-CGCTACTCTCCCAAAACCAA-3'	5'-GGGTCGACCTCGAAGATACA-3'	340
Tg(UAS:myc-Notch1a-intra)^{kca3}	5'-CATCGCGTCTCAGCCTCAC-3'	5'-CGGAATCGTTTATTGGTGTCG-3'	450
p53^{zdf1}	5'-AGCTGCATGGGGGGGAT-3' (WT) 5'-AGCTGCATGGGGGGGAA-3' (Mut)	5'-GATAGCCTAGTGCGAGCACACTCT T-3'	220

7.9 Cell transplantation

Transplantation assays were performed as previously described in (Aman and Piotrowski, 2008). Briefly, donor embryos were injected with 3% lysine-fixable biotinylated-dextran AF568 (D22912) (Invitrogen, USA) at the one cell stage. Alternatively, *Tg(ubi:Zebrabow)* embryos were used as donors in Figure 4-1. Around 50 cells were transplanted from donor embryos into the lateral line region (Kozlowski et al., 1997) of host embryos at blastula stage. Embryos were allowed to develop until the required stage at 28.5°C.

7.10 Heat-shock treatments

Around 100 embryos were placed into 15mL tube filled with pre-heated E2 medium.

The tube was then immersed into the heated water bath. Heat-shock induction was done at various developmental time points, different temperature combinations and time intervals as indicated in the text. After the heat-shock, embryos were allowed to develop at 28.5°C.

7.11 Electron microscopy (EM)

Transmission electron microscopy (TEM): samples were fixed in 2.5% glutaraldehyde and 2% paraformaldehyde in PBS for 1hr at room temperature (then stored in 4°C until processing), followed by a secondary fixation in 1% aqueous osmium tetroxide with potassium ferricyanide overnight at 4°C. Samples were then dehydrated in a graded series of ethanol with propylene oxide as a transitional solvent, and infiltrated in Epon. Sections were cut on a Leica UC6 ultramicrotome in the range of 50nm to 70nm thickness and post stained with 5% uranyl acetate in 70% methanol and Sato's lead stain. Sections were viewed in a FEI Technai Spirit BioTWIN TEM and imaged with a Gatan Ultrascan digital camera. Scanning electron microscopy (SEM): samples were fixed in 2.5% glutaraldehyde and 2% paraformaldehyde in PBS for 1hr at room temperature (then stored at 4°C until processing) and treated with tannic acid, osmium, thiocarbohydrazide, and osmium (TOTO) as described in Jongebloed et al. (1999). Samples were then dehydrated in an ethanol dilution series, critical point dried in a Tousimis Samdri 795 CPD, mounted on stubs and coated with gold palladium. Samples were imaged in a Hitachi TM-1000 tabletop SEM.

7.12 Time-lapse imaging

Time-lapse imaging was performed as described in Galanternik et al. (2016). Briefly, embryos were anesthetized in 0.5X E2 medium with Tricaine (4g/L pH 9.0). Anesthetized embryos were transferred with a fire-polished glass Pasteur pipette on MatTek glass bottom microwell dish in LMP agarose solution (0.8% in 0.5X E2 medium). Once embryo is in correct orientation and agarose solidifies, 2-3mL of 0.5X E2 medium or drug solution

containing Tricaine is added to the MatTek dish. Time-lapse recordings were acquired on Zeiss LSM 780 confocal microscope using 40x/1.2W objective and a tiling function on Zen software.

7.13 RNA sequencing (RNASeq) data analysis

For the RNASeq experiment we cut tails from 36 hpf *Tg(cldnb:lynGFP)* embryos and isolated primordium and neuromast cells by FACS. Reads were mapped to the *Danio rerio* genome version danRer10 from the University of California, Santa Cruz (UCSC) using TopHat version 2.0.13, with gene annotations from Ensembl 84. RNASeq analysis and Gene Ontology (GO) Enrichment analysis was performed in the R environment using the bioconductor packages edgeR, topGO, and biomaRt. Reads counted on Ensembl transcripts from UCSC using HTSeq version 0.6.1 were analyzed with edgeR to generate P values to form comparisons between wildtype and NICD embryos. Of the 32,105 genes detected, only 19,643 genes with a sum across all samples of at least three reads per million were considered for the analysis. P values were adjusted for multiple hypothesis testing using the Benjamini–Hochberg method. The fragments per kilobase of transcript per million mapped reads (FPKM) values were generated using Cufflinks version 2.2.1. To define differentially expressed genes in the NICD embryos, genes were selected with the following criteria: log2 ratio > 0.5 with P value < 0.01 and log2 ratio < -0.5 with P value < 0.01, resulting in 187 genes up- and 502 genes downregulated, respectively. The necessary GO IDs were obtained from Ensembl using biomaRt. Of the 19,643 expressed genes, 11,757 were associated with GO terms. Therefore, only 117 of the 187 genes and 323 of the 502 genes were used in the GO analysis.

The whole-genome sequence data from this study have been submitted to the NCBI Gene Expression Omnibus (GEO; http://www.ncbi.nlm.nih.gov/geo/), accession number GSE86571.

7.14 Image analysis

7.14.1 Cell shape/volume analysis

Individual cells were reconstructed in 3D using Bitplane's Imaris software. Cells were reconstructed manually by drawing the cell boundary in every single z-slice using Imaris' surface function. After the cell boundary was drawn in every z-slice, a surface was created, and the cell volume was exported for analysis.

For illustrative purposes, the cell surfaces were exported, oriented with the cell constriction upward, and placed side by side for comparison. Every attempt was made to export a view of the cells at the same scale, and at an angle, which shows the most representative perspective.

7.14.2 Apical constriction analysis (area)

Rosette constrictions for each cell were analyzed using the ratio of two area measurements in 2D. First we measured the area of the bounding box of the smallest discernable constriction. Second we measured the area of the bounding box of the largest part of the cell. We then used the ratio of those two measurements to determine how much the cell is constricting on the apical side with respect to the bulk of its structure.

7.14.3 Apical constriction analysis (volume)

Rosette constrictions were analyzed using the Imaris surface function. Because so much membrane from multiple cells comes together at a single point, constrictions are the brightest feature in the image. A global threshold was set, selecting the brightest portion of the image. Smaller insignificant features were eliminated using a size threshold, leaving only the largest and brightest rosette constrictions.

7.14.4 Cell counts

Cell counting was performed in Fiji software where every DAPI positive nuclei was counted by hand using a Wand tool. An average number of cells between different neuromasts was calculated and plotted with the standard error bars. Additionally, Student's *t* tests were performed in Microsoft Excel software to assess the significance between the samples.

Contributions

Electron microscopy was performed by Melainia McClain from the Electron microscopy center at Stowers Institute for Medical Research (SIMR). Data analysis in Figure 3-3 was performed by Richard Alexander from the Microscopy center at SIMR. FACS sorting and RNASeq were performed in the Cytometry and Molecular biology facilities at SIMR. RNASeq was analysed by Ryan Jiskra and Xin Gao. Data for Figure 5-1 panels M, N, O was acquired by Andy Aman. Data for Figure 5-3 panels D, D' was acquired by Ren Yi. Illustrations in Figure 5-4 were made by Mark Miller. Stowers Aquatics facility was maintaining fish husbandry.

Appendix

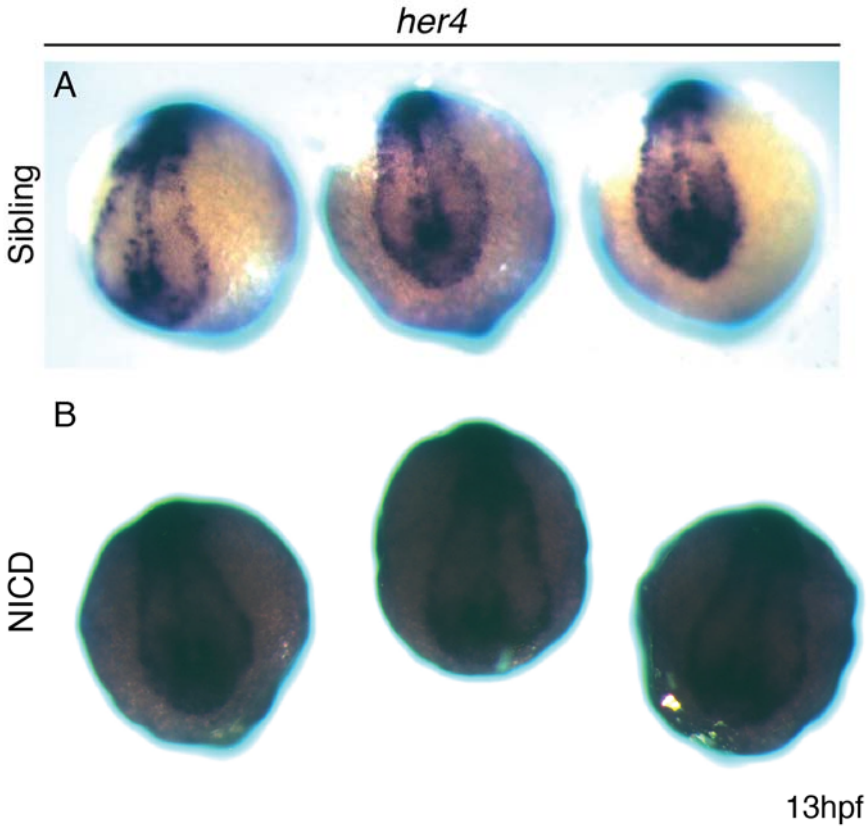

Appendix Figure 1. The NICD transgene is strongly induced in the embryos when the lateral line placode is forming
(A) *her4* expression in three representative wildtype embryos is lower compared to NICD siblings (B) at 13hpf.

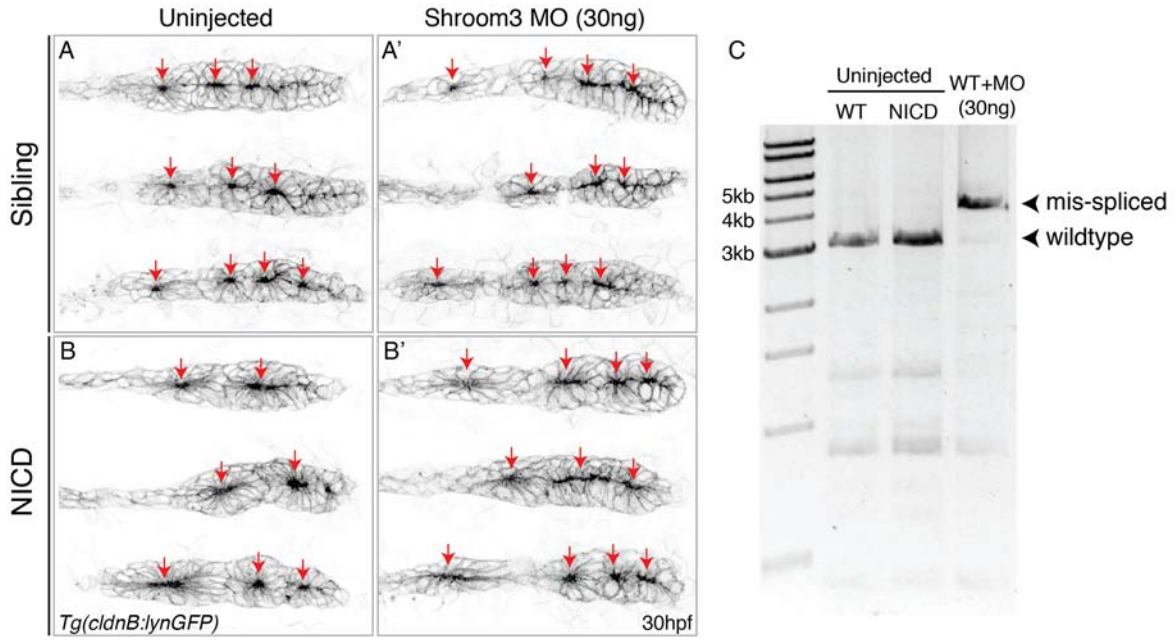

Appendix Figure 2. *shroom3* is not required for proneuromast formation in the wildtype or NICD embryos

Proneuromasts form equally well (marked with red arrows) in the (A and A') wildtype primordia and (B and B') NICD primordia. (C) RT-PCR with *shroom3* specific primers on wildtype embryos injected with *shroom3* morpholino (far right) or uninjected wildtype and NICD embryos (left) showing that *shroom3* morpholino efficiently generates an alternative splice variant by blocking the excision of intron 6, potentially leading to a truncated protein (Ernst et al., 2012).

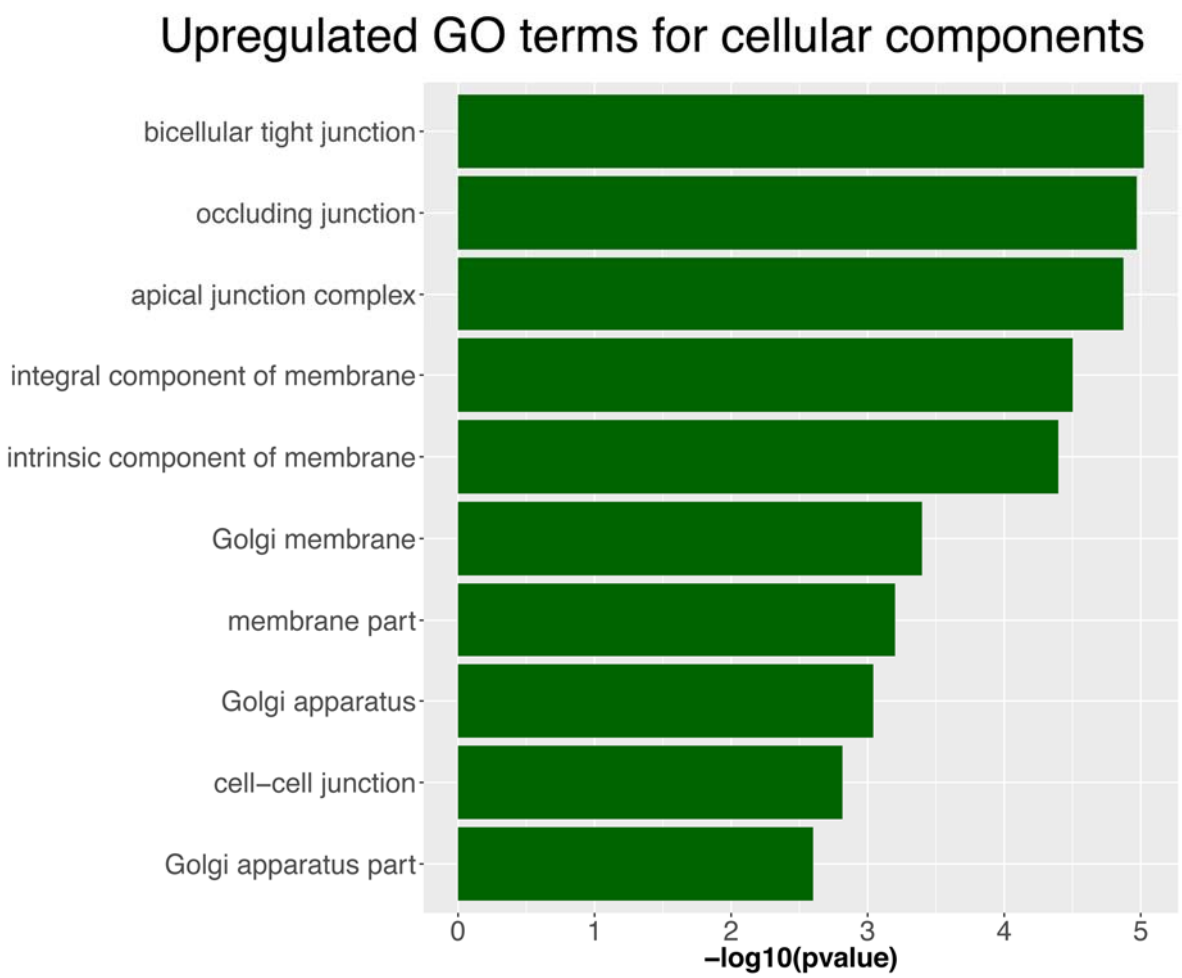

Appendix Figure 3. Upregulated GO terms for cellular components in NICD lateral line primordia

Ten most enriched cellular components in NICD lateral line revealed by GO term analysis.

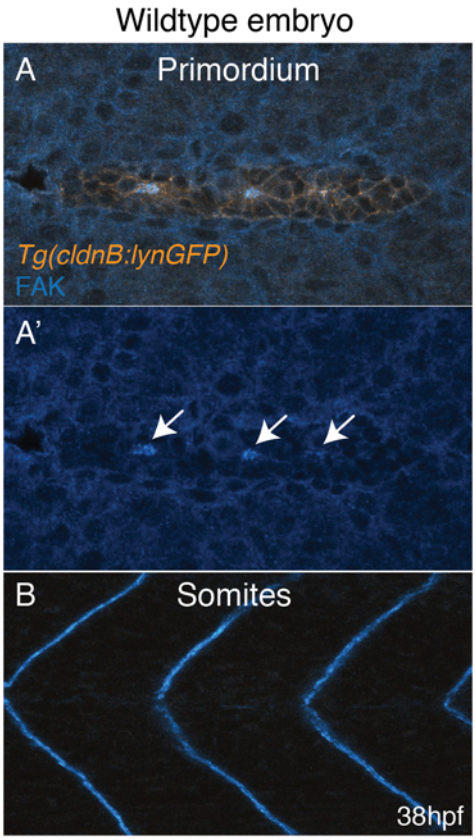

Appendix Figure 4. FAK expression in the wildtype embryo trunk
(A and A') FAK is expressed in the apical constrictions of proneuromasts, marked with arrows in (A'). (B) FAK is expressed in between the somites.

References

Acosta, H., López, S.L., Revinski, D.R., and Carrasco, A.E. (2011). Notch destabilises maternal β-catenin and restricts dorsal-anterior development in Xenopus. Development *138*, 2567-2579.

Agarwala, S., Duquesne, S., Liu, K., Boehm, A., Grimm, L., Link, S., Konig, S., Eimer, S., Ronneberger, O., and Lecaudey, V. (2015). Amotl2a interacts with the Hippo effector Yap1 and the Wnt/beta-catenin effector Lef1 to control tissue size in zebrafish. Elife *4*, e08201.

Aijaz, S., D'Atri, F., Citi, S., Balda, M.S., and Matter, K. (2005). Binding of GEF-H1 to the tight junction-associated adaptor cingulin results in inhibition of Rho signaling and G1/S phase transition. Dev Cell *8*, 777-786.

Aman, A., Nguyen, M., and Piotrowski, T. (2011). Wnt/beta-catenin dependent cell proliferation underlies segmented lateral line morphogenesis. Developmental biology *349*, 470-482.

Aman, A., and Piotrowski, T. (2008). Wnt/beta-catenin and Fgf signaling control collective cell migration by restricting chemokine receptor expression. Dev Cell *15*, 749-761.

Andersen, P., Uosaki, H., Shenje, L.T., and Kwon, C. (2012). Non-canonical Notch signaling: emerging role and mechanism. Trends in cell biology *22*, 257-265.

Anderson, J.M., Van Itallie, C.M., and Fanning, A.S. (2004). Setting up a selective barrier at the apical junction complex. Current opinion in cell biology *16*, 140-145.

Angres, B., Barth, A., and Nelson, W.J. (1996). Mechanism for transition from initial to stable cell-cell adhesion: kinetic analysis of E-cadherin-mediated adhesion using a quantitative adhesion assay. Journal of Cell Biology *134*, 549-558.

Appel, B., and Eisen, J.S. (1998). Regulation of neuronal specification in the zebrafish spinal cord by Delta function. Development *125*, 371-380.

Arnaud, M.P., Vallee, A., Robert, G., Bonneau, J., Leroy, C., Varin-Blank, N., Rio, A.G., Troadec, M.B., Galibert, M.D., and Gandemer, V. (2015). CD9, a key actor in the dissemination of lymphoblastic leukemia, modulating CXCR4-mediated migration via RAC1 signaling. Blood *126*, 1802-1812.

Arnold, K.M., Goeckeler, Z.M., and Wysolmerski, R.B. (2013). Loss of focal adhesion kinase enhances endothelial barrier function and increases focal adhesions. Microcirculation *20*, 637-649.

Artavanis-Tsakonas, S., Rand, M.D., and Lake, R.J. (1999). Notch signaling: cell fate control and signal integration in development. Science *284*, 770-776.

Babb, S.G., and Marrs, J.A. (2004). E-cadherin regulates cell movements and tissue formation in early zebrafish embryos. Developmental dynamics *230*, 263-277.

Barry, E.R., and Camargo, F.D. (2013). The Hippo superhighway: signaling crossroads converging on the Hippo/Yap pathway in stem cells and development. Current opinion in cell biology *25*, 247-253.

Bedzhov, I., and Zernicka-Goetz, M. (2014). Self-organizing properties of mouse pluripotent cells initiate morphogenesis upon implantation. Cell *156*, 1032-1044.

Bermingham, N.A., Hassan, B.A., Price, S.D., Vollrath, M.A., Ben-Arie, N., Eatock, R.A., Bellen, H.J., Lysakowski, A., and Zoghbi, H.Y. (1999). Math1: an essential gene for the generation of inner ear hair cells. Science *284*, 1837-1841.

Bertet, C., Sulak, L., and Lecuit, T. (2004). Myosin-dependent junction remodelling controls planar cell intercalation and axis elongation. Nature *429*, 667-671.

Bhat, A.A., Pope, J.L., Smith, J.J., Ahmad, R., Chen, X., Washington, M.K., Beauchamp, R.D., Singh, A.B., and Dhawan, P. (2015). Claudin-7 expression induces mesenchymal to epithelial transformation (MET) to inhibit colon tumorigenesis. Oncogene *34*, 4570-4580.

Bienz, M. (2002). The subcellular destinations of APC proteins. Nature Reviews Molecular Cell Biology *3*, 328-338.

Bilder, D., and Perrimon, N. (2000). Localization of apical epithelial determinants by the basolateral PDZ protein Scribble. Nature *403*, 676-680.

Blankenship, J.T., Backovic, S.T., Sanny, J.S., Weitz, O., and Zallen, J.A. (2006). Multicellular rosette formation links planar cell polarity to tissue morphogenesis. Dev Cell *11*, 459-470.

Bossuyt, W., Chen, C., Chen, Q., Sudol, M., McNeill, H., Pan, D., Kopp, A., and Halder, G. (2014). An evolutionary shift in the regulation of the Hippo pathway between mice and flies. Oncogene *33*, 1218-1228.

Bray, S. (1998). Notch signalling inDrosophila: three ways to use a pathway. Paper presented at: Seminars in cell & developmental biology (Elsevier).

Bray, S.J. (2006). Notch signalling: a simple pathway becomes complex. Nature reviews Molecular cell biology *7*, 678-689.

Breau, M.A., and Schneider-Maunoury, S. (2015). Cranial placodes: models for exploring the multi-facets of cell adhesion in epithelial rearrangement, collective migration and neuronal movements. Developmental biology *401*, 25-36.

Breau, M.A., Wilson, D., Wilkinson, D.G., and Xu, Q. (2012). Chemokine and Fgf signalling act as opposing guidance cues in formation of the lateral line primordium. Development *139*, 2246-2253.

Brizuela, B.J., Wessely, O., and De Robertis, E.M. (2001). Overexpression of the Xenopus tight-junction protein claudin causes randomization of the left-right body axis. Developmental biology *230*, 217-229.

Bryant, D.M., and Mostov, K.E. (2008). From cells to organs: building polarized tissue. Nature reviews Molecular cell biology *9*, 887-901.

Burridge, K., and Chrzanowska-Wodnicka, M. (1996). Focal adhesions, contractility, and signaling. Annual review of cell and developmental biology *12*, 463-519.

Chitnis, A.B. (1999). Control of neurogenesis—lessons from frogs, fish and flies. Current opinion in neurobiology *9*, 18-25.

Chitnis, A.B., Nogare, D.D., and Matsuda, M. (2012). Building the posterior lateral line system in zebrafish. Dev Neurobiol *72*, 234-255.

Citi, S., Guerrera, D., Spadaro, D., and Shah, J. (2014). Epithelial junctions and Rho family GTPases: the zonular signalosome. Small GTPases *5*, e973760.

Clark, B.S., Cui, S., Miesfeld, J.B., Klezovitch, O., Vasioukhin, V., and Link, B.A. (2012). Loss of Llgl1 in retinal neuroepithelia reveals links between apical domain size, Notch activity and neurogenesis. Development *139*, 1599-1610.

D'atri, F., and Citi, S. (2001). Cingulin interacts with F-actin in vitro. FEBS letters *507*, 21-24.

Dalle Nogare, D., Nikaido, M., Somers, K., Head, J., Piotrowski, T., and Chitnis, A.B. (2016). In toto imaging of the migrating Zebrafish lateral line primordium at single cell resolution. Developmental biology.

Dambly-Chaudière, C., Cubedo, N., and Ghysen, A. (2007). Control of cell migration in the development of the posterior lateral line: antagonistic interactions between the chemokine receptors CXCR4 and CXCR7/RDC1. BMC developmental biology *7*, 23.

David, N.B., Sapède, D., Saint-Etienne, L., Thisse, C., Thisse, B., Dambly-Chaudière, C., Rosa, F.M., and Ghysen, A. (2002). Molecular basis of cell migration in the fish lateral line: role of the chemokine receptor CXCR4 and of its ligand, SDF1. Proceedings of the National Academy of Sciences *99*, 16297-16302.

Dijkgraaf, S. (1963). The functioning and significance of the lateral-line organs. Biological Reviews *38*, 51-105.

Donà, E., Barry, J.D., Valentin, G., Quirin, C., Khmelinskii, A., Kunze, A., Durdu, S., Newton, L.R., Fernandez-Minan, A., and Huber, W. (2013). Directional tissue migration through a self-generated chemokine gradient. Nature *503*, 285-289.

Duguay, D., Foty, R.A., and Steinberg, M.S. (2003). Cadherin-mediated cell adhesion and tissue segregation: qualitative and quantitative determinants. Developmental biology *253*, 309-323.

Dumstrei, K., Mennecke, R., and Raz, E. (2004). Signaling pathways controlling primordial germ cell migration in zebrafish. Journal of cell science *117*, 4787-4795.

Durdu, S., Iskar, M., Revenu, C., Schieber, N., Kunze, A., Bork, P., Schwab, Y., and Gilmour, D. (2014). Luminal signalling links cell communication to tissue architecture during organogenesis. Nature *515*, 120-124.

Ebnet, K., Suzuki, A., Ohno, S., and Vestweber, D. (2004). Junctional adhesion molecules (JAMs): more molecules with dual functions? Journal of Cell Science *117*, 19-29.

Ehrlich, J.S., Hansen, M.D., and Nelson, W.J. (2002). Spatio-temporal regulation of Rac1 localization and lamellipodia dynamics during epithelial cell-cell adhesion. Developmental cell *3*, 259-270.

Endo, Y., Osumi, N., and Wakamatsu, Y. (2002). Bimodal functions of Notch-mediated signaling are involved in neural crest formation during avian ectoderm development. Development *129*, 863-873.

Ernst, S., Liu, K., Agarwala, S., Moratscheck, N., Avci, M.E., Dalle Nogare, D., Chitnis, A.B., Ronneberger, O., and Lecaudey, V. (2012). Shroom3 is required downstream of FGF signalling to mediate proneuromast assembly in zebrafish. Development *139*, 4571-4581.

Fan, Z., Chen, J., Zou, J., Bullen, D., Liu, C., and Delcomyn, F. (2002). Design and fabrication of artificial lateral line flow sensors. Journal of Micromechanics and Microengineering *12*, 655.

Fanning, A.S., Jameson, B.J., Jesaitis, L.A., and Anderson, J.M. (1998). The tight junction protein ZO-1 establishes a link between the transmembrane protein occludin and the actin cytoskeleton. Journal of Biological Chemistry *273*, 29745-29753.

Fanning, A.S., Van Itallie, C.M., and Anderson, J.M. (2012). Zonula occludens-1 and-2 regulate apical cell structure and the zonula adherens cytoskeleton in polarized epithelia. Molecular biology of the cell *23*, 577-590.

Farquhar, M.G., and Palade, G.E. (1963). Junctional complexes in various epithelia. The Journal of cell biology *17*, 375-412.

Feldman, G.J., Mullin, J.M., and Ryan, M.P. (2005). Occludin: structure, function and regulation. Advanced drug delivery reviews *57*, 883-917.

Fritzsch, B. (1987). The amphibian octavo-lateralis system and its regressive and progressive evolution. Acta biologica Hungarica *39*, 305-322.

Galanternik, M.V., Acedo, J.N., Romero-Carvajal, A., and Piotrowski, T. (2016). Imaging collective cell migration and hair cell regeneration in the sensory lateral line. Methods in cell biology *134*, 211-256.

Galanternik, M.V., Kramer, K.L., and Piotrowski, T. (2015). Heparan sulfate proteoglycans regulate Fgf signaling and cell polarity during collective cell migration. Cell reports *10*, 414-428.

Gallardo, V.E., Liang, J., Behra, M., Elkahloun, A., Villablanca, E.J., Russo, V., Allende, M.L., and Burgess, S.M. (2010). Molecular dissection of the migrating posterior lateral line primordium during early development in zebrafish. BMC developmental biology *10*, 120.

Ghysen, A., and Dambly-Chaudiere, C. (2004). Development of the zebrafish lateral line. Current opinion in neurobiology *14*, 67-73.

Gilmour, D.T., Maischein, H.-M., and Nüsslein-Volhard, C. (2002). Migration and function of a glial subtype in the vertebrate peripheral nervous system. Neuron *34*, 577-588.

Gokhale, R.H., and Shingleton, A.W. (2015). Size control: the developmental physiology of body and organ size regulation. Wiley Interdiscip Rev Dev Biol *4*, 335-356.

Gompel, N., Cubedo, N., Thisse, C., Thisse, B., Dambly-Chaudière, C., and Ghysen, A. (2001). Pattern formation in the lateral line of zebrafish. Mechanisms of development *105*, 69-77.

Gonzalez-Mariscal, L., Betanzos, A., Nava, P., and Jaramillo, B.E. (2003). Tight junction proteins. Prog Biophys Mol Biol *81*, 1-44.

Grant, K.A., Raible, D.W., and Piotrowski, T. (2005). Regulation of latent sensory hair cell precursors by glia in the zebrafish lateral line. Neuron *45*, 69-80.

Guruharsha, K., Kankel, M.W., and Artavanis-Tsakonas, S. (2012). The Notch signalling system: recent insights into the complexity of a conserved pathway. Nature Reviews Genetics *13*, 654-666.

Haas, P., and Gilmour, D. (2006). Chemokine signaling mediates self-organizing tissue migration in the zebrafish lateral line. Developmental cell *10*, 673-680.

Haddon, C., Mowbray, C., Whitfield, T., Jones, D., Gschmeissner, S., and Lewis, J. (1999). Hair cells without supporting cells: further studies in the ear of the zebrafish mind bomb mutant. J Neurocytol *28*, 837-850.

Haddon, C., Smithers, L., Schneider-Maunoury, S., Coche, T., Henrique, D., and Lewis, J. (1998). Multiple delta genes and lateral inhibition in zebrafish primary neurogenesis. Development *125*, 359-370.

Harding, M.J., McGraw, H.F., and Nechiporuk, A. (2014). The roles and regulation of multicellular rosette structures during morphogenesis. Development *141*, 2549-2558.

Harding, M.J., and Nechiporuk, A.V. (2012). Fgfr-Ras-MAPK signaling is required for apical constriction via apical positioning of Rho-associated kinase during mechanosensory organ formation. Development *139*, 3130-3135.

Hartenstein, A.Y., Rugendorff, A., Tepass, U., and Hartenstein, V. (1992). The function of the neurogenic genes during epithelial development in the Drosophila embryo. Development *116*, 1203-1220.

Hava, D., Forster, U., Matsuda, M., Cui, S., Link, B.A., Eichhorst, J., Wiesner, B., Chitnis, A., and Abdelilah-Seyfried, S. (2009). Apical membrane maturation and cellular rosette formation during morphogenesis of the zebrafish lateral line. J Cell Sci *122*, 687-695.

Heisenberg, C.P., and Bellaiche, Y. (2013). Forces in tissue morphogenesis and patterning. Cell *153*, 948-962.

Hernández, P.P., Olivari, F.A., Sarrazín, A.F., Sandoval, P.C., and Allende, M.L. (2007). Regeneration in zebrafish lateral line neuromasts: Expression of the neural progenitor cell marker sox2 and proliferation-dependent and-independent mechanisms of hair cell renewal. Developmental neurobiology *67*, 637-654.

Heuberger, J., and Birchmeier, W. (2010). Interplay of cadherin-mediated cell adhesion and canonical Wnt signaling. Cold Spring Harb Perspect Biol *2*, a002915.

Hildebrand, J.D., and Soriano, P. (1999). Shroom, a PDZ domain-containing actin-binding protein, is required for neural tube morphogenesis in mice. Cell *99*, 485-497.

Hirano, S., Kimoto, N., Shimoyama, Y., Hirohashi, S., and Takeichi, M. (1992). Identification of a neural α-catenin as a key regulator of cadherin function and multicellular organization. Cell *70*, 293-301.

Huang, S., and Ingber, D.E. (2005). Cell tension, matrix mechanics, and cancer development. Cancer cell *8*, 175-176.

Hurlstone, A.F., Haramis, A.P., Wienholds, E., Begthel, H., Korving, J., Van Eeden, F., Cuppen, E., Zivkovic, D., Plasterk, R.H., and Clevers, H. (2003). The Wnt/beta-catenin pathway regulates cardiac valve formation. Nature *425*, 633-637.

Hynes, R.O. (2002). Integrins: bidirectional, allosteric signaling machines. Cell *110*, 673-687.

Igaki, T. (2009). Correcting developmental errors by apoptosis: lessons from Drosophila JNK signaling. Apoptosis *14*, 1021-1028.

Irvine, K.D., and Wieschaus, E. (1994). Cell intercalation during Drosophila germband extension and its regulation by pair-rule segmentation genes. DEVELOPMENT-CAMBRIDGE- *120*, 827-827.

Itoh, M., and Chitnis, A.B. (2001). Expression of proneural and neurogenic genes in the zebrafish lateral line primordium correlates with selection of hair cell fate in neuromasts. Mech Dev *102*, 263-266.

Itoh, M., Kim, C.-H., Palardy, G., Oda, T., Jiang, Y.-J., Maust, D., Yeo, S.-Y., Lorick, K., Wright, G.J., and Ariza-McNaughton, L. (2003). Mind bomb is a ubiquitin ligase that is essential for efficient activation of Notch signaling by Delta. Developmental cell *4*, 67-82.

Jacinto, E., Loewith, R., Schmidt, A., Lin, S., Rüegg, M.A., Hall, A., and Hall, M.N. (2004). Mammalian TOR complex 2 controls the actin cytoskeleton and is rapamycin insensitive. Nature cell biology *6*, 1122-1128.

Jarman, A.P., Sun, Y., Jan, L.Y., and Jan, Y.N. (1995). Role of the proneural gene, atonal, in formation of Drosophila chordotonal organs and photoreceptors. Development *121*, 2019-2030.

Jiang, L., Romero-Carvajal, A., Haug, J.S., Seidel, C.W., and Piotrowski, T. (2014). Gene-expression analysis of hair cell regeneration in the zebrafish lateral line. Proc Natl Acad Sci U S A *111*, E1383-1392.

Johnson, G.L., and Nakamura, K. (2007). The c-jun kinase/stress-activated pathway: regulation, function and role in human disease. Biochimica et Biophysica Acta (BBA)-Molecular Cell Research *1773*, 1341-1348.

Jongebloed, W.L., Stokroos, I., Van der Want, J.J., and Kalicharan, D. (1999). Non-coating fixation techniques or redundancy of conductive coating, low kV FE-SEM operation and combined SEM/TEM of biological tissues. J Microsc *193*, 158-170.

Kane, D.A., McFarland, K.N., and Warga, R.M. (2005). Mutations in half baked/E-cadherin block cell behaviors that are necessary for teleost epiboly. Development *132*, 1105-1116.

Keshet, Y., and Seger, R. (2010). The MAP kinase signaling cascades: a system of hundreds of components regulates a diverse array of physiological functions. MAP Kinase Signaling Protocols: Second Edition, 3-38.

Killian, E.C.O., Birkholz, D.A., and Artinger, K.B. (2009). A role for chemokine signaling in neural crest cell migration and craniofacial development. Developmental biology *333*, 161-172.

Kim, M., and Jho, E.-h. (2014). Cross-talk between Wnt/beta-catenin and Hippo signaling pathways: a brief review. BMB Rep *47*, 540-545.

Kim, N.-G., Koh, E., Chen, X., and Gumbiner, B.M. (2011). E-cadherin mediates contact inhibition of proliferation through Hippo signaling-pathway components. Proceedings of the National Academy of Sciences *108*, 11930-11935.

Kimmel, C.B., Ballard, W.W., Kimmel, S.R., Ullmann, B., and Schilling, T.F. (1995). Stages of embryonic development of the zebrafish. Developmental dynamics *203*, 253-310.

Klezovitch, O., Fernandez, T.E., Tapscott, S.J., and Vasioukhin, V. (2004). Loss of cell polarity causes severe brain dysplasia in Lgl1 knockout mice. Genes Dev *18*, 559-571.

Knust, E., and Bossinger, O. (2002). Composition and formation of intercellular junctions in epithelial cells. Science *298*, 1955-1959.

Kok, F.O., Shin, M., Ni, C.W., Gupta, A., Grosse, A.S., van Impel, A., Kirchmaier, B.C., Peterson-Maduro, J., Kourkoulis, G., Male, I.*, et al.* (2015). Reverse genetic screening reveals poor correlation between morpholino-induced and mutant phenotypes in zebrafish. Dev Cell *32*, 97-108.

Kopan, R., and Ilagan, M.X.G. (2009). The canonical Notch signaling pathway: unfolding the activation mechanism. Cell *137*, 216-233.

Kopinke, D., Sasine, J., Swift, J., Stephens, W.Z., and Piotrowski, T. (2006). Retinoic acid is required for endodermal pouch morphogenesis and not for pharyngeal endoderm specification. Developmental dynamics : an official publication of the American Association of Anatomists *235*, 2695-2709.

Kovacs, E.M. (2003). Direct cadherin-activated cell signaling a view from the plasma membrane. The Journal of cell biology *160*, 11-16.

Kovacs, E.M., Verma, S., Ali, R.G., Ratheesh, A., Hamilton, N.A., Akhmanova, A., and Yap, A.S. (2011). N-WASP regulates the epithelial junctional actin cytoskeleton through a non-canonical post-nucleation pathway. Nature Cell Biology *13*, 934-943.

Kozlovskaja-Gumbrienė, A., Yi, R., Alexander, R., Aman, A., Jiskra, R., Nagelberg, D., Knaut, H., McClain, M., and Piotrowski, T. (2017). Proliferation-independent regulation of organ size by Fgf/Notch signaling. eLife *6*, e21049.

Kozlowski, D.J., Murakami, T., Ho, R.K., and Weinberg, E.S. (1997). Regional cell movement and tissue patterning in the zebrafish embryo revealed by fate mapping with caged fluorescein. Biochemistry and cell biology *75*, 551-562.

Kubota, K., Furuse, M., Sasaki, H., Sonoda, N., Fujita, K., Nagafuchi, A., and Tsukita, S. (1999). Ca(2+)-independent cell-adhesion activity of claudins, a family of integral membrane proteins localized at tight junctions. Curr Biol *9*, 1035-1038.

Kwan, K.M., Fujimoto, E., Grabher, C., Mangum, B.D., Hardy, M.E., Campbell, D.S., Parant, J.M., Yost, H.J., Kanki, J.P., and Chien, C.B. (2007). The Tol2kit: a multisite gateway-based construction kit for Tol2 transposon transgenesis constructs. Developmental dynamics : an official publication of the American Association of Anatomists *236*, 3088-3099.

Kwon, C., Cheng, P., King, I.N., Andersen, P., Shenje, L., Nigam, V., and Srivastava, D. (2011). Notch post-translationally regulates [beta]-catenin protein in stem and progenitor cells. Nature cell biology *13*, 1244-1251.

Kwong, R.W., and Perry, S.F. (2013). The tight junction protein claudin-b regulates epithelial permeability and sodium handling in larval zebrafish, Danio rerio. Am J Physiol Regul Integr Comp Physiol *304*, R504-513.

Laplante, M., and Sabatini, D.M. (2012). mTOR signaling in growth control and disease. Cell *149*, 274-293.

Lecaudey, V., Cakan-Akdogan, G., Norton, W.H., and Gilmour, D. (2008). Dynamic Fgf signaling couples morphogenesis and migration in the zebrafish lateral line primordium. Development *135*, 2695-2705.

Lee, C., Scherr, H.M., and Wallingford, J.B. (2007). Shroom family proteins regulate γ-tubulin distribution and microtubule architecture during epithelial cell shape change. Development *134*, 1431-1441.

Lee, Y., Grill, S., Sanchez, A., Murphy-Ryan, M., and Poss, K.D. (2005). Fgf signaling instructs position-dependent growth rate during zebrafish fin regeneration. Development *132*, 5173-5183.

Lehmann, R., Jiménez, F., Dietrich, U., and Campos-Ortega, J.A. (1983). On the phenotype and development of mutants of early neurogenesis inDrosophila melanogaster. Wilhelm Roux's archives of developmental biology *192*, 62-74.

Leung, K.T., Chan, K.Y., Ng, P.C., Lau, T.K., Chiu, W.M., Tsang, K.S., Li, C.K., Kong, C.K., and Li, K. (2011). The tetraspanin CD9 regulates migration, adhesion, and homing of human cord blood CD34+ hematopoietic stem and progenitor cells. Blood *117*, 1840-1850.

Lewis, J. (1998). Notch signalling and the control of cell fate choices in vertebrates. Paper presented at: Seminars in cell & developmental biology (Elsevier).

Li, Y., Hibbs, M.A., Gard, A.L., Shylo, N.A., and Yun, K. (2012). Genome-wide analysis of N1ICD/RBPJ targets in vivo reveals direct transcriptional regulation of Wnt, SHH, and hippo pathway effectors by Notch1. Stem cells *30*, 741-752.

Llense, F., and Martin-Blanco, E. (2008). JNK signaling controls border cell cluster integrity and collective cell migration. Curr Biol *18*, 538-544.

Logan, C.Y., and Nusse, R. (2004). The Wnt signaling pathway in development and disease. Annu Rev Cell Dev Biol *20*, 781-810.

López-Schier, H., and Hudspeth, A. (2005). Supernumerary neuromasts in the posterior lateral line of zebrafish lacking peripheral glia. Proceedings of the National Academy of Sciences of the United States of America *102*, 1496-1501.

Lu, L., Li, Y., Kim, S.M., Bossuyt, W., Liu, P., Qiu, Q., Wang, Y., Halder, G., Finegold, M.J., and Lee, J.-S. (2010). Hippo signaling is a potent in vivo growth and tumor suppressor pathway in the mammalian liver. Proceedings of the National Academy of Sciences *107*, 1437-1442.

Lush, M.E., and Piotrowski, T. (2014). ErbB expressing Schwann cells control lateral line progenitor cells via non-cell-autonomous regulation of Wnt/β-catenin. eLife *3*, e01832.

Manderfield, L.J., Aghajanian, H., Engleka, K.A., Lim, L.Y., Liu, F., Jain, R., Li, L., Olson, E.N., and Epstein, J.A. (2015). Hippo signaling is required for Notch-dependent smooth muscle differentiation of neural crest. Development *142*, 2962-2971.

Marques, S.R., Lee, Y., Poss, K.D., and Yelon, D. (2008). Reiterative roles for FGF signaling in the establishment of size and proportion of the zebrafish heart. Developmental biology *321*, 397-406.

Martin, A.C., and Goldstein, B. (2014). Apical constriction: themes and variations on a cellular mechanism driving morphogenesis. Development *141*, 1987-1998.

Matsuda, M., and Chitnis, A.B. (2010). Atoh1a expression must be restricted by Notch signaling for effective morphogenesis of the posterior lateral line primordium in zebrafish. Development *137*, 3477-3487.

Matsuda, M., Dalle Nogare, D., Somers, K., Martin, K., Wang, C., and Chitnis, A.B. (2013). Lef1 regulates Dusp6 to influence neuromast formation and spacing in the zebrafish posterior lateral line primordium. Development *140*, 2387-2397.

McCubrey, J.A., Steelman, L.S., Chappell, W.H., Abrams, S.L., Wong, E.W., Chang, F., Lehmann, B., Terrian, D.M., Milella, M., and Tafuri, A. (2007). Roles of the Raf/MEK/ERK pathway in cell growth, malignant transformation and drug resistance. Biochimica et Biophysica Acta (BBA)-Molecular Cell Research *1773*, 1263-1284.

McGraw, H.F., Drerup, C.M., Culbertson, M.D., Linbo, T., Raible, D.W., and Nechiporuk, A.V. (2011). Lef1 is required for progenitor cell identity in the zebrafish lateral line primordium. Development *138*, 3921-3930.

Meinhardt, H., and Gierer, A. (1974). Applications of a theory of biological pattern formation based on lateral inhibition. Journal of cell science *15*, 321-346.

Mellman, I., and Nelson, W.J. (2008). Coordinated protein sorting, targeting and distribution in polarized cells. Nature reviews Molecular cell biology *9*, 833-845.

Metcalfe, W.K., Kimmel, C.B., and Schabtach, E. (1985). Anatomy of the posterior lateral line system in young larvae of the zebrafish. Journal of Comparative Neurology *233*, 377-389.

Millimaki, B.B., Sweet, E.M., Dhason, M.S., and Riley, B.B. (2007). Zebrafish atoh1 genes: classic proneural activity in the inner ear and regulation by Fgf and Notch. Development (Cambridge, England) *134*, 295-305.

Millimaki, B.B., Sweet, E.M., and Riley, B.B. (2010). Sox2 is required for maintenance and regeneration, but not initial development, of hair cells in the zebrafish inner ear. In Dev Biol, pp. 262-269.

Mizoguchi, T., Togawa, S., Kawakami, K., and Itoh, M. (2011). Neuron and sensory epithelial cell fate is sequentially determined by Notch signaling in zebrafish lateral line development. J Neurosci *31*, 15522-15530.

Mo, J.S., Park, H.W., and Guan, K.L. (2014). The Hippo signaling pathway in stem cell biology and cancer. EMBO reports *15*, 642-656.

Morgan, T.H. (1917). The theory of the gene. The American Naturalist *51*, 513-544.

Muñoz-Descalzo, S., Tkocz, K., Balayo, T., and Arias, A.M. (2011). Modulation of the ligand-independent traffic of Notch by Axin and Apc contributes to the activation of Armadillo in Drosophila. Development *138*, 1501-1506.

Nagafuchi, A., and Takeichi, M. (1988). Cell binding function of E-cadherin is regulated by the cytoplasmic domain. The EMBO Journal *7*, 3679.

Nechiporuk, A., and Raible, D.W. (2008). FGF-dependent mechanosensory organ patterning in zebrafish. Science *320*, 1774-1777.

Nelson, W.J. (2003). Adaptation of core mechanisms to generate cell polarity. Nature *422*, 766-774.

Nicolson, T. (2005). The genetics of hearing and balance in zebrafish. Annual review of genetics *39*, 9-22.

Niehrs, C. (2006). Function and biological roles of the Dickkopf family of Wnt modulators. Oncogene *25*, 7469-7481.

Nishimura, T., and Takeichi, M. (2008). Shroom3-mediated recruitment of Rho kinases to the apical cell junctions regulates epithelial and neuroepithelial planar remodeling. Development *135*, 1493-1502.

Nüsslein-Volhard, C. (2012). The zebrafish issue of Development. Development *139*, 4099-4103.

Olsauskas-Kuprys, R., Zlobin, A., and Osipo, C. (2013). Gamma secretase inhibitors of Notch signaling. Onco Targets Ther *6*, 943-955.

Ornitz, D.M., and Itoh, N. (2015). The fibroblast growth factor signaling pathway. Wiley Interdisciplinary Reviews: Developmental Biology *4*, 215-266.

Pan, D. (2007). Hippo signaling in organ size control. Genes & development *21*, 886-897.

Parsons, M.J., Pisharath, H., Yusuff, S., Moore, J.C., Siekmann, A.F., Lawson, N., and Leach, S.D. (2009). Notch-responsive cells initiate the secondary transition in larval zebrafish pancreas. Mech Dev *126*, 898-912.

Piotrowski, T., and Baker, C.V. (2014). The development of lateral line placodes: taking a broader view. Developmental biology *389*, 68-81.

Piotrowski, T., and Nüsslein-Volhard, C. (2000). The endoderm plays an important role in patterning the segmented pharyngeal region in zebrafish (Danio rerio). Developmental biology *225*, 339-356.

Plageman, T.F., Chauhan, B.K., Yang, C., Jaudon, F., Shang, X., Zheng, Y., Lou, M., Debant, A., Hildebrand, J.D., and Lang, R.A. (2011). A Trio-RhoA-Shroom3 pathway is required for apical constriction and epithelial invagination. Development *138*, 5177-5188.

Pohl, C., Tiongson, M., Moore, J.L., Santella, A., and Bao, Z. (2012). Actomyosin-based self-organization of cell internalization during C. elegans gastrulation. BMC Biol *10*, 94.

Radosevic, M., Fargas, L., and Alsina, B. (2014). The role of her4 in inner ear development and its relationship with proneural genes and Notch signalling. PloS one *9*, e109860.

Riley, B.B., Chiang, M., Farmer, L., and Heck, R. (1999). The deltaA gene of zebrafish mediates lateral inhibition of hair cells in the inner ear and is regulated by pax2.1. Development *126*, 5669-5678.

Rodriguez-Boulan, E., and Macara, I.G. (2014). Organization and execution of the epithelial polarity programme. Nature reviews Molecular cell biology *15*, 225-242.

Romero-Carvajal, A., Navajas Acedo, J., Jiang, L., Kozlovskaja-Gumbriene, A., Alexander, R., Li, H., and Piotrowski, T. (2015). Regeneration of Sensory Hair Cells Requires Localized Interactions between the Notch and Wnt Pathways. Dev Cell *34*, 267-282.

Rubinfeld, B., Albert, I., Porfiri, E., and Fiol, C. (1996). Binding of GSK3beta to teh APC-beta-catenin complex and regulation of complex assembly. Science *272*, 1023.

Sai, X., Yonemura, S., and Ladher, R.K. (2014). Junctionally restricted RhoA activity is necessary for apical constriction during phase 2 inner ear placode invagination. Developmental biology *394*, 206-216.

Sarrazin, A.F., Villablanca, E.J., Nuñez, V.A., Sandoval, P.C., Ghysen, A., and Allende, M.L. (2006). Proneural gene requirement for hair cell differentiation in the zebrafish lateral line. Developmental biology *295*, 534-545.

Sawyer, J.M., Harrell, J.R., Shemer, G., Sullivan-Brown, J., Roh-Johnson, M., and Goldstein, B. (2010). Apical constriction: a cell shape change that can drive morphogenesis. Developmental biology *341*, 5-19.

Scheer, N., and Campos-Ortega, J.A. (1999). Use of the Gal4-UAS technique for targeted gene expression in the zebrafish. Mech Dev *80*, 153-158.

Scheer, N., Riedl, I., Warren, J., Kuwada, J.Y., and Campos-Ortega, J.A. (2002). A quantitative analysis of the kinetics of Gal4 activator and effector gene expression in the zebrafish. Mechanisms of development *112*, 9-14.

Schwartz, M.A., and DeSimone, D.W. (2008). Cell adhesion receptors in mechanotransduction. Current opinion in cell biology *20*, 551-556.

Shin, J., Poling, J., Park, H.C., and Appel, B. (2007). Notch signaling regulates neural precursor allocation and binary neuronal fate decisions in zebrafish. Development *134*, 1911-1920.

Siddiqui, M., Sheikh, H., Tran, C., and Bruce, A.E. (2010). The tight junction component Claudin E is required for zebrafish epiboly. Developmental dynamics : an official publication of the American Association of Anatomists *239*, 715-722.

Skouloudaki, K., Puetz, M., Simons, M., Courbard, J.R., Boehlke, C., Hartleben, B., Engel, C., Moeller, M.J., Englert, C., Bollig, F.*, et al.* (2009). Scribble participates in Hippo signaling and is required for normal zebrafish pronephros development. Proc Natl Acad Sci U S A *106*, 8579-8584.

Slanchev, K., Carney, T.J., Stemmler, M.P., Koschorz, B., Amsterdam, A., Schwarz, H., and Hammerschmidt, M. (2009). The epithelial cell adhesion molecule EpCAM is required for epithelial morphogenesis and integrity during zebrafish epiboly and skin development. PLoS Genet *5*, e1000563.

Song, H., Mak, K.K., Topol, L., Yun, K., Hu, J., Garrett, L., Chen, Y., Park, O., Chang, J., and Simpson, R.M. (2010). Mammalian Mst1 and Mst2 kinases play essential roles in organ size control and tumor suppression. Proceedings of the National Academy of Sciences *107*, 1431-1436.

Stepniak, E., Radice, G.L., and Vasioukhin, V. (2009). Adhesive and signaling functions of cadherins and catenins in vertebrate development. Cold Spring Harbor perspectives in biology *1*, a002949.

Stoick-Cooper, C.L., Weidinger, G., Riehle, K.J., Hubbert, C., Major, M.B., Fausto, N., and Moon, R.T. (2007). Distinct Wnt signaling pathways have opposing roles in appendage regeneration. Development *134*, 479-489.

Sun, J., Wang, X., Li, C., and Mao, B. (2015). Xenopus Claudin-6 is required for embryonic pronephros morphogenesis and terminal differentiation. Biochem Biophys Res Commun *462*, 178-183.

Svetic, V., Hollway, G.E., Elworthy, S., Chipperfield, T.R., Davison, C., Adams, R.J., Eisen, J.S., Ingham, P.W., Currie, P.D., and Kelsh, R.N. (2007). Sdf1a patterns zebrafish melanophores and links the somite and melanophore pattern defects in choker mutants. Development *134*, 1011-1022.

Takai, Y., and Nakanishi, H. (2003). Nectin and afadin: novel organizers of intercellular junctions. Journal of cell science *116*, 17-27.

Takeichi, M. (2014). Dynamic contacts: rearranging adherens junctions to drive epithelial remodelling. Nature Reviews Molecular Cell Biology *15*, 397-410.

Takke, C., Dornseifer, P., v Weizsacker, E., and Campos-Ortega, J.A. (1999). her4, a zebrafish homologue of the Drosophila neurogenic gene E (spl), is a target of NOTCH signalling. Development *126*, 1811-1821.

Teleman, A.A. (2010). Molecular mechanisms of metabolic regulation by insulin in Drosophila. Biochemical Journal *425*, 13-26.

Terry, S.J., Zihni, C., Elbediwy, A., Vitiello, E., Leefa Chong San, I.V., Balda, M.S., and Matter, K. (2011). Spatially restricted activation of RhoA signalling at epithelial junctions by p114RhoGEF drives junction formation and morphogenesis. Nat Cell Biol *13*, 159-166.

Tsang, M., Maegawa, S., Kiang, A., Habas, R., Weinberg, E., and Dawid, I.B. (2004). A role for MKP3 in axial patterning of the zebrafish embryo. Development *131*, 2769-2779.

Tseng, A.-S., Engel, F.B., and Keating, M.T. (2006). The GSK-3 inhibitor BIO promotes proliferation in mammalian cardiomyocytes. Chemistry & biology *13*, 957-963.

Tsukita, S., Furuse, M., and Itoh, M. (2001). Multifunctional strands in tight junctions. Nature reviews Molecular cell biology *2*, 285-293.

Valdivia, L.E., Young, R.M., Hawkins, T.A., Stickney, H.L., Cavodeassi, F., Schwarz, Q., Pullin, L.M., Villegas, R., Moro, E., and Argenton, F. (2011). Lef1-dependent Wnt/β-catenin signalling drives the proliferative engine that maintains tissue homeostasis during lateral line development. Development *138*, 3931-3941.

Valentin, G., Haas, P., and Gilmour, D. (2007). The chemokine SDF1a coordinates tissue migration through the spatially restricted activation of Cxcr7 and Cxcr4b. Current Biology *17*, 1026-1031.

van der Vos, K.E., and Coffer, P.J. (2011). The extending network of FOXO transcriptional target genes. Antioxidants & redox signaling *14*, 579-592.

Van Itallie, C.M., and Anderson, J.M. (1997). Occludin confers adhesiveness when expressed in fibroblasts. Journal of cell science *110*, 1113-1121.

Van Itallie, C.M., and Anderson, J.M. (2014). Architecture of tight junctions and principles of molecular composition. Semin Cell Dev Biol *36*, 157-165.

Venkiteswaran, G., Lewellis, S.W., Wang, J., Reynolds, E., Nicholson, C., and Knaut, H. (2013). Generation and dynamics of an endogenous, self-generated signaling gradient across a migrating tissue. Cell *155*, 674-687.

Vogelmann, R., and Nelson, W.J. (2005). Fractionation of the epithelial apical junctional complex: reassessment of protein distributions in different substructures. Molecular biology of the cell *16*, 701-716.

Wada, H., Ghysen, A., Asakawa, K., Abe, G., Ishitani, T., and Kawakami, K. (2013). Wnt/Dkk negative feedback regulates sensory organ size in zebrafish. Curr Biol *23*, 1559-1565.

Wada, H., Tanaka, H., Nakayama, S., Iwasaki, M., and Okamoto, H. (2006). Frizzled3a and Celsr2 function in the neuroepithelium to regulate migration of facial motor neurons in the developing zebrafish hindbrain. Development *133*, 4749-4759.

Weston, C.R., and Davis, R.J. (2007). The JNK signal transduction pathway. Current opinion in cell biology *19*, 142-149.

Whitfield, T.T. (2002). Zebrafish as a model for hearing and deafness. Journal of neurobiology *53*, 157-171.

Winston, J.T., Strack, P., Beer-Romero, P., Chu, C.Y., Elledge, S.J., and Harper, J.W. (1999). The SCFβ-TRCP–ubiquitin ligase complex associates specifically with phosphorylated destruction motifs in IκBα and β-catenin and stimulates IκBα ubiquitination in vitro. Genes & development *13*, 270-283.

Wippold, F.J., 2nd, and Perry, A. (2006). Neuropathology for the neuroradiologist: rosettes and pseudorosettes. AJNR Am J Neuroradiol *27*, 488-492.

Wittchen, H.-U., Stein, M.B., and Kessler, R.C. (1999). Social fears and social phobia in a community sample of adolescents and young adults: prevalence, risk factors and co-morbidity. Psychological medicine *29*, 309-323.

Wright, M.R. (1951). The lateral line system of sense organs. The Quarterly review of biology *26*, 264-280.

Wu, C.J., Mannan, P., Lu, M., and Udey, M.C. (2013). Epithelial cell adhesion molecule (EpCAM) regulates claudin dynamics and tight junctions. J Biol Chem *288*, 12253-12268.

Yang, Y., Nguyen, N., Chen, N., Lockwood, M., Tucker, C., Hu, H., Bleckmann, H., Liu, C., and Jones, D.L. (2010). Artificial lateral line with biomimetic neuromasts to emulate fish sensing. Bioinspiration & biomimetics *5*, 016001.

Yu, F.-X., and Guan, K.-L. (2013). The Hippo pathway: regulators and regulations. Genes & development *27*, 355-371.

Zhao, B., Li, L., Lu, Q., Wang, L.H., Liu, C.-Y., Lei, Q., and Guan, K.-L. (2011a). Angiomotin is a novel Hippo pathway component that inhibits YAP oncoprotein. Genes & development *25*, 51-63.

Zhao, B., Tumaneng, K., and Guan, K.-L. (2011b). The Hippo pathway in organ size control, tissue regeneration and stem cell self-renewal. Nature cell biology *13*, 877-883.

Zihni, C., Mills, C., Matter, K., and Balda, M.S. (2016). Tight junctions: from simple barriers to multifunctional molecular gates. Nature reviews Molecular cell biology.

Filename: A036085B
Directory: C:\Users\liw\AppData\Local\Microsoft\Windows\INetCache\Content.MSO
Template: C:\Users\liw\AppData\Roaming\Microsoft\Templates\Normal.dotm
Title: Transcriptional Regulation of Hox genes during hindbrain development
Subject:
Author: Agne Kozlovskaja-Gumbriene
Keywords:
Comments:
Creation Date: 1/27/2017 1:02:00 PM
Change Number: 26
Last Saved On: 2/7/2017 3:12:00 PM
Last Saved By: Hodges, Lisa
Total Editing Time: 184 Minutes
Last Printed On: 2/7/2017 3:41:00 PM
As of Last Complete Printing
Number of Pages: 118
Number of Words: 55,703 (approx.)
Number of Characters: 317,508 (approx.)